

UNIVERSITÉ DU QUÉBEC EN ABITIBI-TÉMISCAMINGUE

ÉCOLE DE GÉNIE

**SELF-HEALING MATERIALS FOR RF ANTENNA AND THEIR
APPLICATION IN MINING**

**SELF-HEALING MATERIAUX POUR ANTENNE RF ET LEUR APPLICATION
DANS L'EXPLOITATION MINIERE**

MÉMOIRE

PRÉSENTÉ

COMME EXIGENCE PARTIELLE

DE LA MAÎTRISE EN INGÉNIERIE

PAR

EHSAN MAJIDI AHI

OCTOBER 2017



BIBLIOTHÈQUE

Cégep de l'Abitibi-Témiscamingue
Université du Québec en Abitibi-Témiscamingue

Mise en garde

La bibliothèque du Cégep de l'Abitibi-Témiscamingue et de l'Université du Québec en Abitibi-Témiscamingue a obtenu l'autorisation de l'auteur de ce document afin de diffuser, dans un but non lucratif, une copie de son œuvre dans Depositum, site d'archives numériques, gratuit et accessible à tous.

L'auteur conserve néanmoins ses droits de propriété intellectuelle, dont son droit d'auteur, sur cette œuvre. Il est donc interdit de reproduire ou de publier en totalité ou en partie ce document sans l'autorisation de l'auteur.

Warning

The library of the Cégep de l'Abitibi-Témiscamingue and the Université du Québec en Abitibi-Témiscamingue obtained the permission of the author to use a copy of this document for non-profit purposes in order to put it in the open archives Depositum, which is free and accessible to all.

The author retains ownership of the copyright on this document. Neither the whole document, nor substantial extracts from it, may be printed or otherwise reproduced without the author's permission.

ACKNOWLEDGMENT

Firstly, I would like to express my sincere gratitude to my supervisors Prof. Fouad Erchiqui, and Prof. Mourad Nedil and to my co-advisers Dr. Brahim Aïssa and Dr. Emile Haddad for their continuous support and inputs for their patience, and especially for having shared their knowledge. Their guidance helped me in all the steps of my current research and in writing my MSc thesis.

A special thanks to my beloved family, to my dear wife, my parents, my sister and my baby daughter for supporting me spiritually throughout writing this thesis and their assistance in my entire life in general.

CONTENTS

<i>Introduction</i>	1
<i>Chapter 1</i>	9
<i>Review</i>	9
<i>RF Self-Healing</i>	9
1.1. Liquid metal	10
1.1.1. Liquid metal in micro channels	10
1.1.2. Liquid Metal in Wire	11
1.1.3. Liquid Metal in Capsules	13
1.1.4. Liquid Metal and Single Walled Carbon Nanotube (SWNT)	18
1.2. Carbon Nano Tube (CNT)	20
1.3. Resettable Fuse	28
1.4. Light Self-Healing	29
1.5. Software Self-Healing	31
1.5.1. Self-Healing by Oscillation principles	31
1.5.2. Feedback Loop	41
<i>Chapter 2</i>	46
2.1. Theory behind the self-healing process	46
<i>Chapter 3</i>	49
<i>experimental Procedures and results</i>	49
3.1. Self-Healing Part	49
3.1.1. Chemical Elements	52
3.1.2. Oven.....	56
3.1.3. Microscope	57
3.1.4. Thermal shock	59

3.2. RF Part	67
3.3. Experimental Results	70
3.3.1. VNA.....	70
3.3.2. Anechoic chamber.....	73
<i>Chapter 4</i>	<i>84</i>
<i>Discussion.....</i>	<i>84</i>
4.1. Irradiation Properties	85
4.2. Self-Healing.....	97
<i>Chapter 5</i>	<i>113</i>
<i>Conclusions and outlook into the future.....</i>	<i>113</i>
<i>Future Works</i>	<i>114</i>
<i>References</i>	<i>116</i>

LIST OF FIGURES

FIGURE 1: <i>SOLDIER-TO-SOLDIER COMMUNICATIONS FOR COVERT BATTLEFIELD OPERATIONS. THE BLACK ARROWS REPRESENT SOME POSSIBLE WIRELESS LINKS ALLOWING DATA TRANSFER FROM ONE SOLDIER TO ANOTHER. [CHAHAT 2014]</i>	2
FIGURE 2: SIMULATED REFLECTION COEFFICIENT OF THE MICROSTRIP PATCH ANTENNA. — IN FREE SPACE. — ON THE SKIN-EQUIVALENT	3
FIGURE 3: REPRESENTATION OF THE BAN SYSTEM IN.....	4
FIGURE 4: (LEFT)MINERS WORKING IN THE UNDERGROUND MINE (RIGHT) MINE GAS SUSPENSION IN AIR.....	6
FIGURE 5: SYNTHETIC MATERIALS AND BIOLOGICAL SYSTEMS ROUTES TO HEALING [BLAISZIK 2010]	7
FIGURE 6: SCHEMATIC EXAMPLES SELF-HEALING; (A) EXTRINSIC, (B) VASCULAR, (C) INTRINSIC [BLAISZIK 2010].....	8
FIGURE 7: (I) ILLUSTRATION OF THE DISCONNECTION AND RECONNECTION OF AN ELECTRONIC CIRCUIT WITH USING A SELF-HEALING WIRE (SHS) (II) DISCONNECTED CIRCUIT (III) EGAIN CHANNEL TO BE ALIGNED FOR RESTORE ELECTRICAL CONDUCTIVITY.....	12
FIGURE 8: ILLUSTRATION SCHEMATIC OF SELF-HEALING CIRCUIT PROCESS.....	14
FIGURE 9: A SCHEMATIC EXAMPLE OF AUTONOMOUS CONDUCTIVITY RESTORATION CONCEPT IN A MICROELECTRONIC DEVICE. A) LIQUID METAL MICROCAPSULES DISTRIBUTED IN A DIELECTRIC MATERIAL TO SELF-HEALING. B) A CRACK LEADS TO BREAKS THE MICROCAPSULES. C) THE LIQUID METAL FLOWS FROM THE MICROCAPSULES TO THE DAMAGE ZONE, AND THEN RESTORING A CONDUCTIVE PATHWAY.....	15
FIGURE 10: SELF-HEALING CIRCUIT COMPONENTS, MULTILAYER TEST SPECIMEN, AND EVIDENCE OF TRIGGERED RELEASE. SEM IMAGES OF: A) CA. 200 M M DIAMETER GA-IN-FILLED UF MICROCAPSULES; B) CA. 10 M M DIAMETER GA-IN UF MICROCAPSULE; AND C) CA. 10 M M DIAMETER CAPSULES PATTERNED ON AN AU LINE. D) SCHEMATIC IMAGE OF A MULTILAYER TEST SPECIMEN CONSISTING OF A GLASS SUBSTRATE WITH A 100 NM THICK AU LINE PATTERN, EPOXY DIELECTRIC WITH DISPERSED GA-IN MICROCAPSULES, NOTCHED GLASS TOP LAYER, AND	

ACRYLIC BOTTOM LAYER. CRACK DAMAGE INITIATES AT THE NOTCH ROOT AND PROPAGATES THROUGH THE SPECIMEN BEFORE ARRESTING AND DEBONDING AT THE ACRYLIC INTERFACE. E) CROSS-SECTIONAL SEM IMAGE SHOWING THE LOCATION OF THE DAMAGED AREA AND SUBSEQUENT LIQUID METAL RELEASE (FALSE COLOR). F) MICRO-CT DATA, WITH SCHEMATIC SUPERIMPOSED, SHOWING MICROCAPSULES AND LIQUID METAL THAT HAS BEEN RELEASED INTO THE CRACK PLANE OF A HEALED SPECIMEN. [BLAISZIK 2011]	17
FIGURE 11: (A) TEM IMAGES OF SWNTs. (B) DIMENSIONS OF THE MICRO STRIP PATCH ANTENNA (C) TOP-VIEW IMAGE OF THE EPOXY/SWNT-BASED FILAMENTS DEPOSITED BY UV-ASSISTED DIRECT WRITING TECHNOLOGY ON THE SUBSTRATE. (D) TOP-VIEW IMAGE OF THE PATCH ANTENNA PROTOTYPE.....	19
FIGURE 12: SKETCH OF THE STUDIED SAMPLES AND EVALUATION TESTS.	20
FIGURE 13: (A) BROKEN CAPSULE (B) INSIDE OF MICROCAPSULE AND (C) OUTSIDE OF MICROCAPSULE TAKEN BY SEM MICROSCOPE.	22
FIGURE 14: (A) MICROGRAPHS OF A CRACK IN ECNT COATING WITHOUT MICROCAPSULES (B) AFTER 24 H (C) IN ECNT COATING WITH MICROCAPSULES CONTAINING EPA: ECNT AFTER CRACKING (D) AFTER 24 H.	23
FIGURE 15: (A) BEFORE ANY DAMAGE; (B) AFTER DAMAGE, FRACTURE OF GOLD LINE AND THEN RELEASE OF SWCNTs AND/OR GRAPHENE FROM MICROCAPSULES; AND (C) AFTER RESTORATION, WHERE THE CONDUCTIVE PARTICLES HAVE BRIDGED THE GAP ON THE GOLD LINE.	25
FIGURE 16: BRIDGING OF CARBON NANOTUBES IN A GAP OF GOLD LINE WITH PREFERENTIAL ORIENTATION DUE TO ELECTRIC FIELD MIGRATION.	26
FIGURE 17: TEM IMAGES OF DRIED SUSPENSION ON CARBON GRIDS (A)–(C), OPTICAL MICROSCOPY IMAGES OF MICROCAPSULES SUSPENDED IN MINERAL OIL (D)–(F), AND SEM IMAGES OF MICROCAPSULES COATED WITH Au/Pd.	27
FIGURE 18: LIGHT-POWERED HEALING OF A CRACK.....	29
FIGURE 19: VARIOUS STAGES OF LIGHT-POWERED HEALING OF LINEARLY CRACKED PDO 3 FILMS BY SEM MICROSCOPE.....	30
FIGURE 20: SELF-HEALING SYSTEM	33
FIGURE 21: THE SELF-HEALING FRAMEWORK FOR RF CIRCUITS.	34
FIGURE 22: SELF-HEALING ARCHITECTURE IN THE RF AMPLIFIER.	35
FIGURE 23: SELF-HEALING ALGORITHM.	36
FIGURE 24: SELF-HEALING LNA ARCHITECTURE.	37

FIGURE 25: SELF-HEALING SiGe RF LNA.....	38
FIGURE 26: SELF-HEALING METHODOLOGY.....	41
FIGURE 27: SELF-HEALING ALGORITHM.....	42
FIGURE 28: SCHEMATIC OF THE DESIGNED SYSTEM.	43
FIGURE 29: DESIGNED SYSTEM.	44
FIGURE 30: RECENT TAXONOMY OF PASSIVE SELF-HEALING CONCEPTS.[AISSA 2014].....	47
FIGURE 31: THE SELF-HEALING PROCESS. (I) THE HEALING AGENT, A MONOMER (E.G. THE DCPD) IS PREPARED AND STORED IN MICROCAPSULES. THE MICROCAPSULES AND A CATALYST ARE SPREAD AND EMBEDDED WITHIN THE STRUCTURE (MATRIX). (II) WHEN A CRACK REACHES A MICROCAPSULE, IT CAUSES THE RUPTURE WHICH RELEASES THE MONOMER-HEALING AGENT. (III) SELF-HEALING IS REALIZED BY POLYMERIZATION BETWEEN THE MONOMER AND EMBEDDED CATALYST.[AISSA 2014]	48
FIGURE 32: VACUUM SYSTEM.....	50
FIGURE 33: EPON 828.....	53
FIGURE 34: HARDENING AGENT (EPICURE 3046).....	54
FIGURE 35: MICROCAPSULE LESS THAN 200 MICROMETER DIAMETER.....	55
FIGURE 36: GRUBBS CATALYST UNDER THE MICROSCOPE.....	56
FIGURE 37: OVEN FOR POST CURING PROCESS.....	57
FIGURE 38: LEICA ZOOM 2000 MICROSCOPE	58
FIGURE 39: OMAX A35140U MICROSCOPE	59
FIGURE 40: SCHEMATIC PICTURE OF THERMAL SHOCK TEST.....	60
FIGURE 41: THERMAL SHOCK FOR RF ANTENNA.....	60
FIGURE 42: THERMAL SHOCK FOR ANTENNA WITH SELF-HEALING MATERIAL AFTER FIRST LIQUID NITROGEN, (RIGHT) AFTER FIRST OVEN.....	61
FIGURE 43: THERMAL SHOCK FOR ANTENNA WITH SELF-HEALING MATERIAL, (LEFT) AFTER SECOND LIQUID NITROGEN, (RIGHT) AFTER SECOND OVEN.....	62
FIGURE 44: THERMAL SHOCK FOR ANTENNA WITH SELF-HEALING MATERIAL, (LEFT) AFTER THIRD LIQUID NITROGEN, (RIGHT) AFTER THIRD OVEN	63
FIGURE 45: THERMAL SHOCK FOR ANTENNA WITH SELF-HEALING MATERIAL PLUS CNTs, (LEFT) AFTER FIRST LIQUID NITROGEN, (RIGHT) AFTER FIRST OVEN.....	64
FIGURE 46: THERMAL SHOCK FOR ANTENNA WITH SELF-HEALING MATERIAL PLUS CNTs, (LEFT) AFTER SECOND LIQUID NITROGEN, (RIGHT) AFTER SECOND OVEN	65

FIGURE 47: THERMAL SHOCK FOR ANTENNA WITH SELF-HEALING MATERIAL PLUS CNTs, (LEFT) AFTER THIRD LIQUID NITROGEN, (RIGHT) AFTER THIRD OVEN.....	66
FIGURE 48: RF PATCH ANTENNA.....	67
FIGURE 49: ANECHOIC CHAMBER IN THE ECOLE POLYTECHNIQUE DE MONTREAL	69
FIGURE 50: MEASURED S-PARAMETERS FOR ANTENNA 1 BY VN.....	70
FIGURE 51: MEASURED S-PARAMETERS FOR ANTENNA 2 BY VNA.....	71
FIGURE 52: RADIATION PATTERN BY ANECHOIC CHAMBER FOR ANTENNA 1	73
FIGURE 53: RADIATION PATTERN FOR ANTENNA 1 WITH SELF-HEALING MATERIAL IN 0 DEGREE(LEFT) AND 90° DEGREE(RIGHT)	74
FIGURE 54: RADIATION PATTERN FOR ANTENNA 1 WITH SELF-HEALING MATERIAL AFTER THERMAL SHOCK	75
FIGURE 55: RADIATION PATTERN FOR ANTENNA 2 WITH ONLY RESIN.....	76
FIGURE 56: RADIATION PATTERN FOR CLEANED (FROM RESIN) ANTENNA 2	77
FIGURE 57: RADIATION PATTERN FOR ANTENNA 2 WITH SELF-HEALING MATERIAL PLUS CNT	78
FIGURE 58: RADIATION PATTERN FOR ANTENNA 2 WITH SELF-HEALING MATERIAL PLUS CNT AFTER THERMAL SHOCK.....	79
FIGURE 59: RADIATION PATTERN FOR ANTENNA 2 WITH SELF-HEALING MATERIAL WITH MICROCAPSULES CONTAINING CNT	80
FIGURE 60: RADIATION PATTERN FOR ANTENNA 2 WITH SELF-HEALING MATERIAL.....	81
FIGURE 61: MEASURED S-PARAMETERS FOR ANTENNA 1	85
FIGURE 62: MEASURED S-PARAMETERS WITH DIFFERENT MATERIALS FOR ANTENNA 2	86
FIGURE 63: RADIATION PATTERN BY ANECHOIC CHAMBER FOR ANTENNA 1 IN THE 0 DEGREE.....	88
FIGURE 64: ZOOMED OF PEAK AREA OF RADIATION PATTERN BY ANECHOIC CHAMBER FOR ANTENNA 1 IN THE 0 DEGREE.....	89
FIGURE 65: RADIATION PATTERN BY ANECHOIC CHAMBER FOR ANTENNA 1 IN THE 90 DEGREE.....	90
FIGURE 66: ZOOMED OF PEAK AREA OF RADIATION PATTERN BY ANECHOIC CHAMBER FOR ANTENNA 1 IN THE 90 DEGREE.....	91
FIGURE 67: RADIATION PATTERN BY ANECHOIC CHAMBER WITH DIFFERENT MATERIALS FOR ANTENNA 2 IN THE 0 DEGREE.....	92
FIGURE 68: ZOOMED OF PEAK AREA OF RADIATION PATTERN BY ANECHOIC CHAMBER WITH DIFFERENT MATERIALS FOR ANTENNA 2 IN THE 0 DEGREE.....	93
FIGURE 69: RADIATION PATTERN BY ANECHOIC CHAMBER WITH DIFFERENT MATERIALS FOR ANTENNA 2 IN THE 90 DEGREE.....	95

FIGURE 70: ZOOMED OF PEAK AREA OF RADIATION PATTERN BY ANECHOIC CHAMBER WITH DIFFERENT MATERIALS FOR ANTENNA 2 IN THE 90 DEGREE.....	96
FIGURE 71: ZOOMED SELECTED DAMAGED AREA OF ANTENNA IN 4X	98
FIGURE 72: MANY BROKEN MICROCAPSULES IN 10X	99
FIGURE 73: WELL DISTRIBUTED CATALYST IN THE RESIN BAS(10X)	100
FIGURE 74: MANY UNBROKEN MICROCAPSULES IN 10X	101
FIGURE 75: BROKEN MICROCAPSULES IN THE PATH OF CRACK (20X).....	102
FIGURE 76: MORE MAGNIFIED BROKEN MICROCAPSULES IN THE PATH OF CRACK (40X, 80X).....	103
FIGURE 77: ZOOMED SELECTED DAMAGED AREA OF ANTENNA WITH SELF-HEALING PLUS CNTs IN 4X.....	104
FIGURE 78: SURFACE OF DAMAGED ZONE IN 10X	105
FIGURE 79: SURFACE OF DAMAGED ZONE IN 20X	106
FIGURE 80: DIFFERENT FOCUS POINTS IN 20X.....	107
FIGURE 81: TWO POSITIONS IN ANECHOIC CHAMBER TEST.....	109
FIGURE 82: MONTHLY EFFECTIVE MASS OF OBJECTS IN EARTH ORBIT BY REGION (OFFICIALLY CATALOGUED BY THE U.S. SPACE SURVEILLANCE NETWORK. DIVIDED INTO ORBITAL ALTITUDE REGIONS, “EFFECTIVE MASS” ACCOUNTS FOR THE FRACTION OF ITS ORBIT THAT AN OBJECT MAY SPEND IN THE DIFFERENT REGIONS).....	122
FIGURE 83: (A) SCHEMATIC OF THE OPTICAL FIBER (B) LIGHT PHENOMENA IN THE FBG SENSOR. [AISSA 2014].....	124

LIST OF TABLES

TABLE 1: REASONING FOR SELF-HEALING ELECTRONICS [FREI 2013]	9
TABLE 2: SUMMARY OF TESTED COMPOSITIONS (DETA CONCENTRATION IN ALL CASES WAS 12.4 WT%), AND AVERAGE INITIAL ELECTRICAL RESISTANCE VALUES (R0)	21
TABLE 3: EXAMPLES OF THE SOFTWARE RF SELF-HEALING METHODS (FEEDBACK LOOP AND eDNA ARCHITECTURE)	40
TABLE 4: SUMMARY OF FEEDBACK LOOP SELF-HEALING BASED ON HUSIKAMP STUDY	45
TABLE 5: SELF-HEALING PREPARATION	51
TABLE 6: SELF-HEALING ELEMENTS	52
TABLE 7: EPON SPECIFICATIONS	53
TABLE 8: HARDENING AGENT SPECIFICATIONS	54
TABLE 9: SUMMARY OF RADIATION PATTERN INFORMATION FOR ANTENNA 1	82
TABLE 10: SUMMARY OF RADIATION PATTERN INFORMATION FOR ANTENNA 2	83
TABLE 11: MEASURED S-PARAMETERS BY VNA AND CALCULATED INFORMATION FOR ANTENNA 1	86
TABLE 12: MEASURED S-PARAMETERS BY VNA AND CALCULATED INFORMATION FOR ANTENNA 2	87
TABLE 13: RADIATION PATTERN DESCRIPTION FOR ANTENNA 1	90
TABLE 14: RADIATION PATTERN DESCRIPTION IN DIFFERENT DIRECTION FOR ANTENNA 1	92
TABLE 15: RADIATION PATTERN DESCRIPTION FOR ANTENNA 2	94
TABLE 16: RADIATION PATTERN DESCRIPTION IN DIFFERENT DIRECTION FOR ANTENNA 2	97
TABLE 17: COMPARISON OF IRRADIATION PROPERTIES IN THE FIRST POSITION OF ANECHOIC CHAMBER TEST (0° POSITION)	108
TABLE 18: COMPARISON OF IRRADIATION PROPERTIES IN THE SECOND POSITION OF ANECHOIC CHAMBER TEST (90° POSITION)	110
TABLE 19: COMPARISON OF IRRADIATION PROPERTIES IN THE FIRST POSITION OF ANECHOIC CHAMBER TEST (0° POSITION) AFTER THE THERMAL SHOCK	111

TABLE 20: COMPARISON OF IRRADIATION PROPERTIES IN THE FIRST POSITION OF ANECHOIC CHAMBER TEST (90° POSITION) AFTER THE THERMAL SHOCK..... 111

TABLE 21: REVIEW TABLE OF PAPERS ABOUT GRAPHENE SELF-HEALING 115

RÉSUMÉ

Certains systèmes de télécommunication (BAN) ont été proposés pour surveiller les accidents, l'emplacement des mines et l'existence de gaz toxiques dans les galeries des mines. Les BAN sont des systèmes de communication sans fil qui permettent la communication entre les dispositifs électroniques portables et implantés sur le corps humain. En raison de défaillances mécaniques et électriques des opérations de télécommunication dans l'environnement minier, ainsi que de la difficulté, du coût et du temps nécessaire à la réparation ; L'utilisation de matériel Self-Healing pour les systèmes de télécommunications devient importante. Le matériau Self-Healing peut les réparer avec ou sans influence externe. L'idée actuelle pour le travail de cette maîtrise à partir de mes recherches récentes sur les composites Self-Healing pour les applications spatiales. Pour éliminer les dommages possibles et également pour la surveillance de la santé des systèmes électroniques, une nouvelle génération de matériel intelligent pourrait être une alternative appropriée.

Il existe de nombreuses méthodes pour organiser des matériaux Self-Healing qui comprennent des microcapsules, des Ionomères, des Céramiques, etc., qui sont actuellement utilisés. Dans un premier temps, l'effet du matériau Self-Healing sur les propriétés électromagnétiques d'une fréquence radio(RF) est évalué. Deuxièmement, la capacité de Self-Healing pour protéger l'antenne est atteinte expérimentalement.

ABSTRACT

Some telecommunication systems (Body area networks, BANs) were proposed to monitor accidents, miner location and the existence of toxic gases in the mines galleries. BANs are wireless communication systems that enable communications between wearable and implanted electronic devices on the human body. Due to mechanical and electrical failures of telecommunications operations in the mines environment, and also to the difficulty, cost and time needed for repairing; using self-healing material for telecommunications systems become important. Self-healing material can repair them either with or without external influence.

The present idea for this Master's work came from my recent research on self-healing composites for space applications. For eliminating the possible damage and also for health monitoring of electronic systems, new generation of smart material could be a suitable technological alternative. There are numerous methods for organising self-healing materials that include microcapsules, ionomers, ceramics, etc., which are currently used. In the first step, the effect of self-healing material on the electromagnetic properties of a radio frequency antenna is evaluated.

Second, the capability of self-healing to protect the RF antenna is experimentally achieved.

LIST of ACRONYMS

Carbon nanotubes (CNT)	Process-Voltage-Temperature Environment (PVT-E)
Chemical vapour deposition (CVD)	Power amplifier's (PA)
Diethylenetriamine (DETA)	Power management unit (PMU)
Device under test (DUT)	Radio Frequency (RF)
Dichlorobenzene (DCB)	Radio Frequency Identification (RFID)
Electrically conductive epoxies (ECAs)	Self-healing wire (SHS)
EPA (ethyl phenyl acetate)	Scanning electron microscope (SEM)
Electrochemical impedance spectroscopy (EIS)	Single Walled Carbon Nanotube (SWNT)
GPS (Global positioning System)	System-On-Package (SOP)
Low noise amplifier (LNA).	System-In-Package (SIP)
Multivariate adaptive regression splines (MARS)	System-On-Chip (SOC)
Polymeric urea-formaldehyde (UF)	Transmission electron microscope (TEM)
Polymer poly (3-hexylthiophene-2, 5-diyl) (P3HT)	Ultraviolet (UV)
Polymeric Positive Temperature Coefficient (PPTC)	Vector network analyzer (VNA)
	Wireless body area network (WBAN)

INTRODUCTION

Recently, underground wireless communication has become one of the main research areas in the telecommunications field.

Underground environments like mines are challenging for wireless communication mainly because of the high path loss and also dynamic channel conditions. However, many research studies have focused on the implementation of wireless communication systems in underground environments to increase the safety of the workers. In fact, underground mines are subjected to many fatal events. In addition to the accident occurring in mines, other hazardous elements like toxic gases such as carbon monoxide (CO), flammable gases like methane (CH₄), fires, and insufficient oxygen concentration could be appeared. Thus, there is necessity to develop and improve advanced and updated technologies for underground safety of miners, especially to the sensing process and monitoring. [El Azhari 2015]

Using of wireless body area network (WBAN) is one way for the monitoring of miners in underground environment. WBAN is a kind of wearable sensors located on, off, or in the body. Also, they can benefit civilian parts such as healthcare, personal entertainment, sports training, and emergency services. For example, in hospitals, clinics, and public transportation system, there is a need to relay personalized data to and from individuals, in crowds, where the high frequency and highly directive beams from small millimeter-wave antennas will reduce interference between users and other communication system. Figure 1 show a scenario of soldier-to-soldier communications for a battlefield operation where co-located soldiers are wirelessly networked to allow

high-speed communications within a disarranged urban warfare environment [Figure 1].

Moreover, for each soldier, there is an advanced technology which improves situational awareness, lethality and survivability such as GPS (Global positioning System), helmet mounted display, RADAR bullet detector, etc. [Chahat 2014]

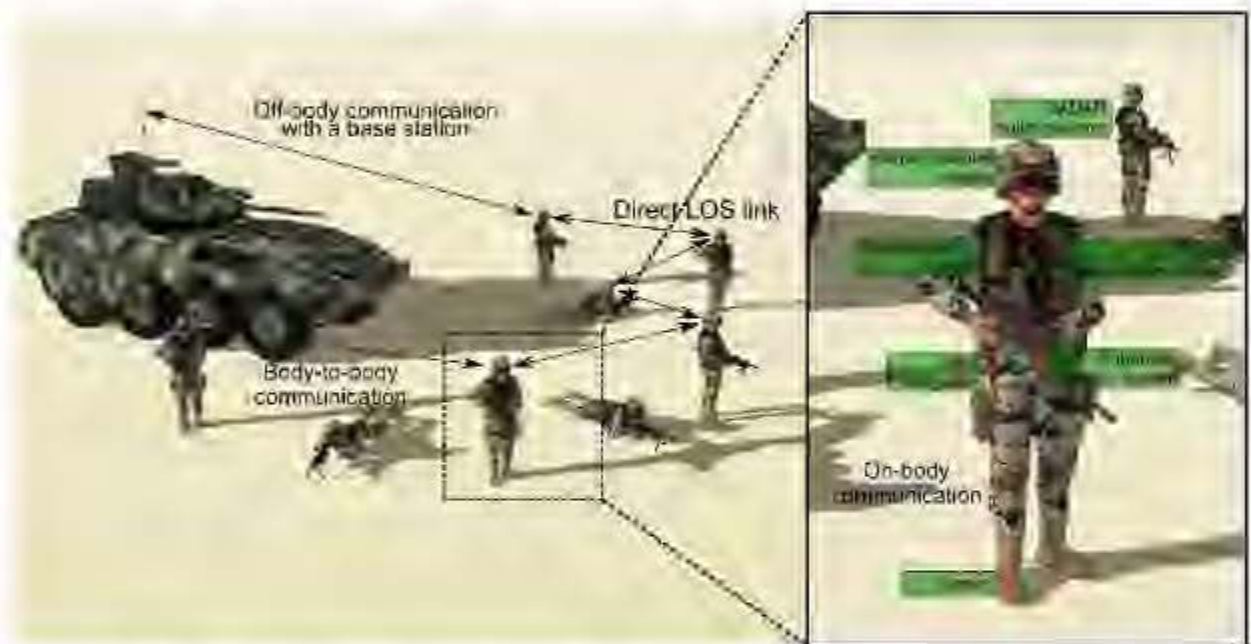


Figure 1: Soldier-to-soldier communications for covert battlefield operations. The black arrows represent some possible wireless links allowing data transfer from one soldier to another. [Chahat 2014]

When WBANs is placed close to the human body, wearable antennas need to be designed in such a way to operate in a robust manner to minimize the body effect on the antenna performance. In fact, Patch antennas are one of the best options for off-body communications. Because they are simple to design and low-cost structure in

addition, their radiation at broadside allows maximizing radiations at the opposite side of the human body while reducing radiation towards the body. [Chahat 2014]

Wearable antennas which have to be integrated with the transceiver need to be as compact as possible. They have to be efficient with minimal power absorption inside the human body that behaves as a highly lossy dispersive dielectric media. In addition, they have to be light weight and, in some particular cases, conformable to the human body shape. Recently, researchers are working on the influences of human body on irradiation properties of antenna. Chahat has demonstrated that the reflection coefficient is very slightly affected by the human body, and the radiation pattern remained stable at the opposite side of the human body as well [Figure 2]. These results have shown that micro strip patch antennas are only slightly sensitive to the human body proximity at 60 GHz. [Chahat 2014]

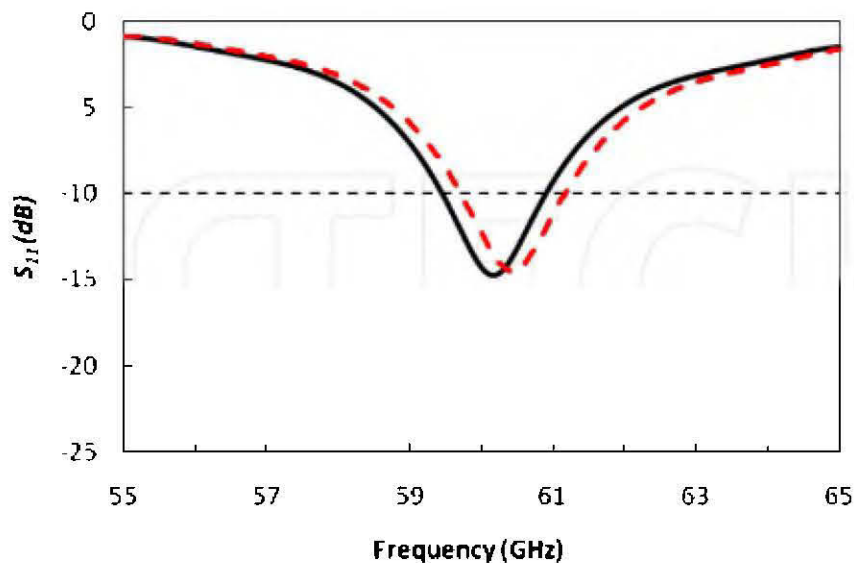


Figure 2: Simulated reflection coefficient of the microstrip patch antenna. — In free space. - - On the skin-equivalent phantom. [Chahat 2014]

WBAN used widely applications in biomedical therapy, healthcare and entertainment as well. Recently, researchers have focused more to developing its system technologies which have been conducted in several directions, such as on- or off-body wearable antenna design and optimization, WBAN body channel modeling, and analysis of the effects of human body on wireless performance. [Gao 2012]

Underground mining is one of the most dangerous and hazardous environment. However, for mining industry, safety is undoubtedly the most important factor. Figure 3 displays a schematic of WBAN technology in the mine gallery.



Figure 3: Representation of the BAN system in a mine environment. [El Azhari 2015]

There is permanently potential of accident events in the underground mines, and these accidents lead to fatal injuries, death of miners, and huge economic losses for the mining sector. For example, there were 300 coal mine explosions reported with 1037 deaths and over 600 injuries of coal mine workers between the period of 1981 and 2007 in the South African underground mines. There is a report in 1994, which presents rates for mining occupational injuries (per 10000 full-time workers) of 11:8 for disorder associated with repeated trauma, 6:6 for dust diseases of lungs, 3:0 for skin diseases and disorders, 1:8 for disorders due to physical agents, 1:2 for respiratory conditions due to toxic agents, and 1:4 for all other occupational diseases. To avoid the great loss lives of workers, safety is as mentioned earlier an important factor in the underground mining environment. The automated real-time remote monitoring system is established to monitor the gas levels in three different areas: entrance, stop, and stair regions in the underground mine. Remote monitoring refers to the access and monitoring of a device (in this case gas levels) from a distance location. [Raheem 2012]

Toxic gases are extremely prevalent in the underground mines and they cannot be easily detected by human senses. One of the solutions for monitoring of toxic gas in the mines is RF technology. Radio Frequency Identification (RFID) tag is used to monitor the toxic gas location and transmit signals to the connected sensors to read the gas levels at a specified time and store them via the gateway to the mine server.

This technology is suitable to observe even the critical level; and alerts the mine safety officers on the critical situations in the underground mine regions. Then the mine managers should have communicating with the miners about the actions to take. Figures 4 shows photography of miners working in an underground mine and, a mine with a cloud of gas suspended in the air, respectively. [Raheem 2012]



Figure 4: (left) Miners working in the underground mine (right) Mine Gas Suspension in air

On the other hand, failure occurs due to a disruption of electrical conductivity as a result of fracture or debonding, both within conductive pathways and at interconnects lead to limiting of lifetime of an electronic device. Moreover, mechanical affects the long-term performance of lithium-ion batteries in the integrated circuits. In the batteries, repetition of lithiation and delithiation of electrodes lead to particle fracture and electrical isolation, and finally resulting in a decrease in battery capacity. Actually, the lifetime of electronic materials by restoring of autonomous conductivity through the release of conductive materials from embedded capsules can be extended without requiring any disassembly and repair of damaged components. [Odom 2012]

Basically, when a material is under stress, the defects like cracks or voids developed during the life time and lead to its failure. Consequently, it's repairing necessities human intervention. Inspired by the nature and biology science, material scientists came out with a solution where the material can repair itself. Indeed, either in human or animal body, when an injury happened, body starts to repair itself by which is called "Self-Healing" or "Self-Repairing" process. The healing can be autonomic or externally assisted like heat, light or electrical signal. A considerable point is that when a defect like crack starts to propagate, the healing process will start instantly. The self-healing divided to two classes, extrinsic and intrinsic (Figures 5 and 6).

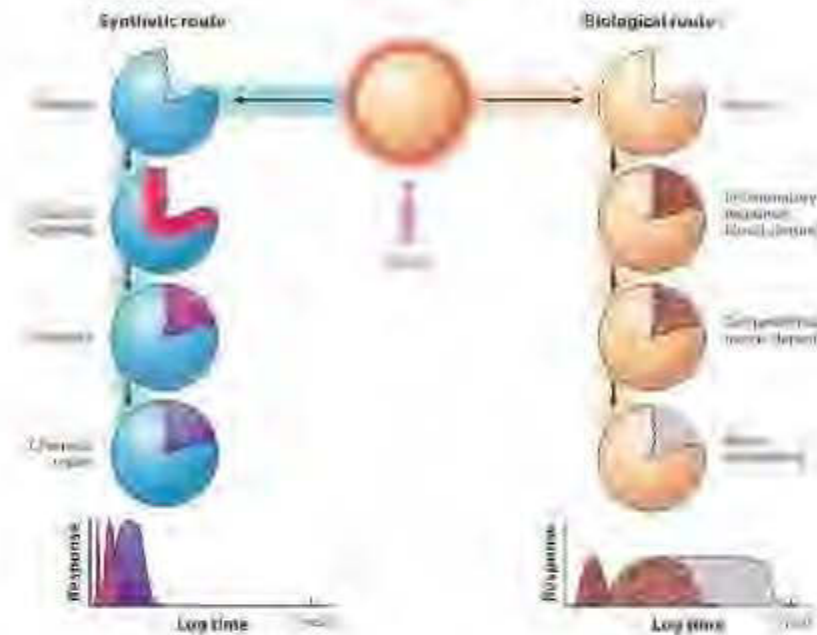


Figure 5: Synthetic materials and biological systems routes to healing [Blaiszik 2010]

In the extrinsic part, the healing agent is an extra material, embedded within the original structure, for example placed inside microcapsules. When a crack appears, it leads to break the microcapsule and filling the crack with healing agent.



Figure 6: Schematic examples self-healing; (a) Extrinsic, (b) Vascular, (c) Intrinsic [Blaiszik 2010]

In the case of intrinsic self-healing process, the materials (e.g. polymer) will repair themselves under certain condition, like mechanical stress or temperature. [Francesconi 2012]

The goal of study is the protection of RF antenna circuits and RF instruments in general that are operating in the underground mine environment, by self-healing material film. Also, to increase their lifetime, resin epoxy and microcapsules are added to mixture. Moreover, carbon nanotubes (CNTs) were added to improve the mechanical properties, and in some extend the electrical properties as well.

State of Art

To the best of our knowledge, this is first application of self-healing material for a RF antenna operating in underground mines.

CHAPTER 1

REVIEW

RF SELF-HEALING

Recently, self-healing for RF antennas and circuits attracted increasing attention. There is potential for circuits to have various defects and then lead to break. Especially for the miniaturized systems, for economical reasons and for saving the time, self-healing phenomena can be considered. Scientists are working on different kind of self-healing technologies for multiples purposes. Table 1 shows different kind of self-healing reasoning.

Table 1: Reasoning for self-healing electronics [Frei 2013]

Method	Reasoning
Data-restoring algorithm	Development of algorithm; laboratory hardware demonstration
DNA approach	Theoretical development awaiting hardware implementation
Healing nano-tubes	Nano-tube suspension in capsules demonstrated; healing of electronic material to be demonstrated
Healing capsules	Laboratory demonstrations showing healing of electronic material
Melting fuse	In active use for several years for production repair and in-use self-repair
Embryonic	Hardware/software at conceptual stage; some instances of hardware validated in a laboratory environment
Software and formal methods for redundancy	Technology concept formulated
Sharing of local/global diagnosis information	Technology concept formulated

1.1. *Liquid metal*

1.1.1. **Liquid metal in micro channels**

Dickey et al. used liquid metal as microcapsules to self-healing applications. [Dickey 2014]

Liquid metal (Eutectic Gallium Indium, EGaIn) was injected into the elastomeric micro channels. By cutting the wires with a blade, oxidation allows the liquid metal to remain in the channels and also stay flush when interfaces are made by cutting. With pushing the wire to back, initial shape physically, then polymer self-heals by hydrogen bonding and establish the electrical conductivity again.

Because mercury is a toxic element, another alternative like EGaIn which forms a thin oxide layer on its surface, was considered. Participation of oxide interferes with electrochemical measurements, alters the metal fluid dynamic behavior. Dickey has showed that solid oxide “skin” leads to new usages for liquid metals, including self-healing circuits, shape reconfigurable conductors, and stretchable antennas, wires, and interconnects.

Most of the metallic elements are solid at room temperature, but there is another group of metals which are liquid at room temperature, like Mercury, francium, caesium, gallium, and rubidium. Francium is radioactive, caesium and rubidium are both explosives, and mercury is toxic. So, only gallium and its alloys are proper for safe applications.

In the presence of oxygen, gallium surface makes a passivating oxide layer, which provides a physical, chemical, and electrical barrier which can hinder the metal to be in direct contact with the environment.

Self-healing wires made by injecting EGaIn into microchannels which is composed of self-healing polymer. Another possible way to make self-healing wires is dispersing liquid metal droplets in polymer which is then placed on the conductive traces of gold. After the cutting by blade, the gold breaks, and liquid metal escape from the polymer matrix and contacts the resulting gap. Hence, alloys with the gold material could help to regain electrical conductivity along the gold pathway. [Dickey 2014]

1.1.2. Liquid Metal in Wire

Palleau has fabricated a wire of liquid metal which was injected into microchannels composed of self-healing polymer [Figure 7]. Cutting by razor leads to oxidation the surface of the liquid metal, and forms a thin oxide film. The film prevents the metal from escaping from the microchannels and also makes it flush with the interface of the channel. [Palleau 2013]

This film also helps the metallic element to adhere to the polymer. EGaIn was used as liquid metal because of its conductive pathways with high electrical conductivity that benefits from the low melting point (15.7°C) and low viscosity, showing a promising way to create both mechanically and electrically self-healing composite. Metal is able to be shaped via its injection in microchannels, which could be useful for antennas, interconnects, soft electronics, reconfigurable optics, and micro fluidic devices.

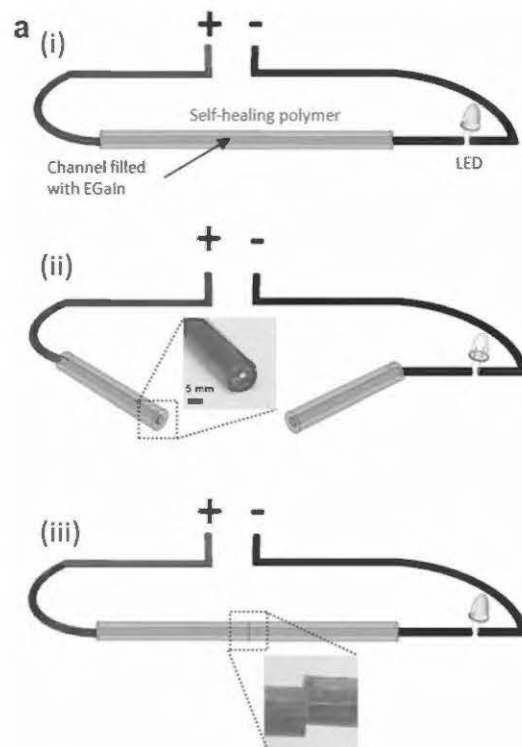


Figure 7: (i) Illustration of the disconnection and reconnection of an electronic circuit with using a self-healing wire (SHS) (ii) Disconnected circuit (iii) EGaIn channel to be aligned for restore electrical conductivity.

Self-healing wires can increase the electronic components lifetime and are also important for the field of stretchable electronics in which components could undergo significant deformation.

The self-healing wires offer a new solution to self-rewire electronic circuits and are a potential way for reconfiguring micro fluidic channels into more complex shapes

by a razor. On the other hand, coverage of liquid metal as microencapsulated droplets in the polymeric material could lead to a damaged film of gold to self-heal electrically. The mixture of self-healing polymer (Reverlink®) structured with microchannels filled with liquid metal (EGaIn) is a new method to the manufacturing of shape-reconfigurable and electrical self-healing stretchable circuits.

After cutting by razor, with joining the two parts of the self-healing wire, the electrical conductivity restores instantly. Alignment of two wires by hand depends on hand-eye coordination. Palleau has succeeded to align the wires with a diameter of 100 μm . After alignment, the liquid metal (EGaIn) components connect together forming a conductive wire again. [Palleau 2013]

1.1.3. Liquid Metal in Capsules

Dadi et al. have used liquid metal as healing capsules having diameter of 10 μm . They were coated along the external part of the component with self-healing material. By initiating a crack, the microcapsules are broken and then release the liquid metal into the crack. After filling the crack, electrical flow is established again. [Dadi 2012] Figure 8 and 9 showing a schematic of this self-healing method as capsules.

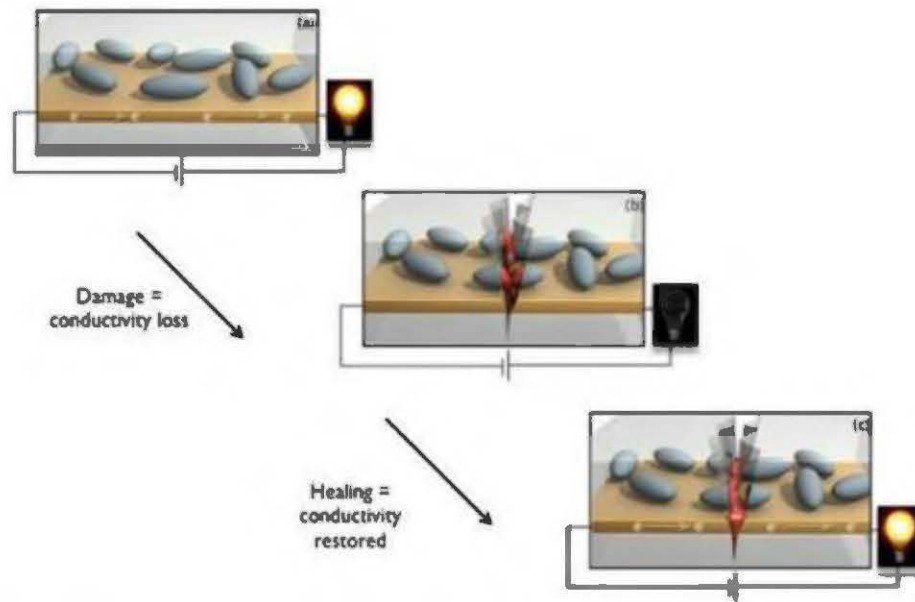


Figure 8: Illustration schematic of self-healing circuit process.

In another work, Blaiszik has proposed an electrical self-healing method to restore electrical conductivity in a broken circuit automatically.

Release and transfer of liquid metal microcapsules to the area of damage are the bases to this self-healing method. Because EGaIn alloy has relatively high conductivity of 3.40×10^4 S/cm and a melting point around 16°C , proposed as the healing agent. Also polymeric urea-formaldehyde (UF) was used as shell wall for encapsulation of EGaIn. [Blaiszik 2011]

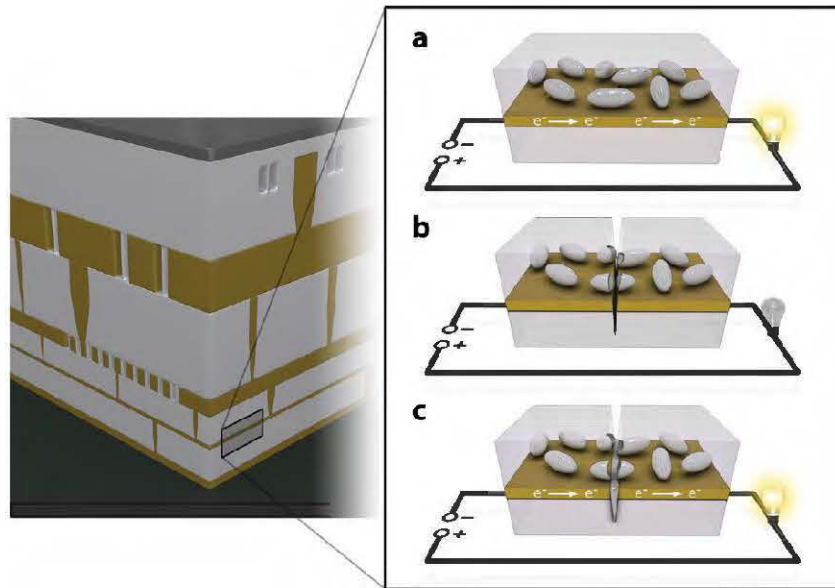


Figure 9: A schematic example of autonomous conductivity restoration concept in a microelectronic device. a) Liquid metal microcapsules distributed in a dielectric material to self-healing. b) A crack leads to breaks the microcapsules. c) The liquid metal flows from the microcapsules to the damage zone, and then restoring a conductive pathway.

In fact, electrical conductivity was recovered with low quantity of smaller EGeIn microcapsules specifically located at the damage site. With decreasing the microcapsule size or increasing of their volume fraction, probability of intersecting and rupturing a capsule with the propagating crack will increase as well. After the propagation of the crack and the rupture a microcapsule, the liquid metal is released and makes an electrically conductive pathway where the electrical conduction

restoration happens with high efficiency. With considering the size scales of the circuit damage, optimal conductance restoration may need a variety of capsule sizes. Self-healing procedure and some SEM images of system shown in the figure 10.

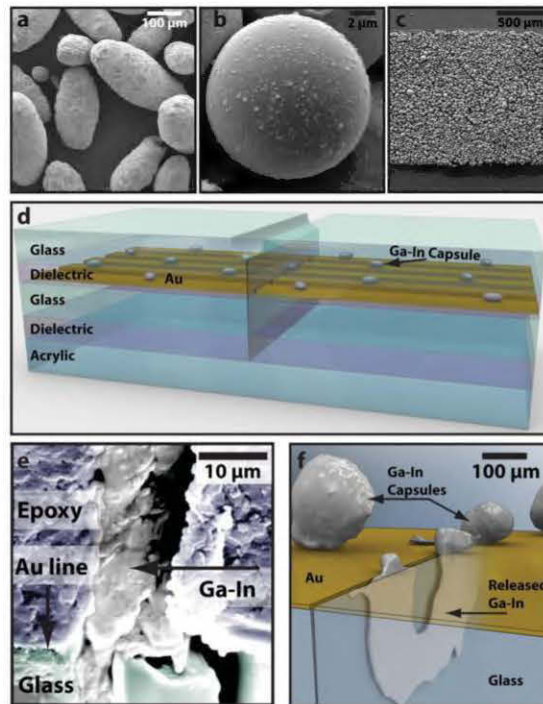


Figure 10: Self-healing circuit components, multilayer test specimen, and evidence of triggered release. SEM images of: a) ca. 200 μ m diameter Ga-In-filled UF microcapsules; b) ca. 10 μ m diameter Ga-In UF microcapsule; and c) ca. 10 μ m diameter capsules patterned on an Au line. d) Schematic image of a multilayer test specimen consisting of a glass substrate with a 100 nm thick Au line pattern, epoxy dielectric with dispersed Ga-In microcapsules, notched glass top layer, and acrylic bottom layer. Crack damage initiates at the notch root and propagates through the specimen before arresting and debonding at the acrylic interface. e) Cross-sectional SEM image showing the location of the damaged area and subsequent liquid metal release (false color). f) Micro-CT data, with schematic superimposed, showing microcapsules and liquid metal that has been released into the crack plane of a healed specimen. [Blaiszik 2011]

Blaiszik et al. have also demonstrated successful autonomous recovery of electrical conductivity in mechanically damaged circuit. This kind of Self-healing method of circuits will increase the lifetime and reliability of devices in mechanical environments, and also it is enabling new applications in microelectronics, advanced batteries, and electrical systems. [Blaiszik 2011]

1.1.4. Liquid Metal and Single Walled Carbon Nanotube (SWNT)

Aissa et al. have designed by the UV assisted direct-writing technology a fluid patch antenna which is operating at the S-band frequency domain, and based on an electrically conductive nanocomposite, that is composed of EGaIn and Single Walled Carbon Nanotube (SWNT) material. [Aissa 2013]

The fabricated fluidic antennas have shown an increase both in their electrical conductivity and reflection coefficient as a function of the integrated quantity of SWNT (results were supported by simulations works). As mentioned, Aissa et al. have first utilized a UV-assisted direct-writing technology to design the patch antenna onto a PDMS substrate, followed by injecting and encapsulating the conductive EGaIn/SWNT nanocomposition. [figure 11]

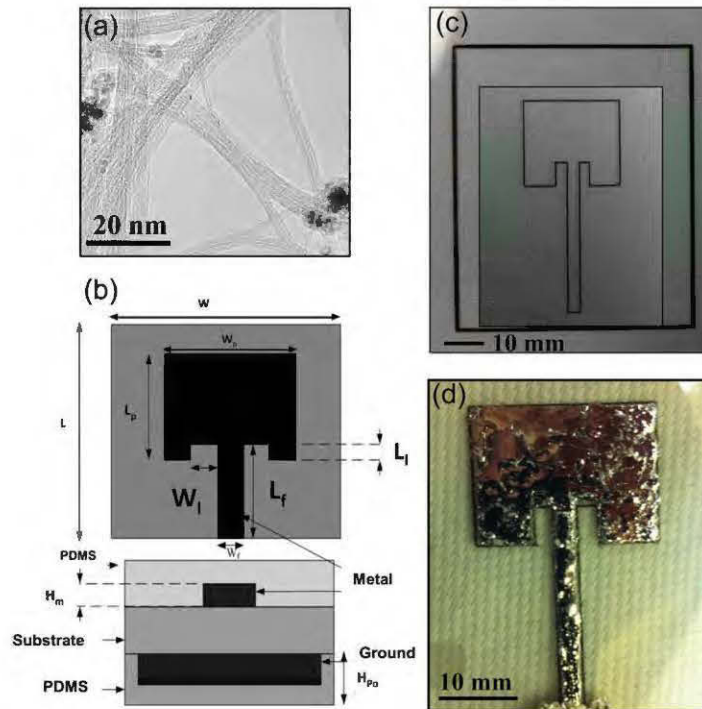


Figure 11: (a) TEM images of SWNTs. (b) dimensions of the micro strip patch antenna (c) top-view image of the epoxy/SWNT-based filaments deposited by UV-assisted direct writing technology on the substrate. (d) top-view image of the patch antenna prototype.

On the other hand, they have demonstrated that SWNTs have a direct effect on the long-term stability of the antennas by mechanically bending them more than 12 months.

1.2. Carbon Nano Tube (CNT)

1.2.1. CNT as a Microcapsule

Baileya et al. have used the CNT as microcapsule with epoxy for self-healing purpose. Having an EPA (healing solvent: ethyl phenyl acetate): CNT core in microcapsules, contribute to electrical conductivity and mechanical properties were restored to be 64 % and 81 %, respectively. Figure 12 shows when a crack occurred, the microcapsules are broken and fill the crack path by the healing solvent. Using the electrically conductive epoxies (ECAs) for external coatings will contribute to electrically self-healing. [Baileya 2015]

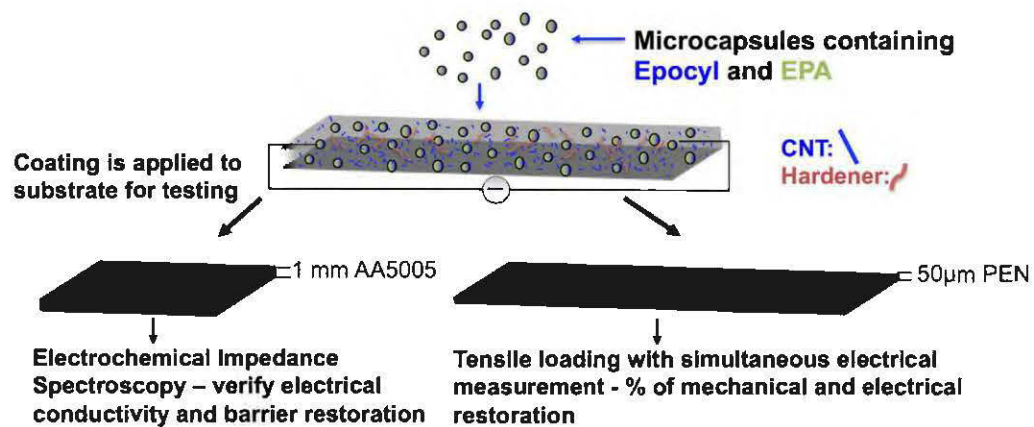


Figure 12: Sketch of the studied samples and evaluation tests.

However, the main element that ensures an electrically conductive self-healing is the carbon nanotube material. Because of their excellent electrical conductivity and also high aspect ratio, CNT are an excellent option for regenerating the electrical conductivity. Using the CNTs may increase brittleness and then cracking. They made two self-healing coatings contained microcapsules filled with EPA and either epoxy with CNTs or without CNTs [Table 2]. Therefore, two different methods were used for self-healing evaluation. First, electrochemical impedance spectroscopy (EIS) which is a non-destructive method and, second, test method was a novel in situ electro-tensile test. In fact, EIS was utilized to assess the potential of the CNT and without-CNT microcapsules to bridge and restore cracks.

Table 2: Summary of tested compositions (DETA concentration in all cases was 12.4 wt%), and average initial electrical resistance values (R₀).

Purpose	Microcapsule core composition	Coating composition	Average initial resistance (R ₀) [MΩ]
Mechanical and electrical healing	97.5 wt% EPA:2.5 wt% ECNT	ECNT + Microcapsules: diethylenetriamine(DETA)	0.86±0.12
Mechanical healing	97.5 wt% EPA:2.5 wt% EPON	ECNT + Microcapsules: diethylenetriamine(DETA)	1.30±0.22
Control (Electrochemical Impedance spectroscopy –EIS- and in situ electro tensile loading)–effect of microcapsules on coating properties	100% hexylacetate (HA)	ECNT + Microcapsules: diethylenetriamine(DETA)	1.55±0.26
Control (EIS and in situ electro tensile loading)	No microcapsules	ECNT: diethylenetriamine(DETA)	0.45±0.23
Control (EIS)–effect of conductive capsule solution on	No microcapsules impedance	EPON: diethylenetriamine(DETA)	-

They used 97.5 wt. % EPA: 2.5 wt. % ECNT for Microcapsule core composition and ECNT + Microcapsules: DETA for coating composition and for mechanical and electrical healing.

Figure 13 shows a cross-section view of the microcapsule, which it's inside smooth and rough outside. The detailed view of the internal surface of microcapsule which is in contact with the healing solvent (EPA: ECNT) is available in Fig. 13b. This surface is capable to decrease mass transport of the material through the microcapsule shell. Then, it leads to relatively better containing healing agent in the microcapsule until damage occurs. In contrast, Fig. 13c shows outside surface of the microcapsule which is rough due to agglomeration of UF Nano particles.

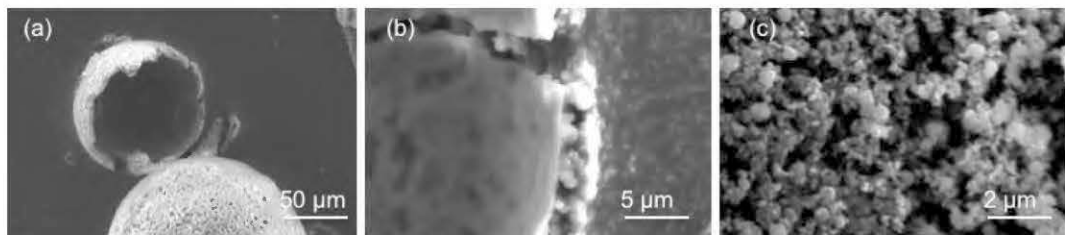


Figure 13: (a) broken capsule (b) inside of microcapsule and (c) outside of microcapsule taken by SEM microscope.

Figures 14a and 14b show the optical micrographs of original and healed cracks of a sample of pure ECNT deposited on substratum where the crack is still present after 24 hours. Also, there are similar results for HA capsules were added into the film. Crack width values are shown in the micrographs.

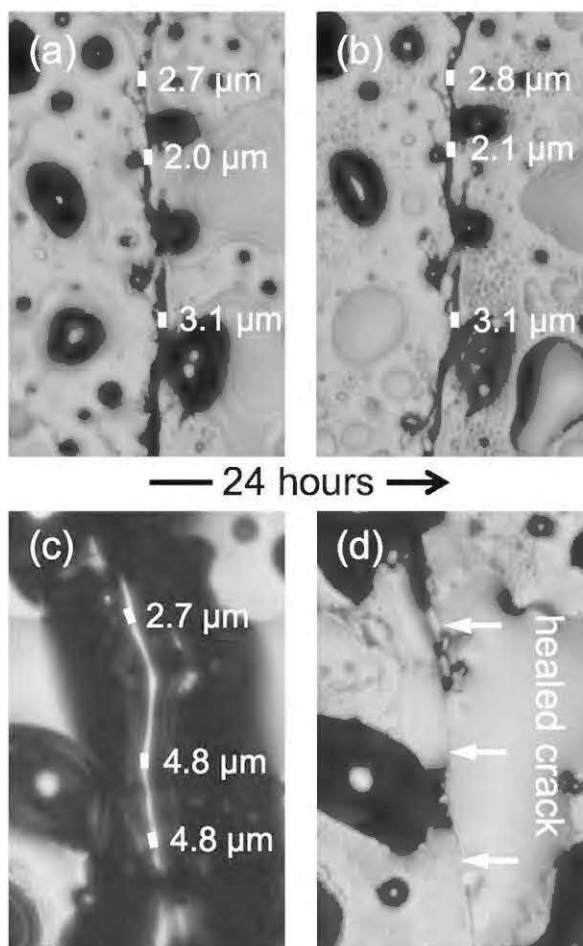


Figure 14: (a) micrographs of a crack in ECNT coating without microcapsules (b) after 24 h (c) in ECNT coating with microcapsules containing EPA:ECNT after cracking (d) after 24 h.

EIS testing demonstrated that coatings containing microcapsules with an EPA: ECNT or EPA: EPON core lead to improved barrier restoration, and also when microcapsules with an EPA: ECNT core were incorporated into the coating, electrical conductivity and mechanical properties were restored to 64 % and 81 % respectively.

1.2.1. SWNT and Graphene as Microcapsule

Odom used microcapsules including suspensions of polymer-stabilized carbon nanotubes and/or graphene flakes for the conductivity self-healing in fractured gold lines. Advantage of using the CNT is bridging a gap in gold line with preferential orientation because of electric field migration.

When the sample broken, a crack formed in the gold line, then conductivity will be lost. Once the carbon nanotubes and/or graphene suspensions from capsule cores released in the same time, conductivity restored instantly. Electronic materials lifetime can be extended with conductivity self-healing via the releasing of conductive materials from embedded capsules, without repairing of damaged components. Autonomic restoration of conductivity of fractured patterned gold lines by damage triggered release of polymer-stabilized carbon nanotube and/or graphene suspensions is shown in Figure 15.

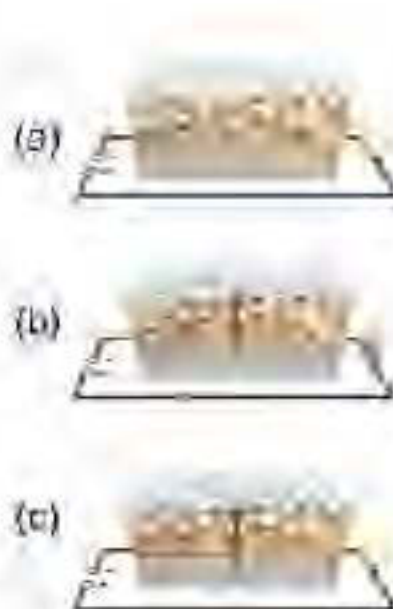


Figure 15: (a) before any damage; (b) after damage, fracture of gold line and then release of SWCNTs and/or graphene from microcapsules; and (c) after restoration, where the conductive particles have bridged the gap on the gold line.

Additionally, Microcapsules can decrease the potential of short circuiting of electronic circuit components when electric field migration navigates the carbon nanomaterials preferentially to the fracture zones within each gold line, as opposed to a random crystallization of charge transfer salt or capillary-driven delivery of liquid metal. (See Figure 16)

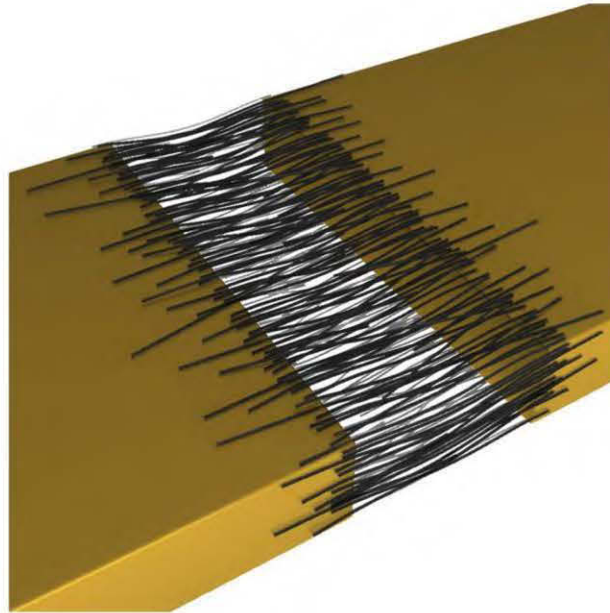


Figure 16: bridging of carbon nanotubes in a gap of gold line with preferential orientation due to electric field migration.

This method doesn't need any external intervention or reliance on back-up circuits. These microcapsules compare to the transfer salts and liquid metal eutectics, are more compatible in environments like lithium-ion batteries where anodes are often made with graphitic materials. Also, microcapsules reduce the potential for short circuit. Odom et al. have used the conducting polymer poly (3-hexylthiophene-2, 5-diyl) (P3HT) as an additive to gain stable CNT and/or graphene suspensions in the solvent o-dichlorobenzene (DCB) to improve the efficient release and assembly of carbon nanomaterials from broken microcapsule.

Deposition of the solution on gold lines with pre-fabricated 5 μm gaps, helped to analyze the electrical behaviour of these suspensions. [Figure 17]

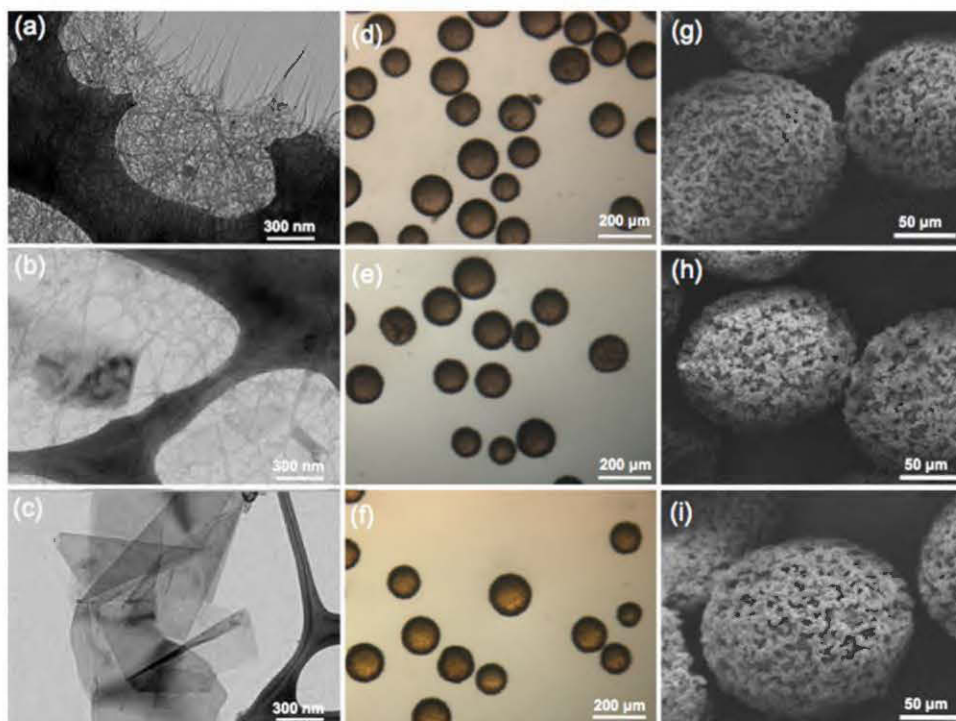


Figure 17: TEM images of dried suspension on carbon grids (a)–(c), optical microscopy images of microcapsules suspended in mineral oil (d)–(f), and SEM images of microcapsules coated with Au/Pd

By applying a 5V potential across the gap, the carbon nanotubes moved to the gap in the gold line preferentially with the direction of the applied electrical field.

They fabricated microcapsules including suspensions of graphene and a combination of SWNTs and graphene. In fact, both suspensions of SWNT and graphene are being able to efficient self-healing. Averagely, complete conductivity self-healing happened in 25% of samples and also partial self-healing occurred in 50% of samples, and only 25% with no healing response.

1.3. Resettable Fuse

This kind of fuses utilize a thermoplastic conductive element known as a Polymeric Positive Temperature Coefficient (PPTC) thermistor that impedes the circuit during an over current condition (by increasing device resistance). The PPTC thermistor is self-resetting in that when current is removed, the device will cool and revert to low resistance. These devices are often used in aerospace/nuclear applications where replacement is difficult, or on a computer motherboard so that a shorted mouse or keyboard does not cause motherboard damage. [Kishore 2014]

1.4. Light Self-Healing

Kang et al. have proposed a light-powered self-healing electrical conductor for wearable devices (e.g., the electronic skin, sensitive to mechanical motion). Compare to other self-healing methods, his method with helping the green light radiation can heal the damaged electrical conductor much faster (less than 3 min). [Kang 2014]

Figure 18 shows how cracks be healed by light. They have used an epoxy based amorphous polymer, poly(disperse orange) 3 (PDO3) as azobenzene material.

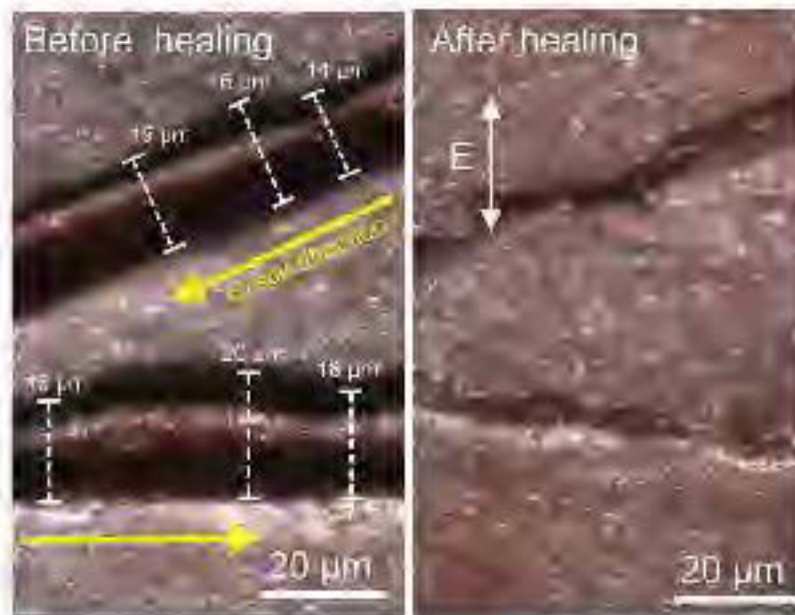


Figure 18: Light-powered healing of a crack

Kang et al. have also used a photochromic soft material or photofluidic diffusible polymeric backing layer (azobenzene material), and this material was found to be able to be directionally diffused along the light polarization.

Also, regardless of crack propagation direction, light incident angles, and the number of cracks with respect to light polarization, this material diffusion directionality enables an efficient healing method. [Figure 19]

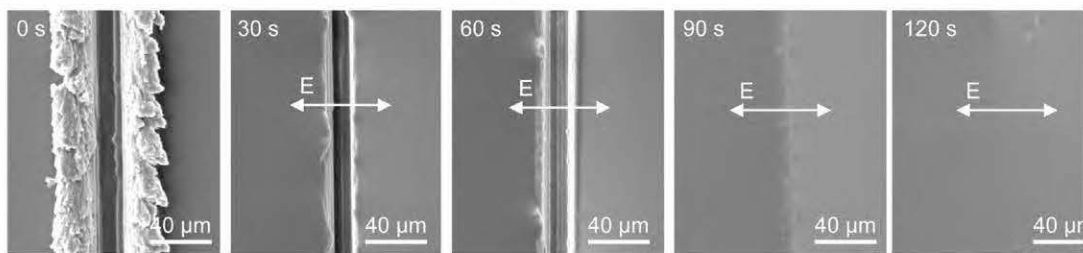


Figure 19: Various stages of light-powered healing of linearly cracked PDO 3 films by SEM microscope.

By light healing method, silver nanowires can be deposited as conducting material on the top layer of the photochromic soft material.

Also, healing method can be repeated for 3 times. Directional photofluidic diffusion of AgNW (Silver nanowire) mesh/azobenzene material, distributes the basic concept of light-powered healing for remote restoration of multiple irregular cracks on

curvilinear substrate (for wearable devices applications). Light-powered healing needs improvement in the repeatability and this is crucial for realistic wearable electronic devices applications.

1.5. Software Self-Healing

1.5.1. Self-Healing by Oscillation principles

During the last decade, System-On-Chip (SOC) method has been performed to integrate digital, analog and RF circuits on a single chip to miniaturize wireless communication systems. In addition, SOC method is a promising solution for the miniaturization of RF systems, but it is restricted by Low-Q passives and substrate coupling. Other approaches for miniaturization are System-On-Package (SOP) and System-In-Package (SIP) approaches which have shown potential to better integration of digital, analog and RF performances. Even though, these related technological advances have been reduced many problems associated with manufacturing complex integrated RF systems.

The manufacturing cost of RF systems is still a major concern for industry because of high test cost and yield issues of RF circuits.

Reducing the transistors size will lead to:

- Lower power consumption
- Higher integration of systems on chip

In addition, the power amplifiers will suffer from lower supply voltages and Process-Voltage-Temperature and Environment (PVT-E). A self-healing method can help to repair any differences in the RF-power amplifier caused by PVT-E variations and decrease overhead on the RF-power amplifier system. By performing self-healing, the efficiency of the RF-power amplifier can be increased.

There are several methods for acquire the data required for RF self-healing:

- A common method is based on the self-resonance method. In this case, the RF circuit is brought into oscillation and its output signal is investigated. The resulting waveform can then be used as input parameters for the self-healing algorithm.
- Another method is to determine the amplitude of relevant signals and uses these in the self-healing feedback loops. Most amplitude detectors consist of simple circuits and use little space and power. One of the main disadvantages of this method is that the phase and shape of the signal is disappearing, and then smart measurement points and relations should be used to measure the relevant parameters.

It is possible to gain detailed information on the power amplifier's (PA) performance conditions by utilizing expensive measurement equipment. The acquired information from these measurements can then be used to improve the sub-optimum performance of the PA which would lead to decreased design margins, but this is a time consuming and costly. Also the information of input and output signal of the RF-power amplifier is limited.

As a solution to this problem is the development and use of self-healing method.

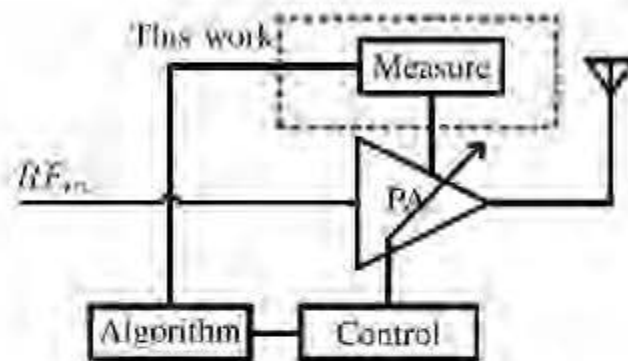


Figure 20: Self-healing system

Power amplifiers suffer from PVT-E (Process-Voltage-Temperature and Environment) variations which are normally slow processes, but have high impact on the amplifier behavior and performance. These variations caused by PVT-E can be removed by a self-healing system [Figure 20]

In a self-healing system, amplifier properties are adjusted to compensate any PVT-E differences that occurred during production or operation, which is achieved by assuming that the amplifier is different from the ideal one.

Recently, miniaturizing of the RF systems can be done by System-On-Chip (SOC), System-On-Package (SOP) and System-In-Package (SIP) approaches. In fact, SOC integrate the digital, analog, and RF circuits to a uniform chip. Although all of these

methods can reduce the manufacturing problems but high test cost and yield issue of RF circuits are the main concern of industries.

Abhilash proposed a framework for this problem. This framework included low cost testing methodology for RF amplifier [Figure 21]. It uses low frequency signal and try to integrate RF substrates to an embedded RF passive filter. Oscillation principle used to enable testing of RF circuits without any external influences. Second part of this framework is increasing the RF circuit yield for parametric defect which included a diagnosis algorithm for identify damaged circuits. [Abhilash 2011]

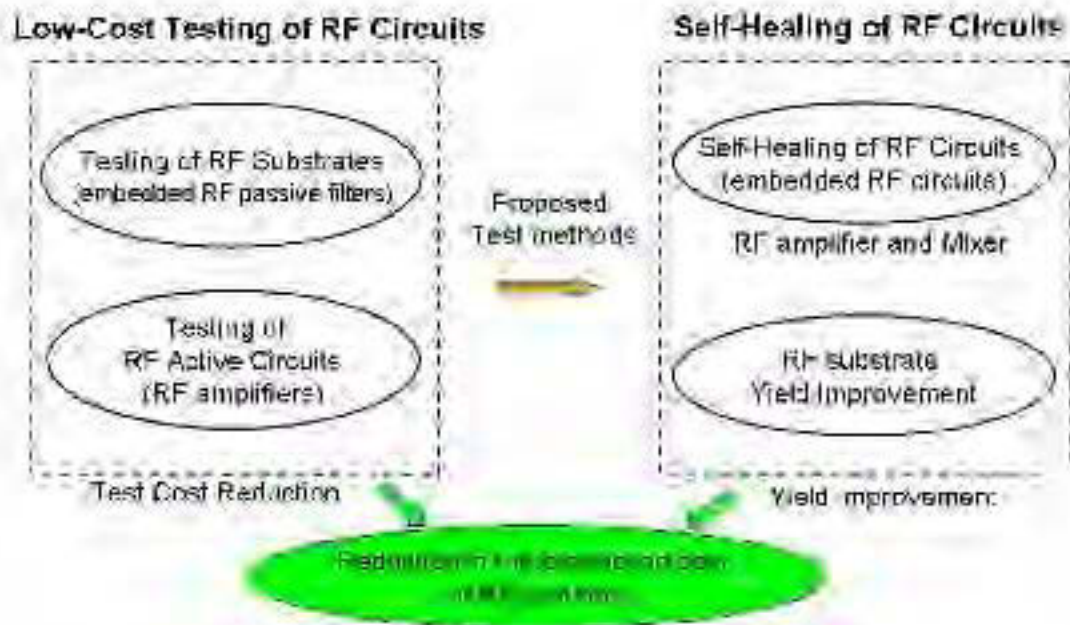


Figure 21: The self-healing framework for RF circuits.

Self-healing method is integrating the measurement circuits in the same chip and uses the determined RF-signals in a feedback loop to correct the performance of the RF-circuit. The final goal of self-healing is to increase the post manufacturing yield against parametric defects. Abilash et al. have used a methodology based on oscillation principle in device under test (DUT) which itself generate the test signature. The stimulus uses to assess the impact of process variations on the DUT operation. In addition, compensation for loss of DUT performance due to variations comes out by adjusting the calibration/tuning knobs. In the self-healing mode, external feedback enables across the low noise amplifier (LNA). [Figure 22]

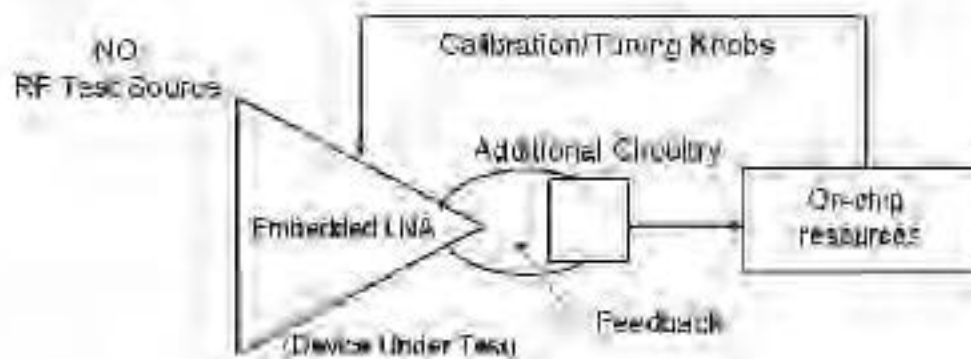


Figure 22: Self-Healing architecture in the RF amplifier

Thus, LNA oscillate and generate a sinusoidal signal for testing and calibration. In fact, the feedback network is a phase shifter which can be accomplished on-chip or off-chip on the circuits. Actually, phase shifter is connected to input and output ports of LNA by RF switches to complete the feedback loop. Figure 23 shows the algorithm of self-healing.

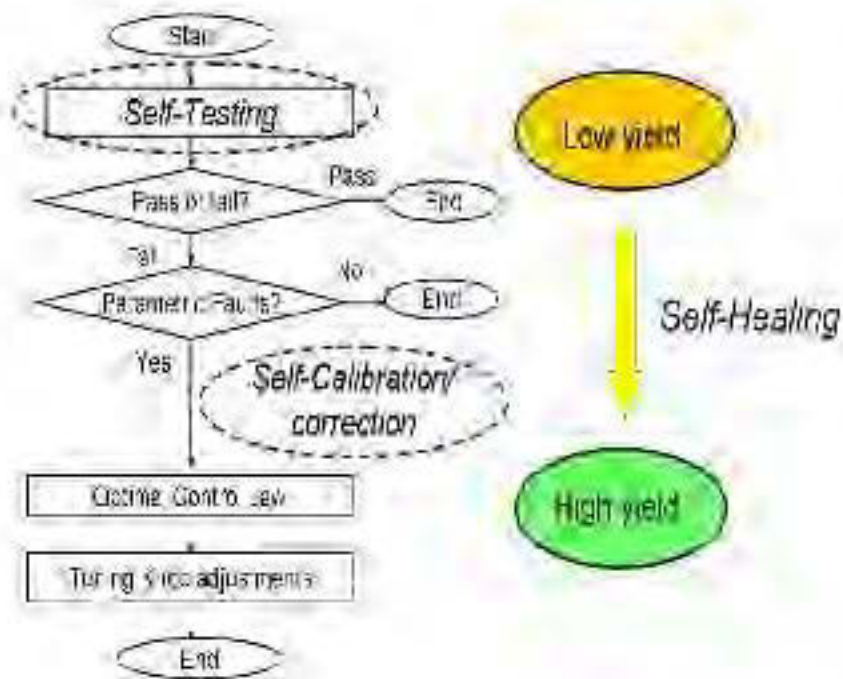


Figure 23: Self-healing algorithm

In the presence of variations, self-healing of the LNA attained by adjusting the LNA tuning knobs from on-chip power management unit(PMU) with is using the essential necessities for wireless communication, like on-chip RF mixer, ADC, low pass filter, image reject filter and DCP.

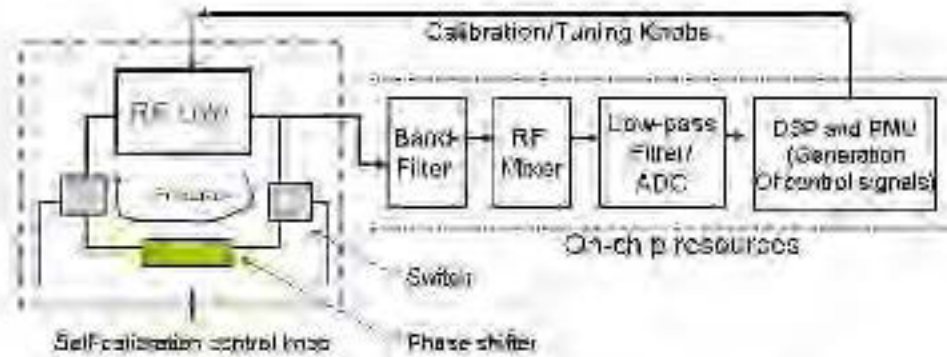


Figure 24: Self-healing LNA architecture

In the current self-healing methodology, failure detection performed by predictive oscillation-based testing which is developed for on-chip testing of RF amplifier. Therefore, detection of faults will be possible, because of existence mapping between test signature and LNA specifications. Abilash et al. have proposed for first time, yield improvement utilizing oscillation principles. In addition, self-healing RF circuits can be controlled by calibration/ tuning knobs. Also, the design of knobs must be to that DUT specifications be independent of other specifications, this allows all specifications to be controlled indecently to yield recovery. [Figure 24]

Actually, calibration/correction procedure can be one-time or iterative. Also, the iterative procedure leads to high yield recovery but time consuming. Abilash for demonstrate the self-healing; simulate two LNAs, SiGe HBT LNA and CMOS RF LNA. For the first one, two tuning knobs used for change the bias current (I_{bias}) and voltage to change capacitance in the LC tank. [Figure 25]

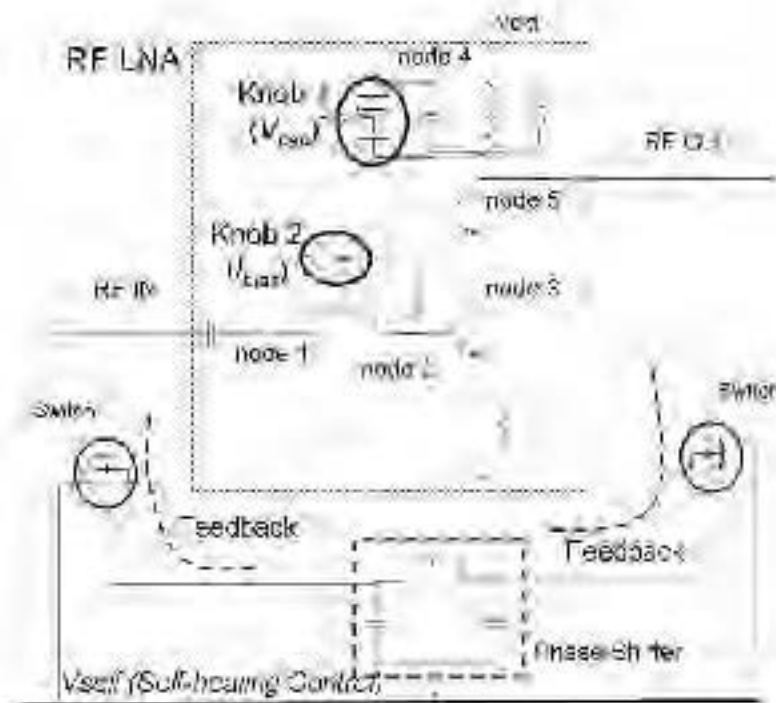


Figure 25: Self-healing SiGe RF LNA

Also, to determine the LNA samples for self-calibration/correction, a nonlinear prediction model developed from Monte Carlo simulation method by multivariate adaptive regression splines (MARS). Monte Carlo simulation conducted with 300 LNAs. This prediction model applied to predict small signal transmission gain and 1-dB compression point (P1dB, dBm). The prediction model performed to find specifications and predicted gain.

The Abilash methodology has been showed on an embedded RF LNA in the RF front-end systems. It has been shown through simulations that a significant yield improvement of the RF amplifier can be obtained by this methodology. Both a board-

level prototype and a chip-level prototype of the self-healing LNA have been demonstrated. Also the performed experiments results were encouraging and it can be concluded that the methodology can be considered as a new solution for the development of future self-healing RF systems. Also, Abilash demonstrated for the first time that RF amplifiers can be tested for their specifications using oscillation principles and yield improvement using oscillations principles for active RF circuits. As shown in the table 8, the novel achievements of Abilash thesis are summarized. Table 3 exhibits the example of the software RF self-healing methods.

Table 3: Examples of the software RF self-healing methods (feedback loop and eDNA architecture).

SH method	Innovation and Important points	Method
eDNA Architecture	eDNA architecture and the eDNA program	In fact, eDNA architecture included a distributed array of multiple homogenous processing units called electronic cells and The duty is to implement the eDNA program, which is specified by the programmer. Also eCell contain a microprocessor and a 32 bit ALU which is configured by the microprocessor to do a function described by the gene. The DNA is a program written for the eCell microprocessor, which performs self-organizing and self-healing of the eDNA architecture. All eCells contain a copy of this program.[Boesen 2011]
Feedback loop	Yield improvement utilizing oscillation principles. Self-healing RF circuits can be controlled by calibration/ tuning knobs.	The proposed methodology is based on oscillation principles in which the Device-Under-Test (DUT) itself generates the output test signature with the help of additional circuitry. In the proposed methodology, the self-generated test signature from the DUT is analyzed by using on-chip resources for testing the DUT and controlling its calibration knobs to compensate for multi-parameter variations in the DUT's manufacturing process. This methodology does not require the use of external test stimulus for performing self-healing because the stimulus is self-generated by the RF amplifier, with the help of additional circuitry and by using oscillation principles (feedback loop).[Abhilash 2011]
Feedback loop	A low power signal waveform sampling system for self-healing RF-power amplifiers is designed and simulated.	Integrating the measurement circuits in the same chip and use the measured RF-signals in a feedback loop to correct the performance of the RF-circuit.[Huiskamp 2015]

1.5.2. Feedback Loop

Husikamp et al. have proposed a self-healing methodology that integrates the measurement circuits in the same chip with using measured RF signal in feedback loop. [Husikamp 2015]

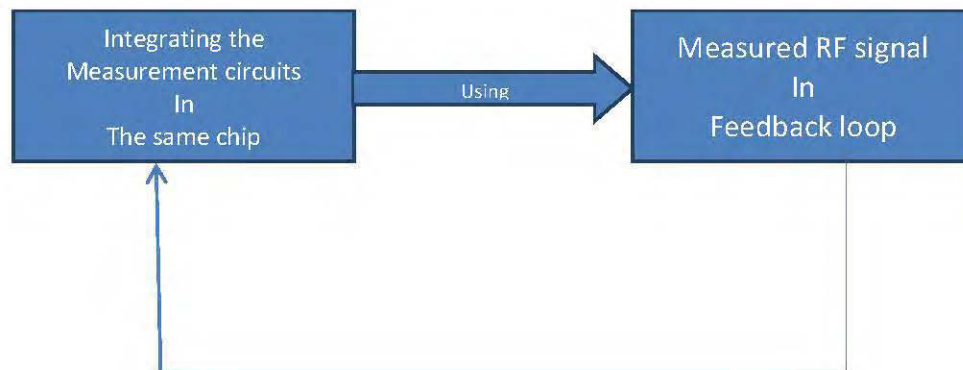


Figure 26: Self-Healing methodology.

In this system, if assuming that the amplifier is different from the ideal amplifier, its duty is compensating for any PVT-E changes that occurred during production or operation. In addition, controllable parameters like biasing voltages, bias currents and

matching networks must be changeable to compensate to PVT-E influences. [Figure 26 & 27]

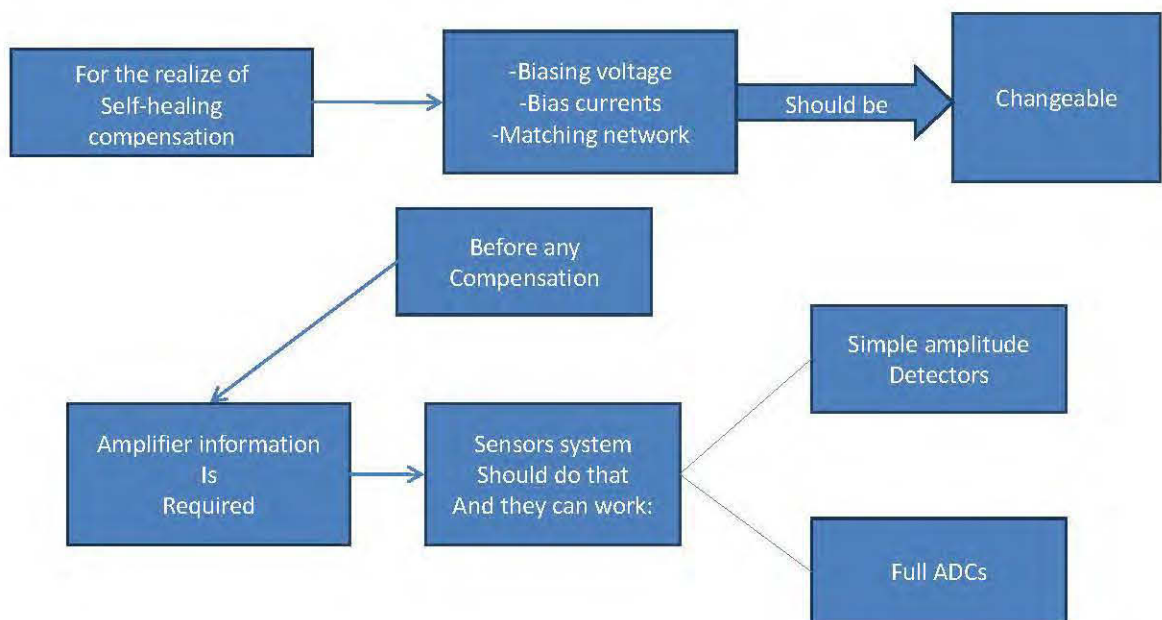


Figure 27: Self-healing algorithm

Basically, for performing the compensation, amplifier information is required, so some sensors should be adjusted in design. They could range from simple amplitude detectors to full ADCs. Although, DC sensors could be applying to measure bias points, but they cannot return amplifier information.

However, Sampling the RF-waveform with an ADC will return the information, but that is power inefficient. This approach the baseband ADC of the baseband

processor can be utilized to sample is energy efficient. This way focused on the clock generation and the sampling system. However, the baseband processor and ADC are outside of the scope of this project.

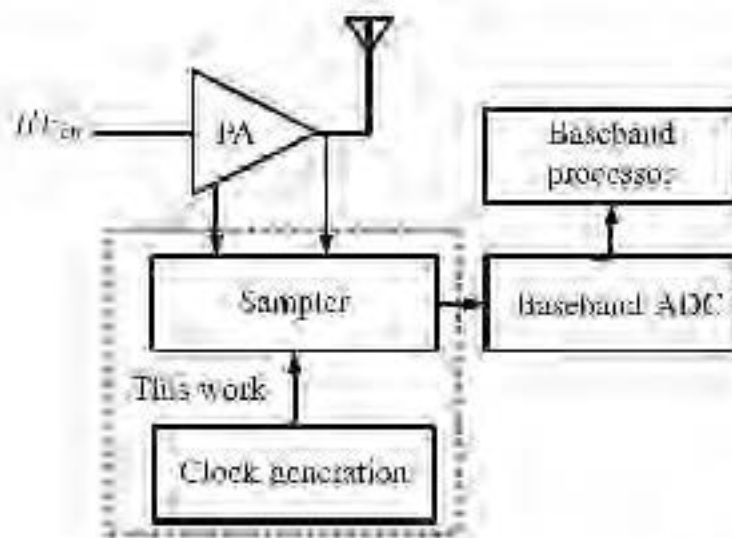


Figure 28: Schematic of the designed system.

Actually, in the modern electronic transmitter systems, the signal is produced by a digital baseband processor which modulates the data signal. After, the signal convert to the analog domain and the modulated data signal is then converted to the carrier frequency [Figure 28]

Usually, in the current system, the delayloop is clocked with the PA frequency and creates the different phases for sample the relevant RF-wave forms of the PA. Also, the sample and circuits return the equally spaced samples over one period of the waveform. Hence, they convert by the ADC from the analog domain to the digital domain and also, the digital samples convert by the DFT to the sinusoids. The current system

can acquire the RF-signal characteristics by converting the high frequency RF-signal to DC values. In addition, they can be sampled at low frequencies. Because the ADC can work at very low speeds, so this saves a lot of energy compared to the Nyquist speed ADC. In the Figure 29, proposed system is shown;

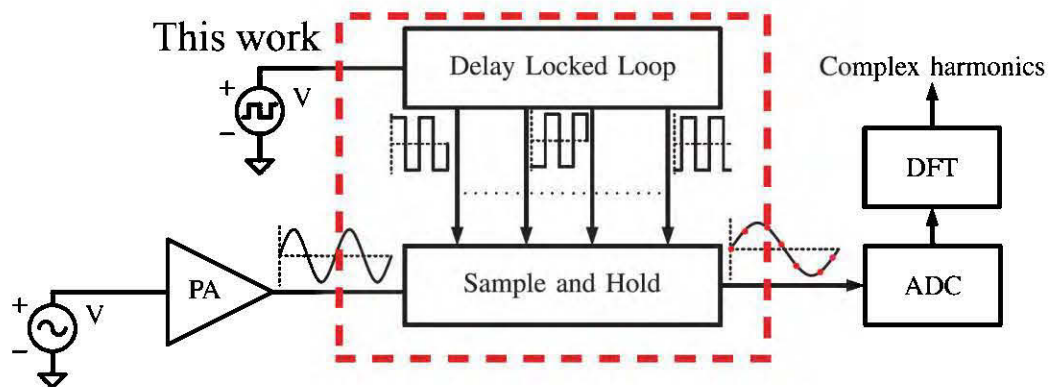


Figure 29: Designed system.

Huiskamp et al. have designed a low power signal waveform sampling system for self-healing RF-power amplifiers is designed and simulated. Also, the sampling system samples RF-waveforms at equally spaced points across one period of the fundamental frequency. Seven samples are needed to define the RF-waveform up to the third harmonic. The information about the RF power amplifier can be returned and this information can be utilized in a self-healing system. However, table 4 illustrate the comparison of two methods. Table 4 shows summary of feedback loop self-healing;

Table 4: Summary of feedback loop self-healing based on Husikamp study

Self-Healing method	Comment
Integrating the measurement circuits in the same chip and use the measured RF-signals in a feedback loop to correct the performance of the RF-circuit.	Compensation of PVT-E (Process-Voltage-Temperature and Environment) variations which are normally slow processes but has great impact on the behaviour and performance of an amplifier by self-healing method.

CHAPTER 2

2.1. Theory behind the self-healing process

In general, the self-healing processes are divided into 4 main categories [Aissa 2014]:

- Capsules and/or particles randomly distribute into the structure;
- Organized net based on hollow fibers system;
- Organized net based on wires (shape memory alloys, fibers and conductive metallic wires).
- Organized net with an external triggering system.

For example, repair process implemented within composite materials is a kind of self-healing with capsules. In this system, a monomer is encapsulated within a microcapsule and then dispersed along with a catalyst (generally a Ruthenium based catalyst is employed). Once the microcapsules break (rupture) upon a mechanical impact for e.g., the monomer flows within the crack and is polymerized once in contact with the dispersed catalyst. In this way, the micro-fissure is repaired.

Another approach is to add a triggering mechanism to a passive system. In such a case, the repairing process is activated externally. For example, the sunlight may serve as the triggering mechanism. At the same time, the sunlight may be used to improve the efficiency of curing process.

Healing materials increase the safety, reliability and lifetime of airframe, launcher, and space structures, by reducing the propagation of fatigue damage and mitigating the growth of small cracks in the structural materials. However, adding the healing agents could affect the intrinsic properties of the host material, requiring a complete verification of the material strength, manufacturing process and its lifetime.

Figure 30 summarizes the taxonomy of the passive self-healing concepts, approaches and methods used to validate the self-healing technology. Self-healing is usually considered as the recovery of mechanical strength through crack healing. However, there are other types of damages, e.g., such as small pinholes that can be healed to ensure the proper performance of various materials. Self-healing polymers may be used to repair small punctures and pinholes. They show a great promise to mitigate potentially catastrophic damage from events such as micrometeoroid penetration and/or atomic oxygen effects. Effective self-repair requires these materials to heal instantaneously following projectile penetration while retaining structural integrity.

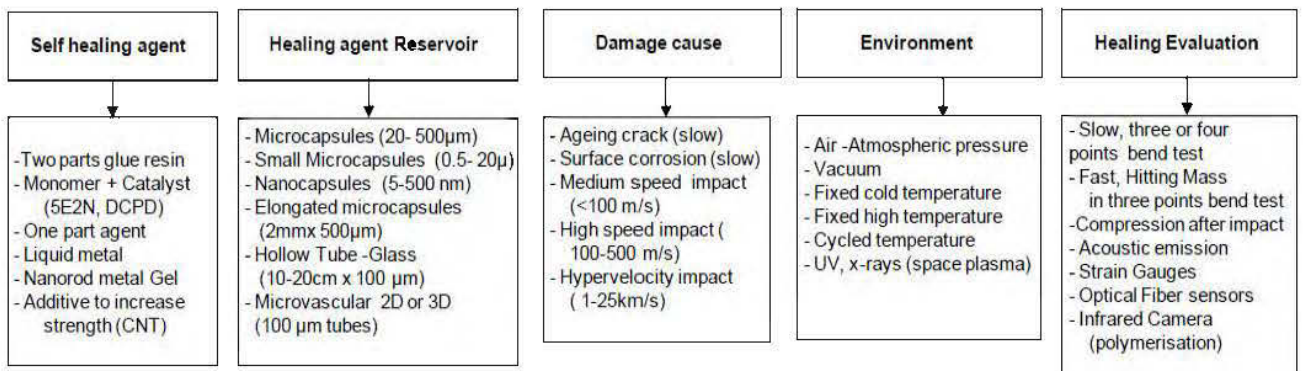


Figure 30: Recent Taxonomy of Passive Self-Healing Concepts.[Aissa 2014]

The concept was developed by the group of the University of Urbana, Illinois and their system is based on an encapsulated healing agent that is embedded in a polymer. Results from different tests confirmed that the self-healed composite material regained as much as 90 % of its original strength. Actually, proposed material is able to sense damage and begin to repair without the need of external trigger. Such a process is referred to as self-healing. Figure 31 shows, In the case of a crack on the material, healing agent (cross-linking polymer) forms a bond between the 2 crack faces, and heals the structure. [Aissa 2014]

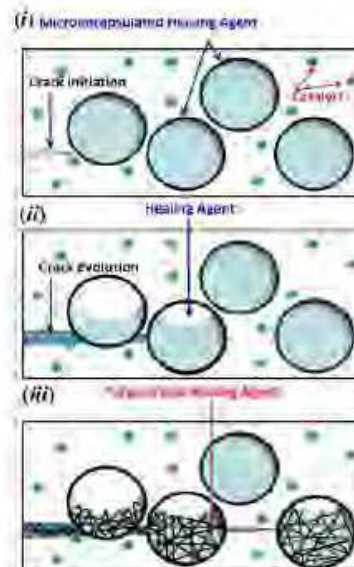


Figure 31: The self-healing process. (i) The healing agent, a monomer (e.g. the DCPD) is prepared and stored in microcapsules. The microcapsules and a catalyst are spread and embedded within the structure (matrix). (ii) When a crack reaches a microcapsule, it causes the rupture which releases the monomer-healing agent. (iii) Self-healing is realized by polymerization between the monomer and embedded catalyst.[Aissa 2014]

CHAPTER 3

EXPERIMENTAL PROCEDURES AND RESULTS

3.1. Self-Healing Part

As we mentioned earlier, the self-healing material has the ability to make possible an autonomous repair of cracks and/or holes occurring in a composite material. It can be used in different applications, including aerospace, electronics and construction. In recent project, we could use self-healing material as a specific composite for the efficient self-repair of polymeric based materials, also in the light to decrease the repairing time, the cost and man power. The same idea behind the same reasons we plan to apply for RF antenna in mining environment.

The matrix element of Self-healing material used in this work was the epoxy polymer (namely the Epon 828), and the hardening agent. By mixing Epon 828 with the hardener part, a polymerized epoxy is obtained.

Self-healing microcapsules are containing healing agent. Once they broke, in the presence of ruthenium Grubbs catalyst, polymerization starts. Thus, cracks will be likely filled by the self-healing composite material.

First, epoxy mix with proportional ratio of microcapsules and then catalyst. The last step is adding the hardener Epicure. After adding the Epicure, mixture starts to

polymerize. This is reason for adding it in last step. (For preparation non self-healing material, should just mix the epoxy and curing agent)

Then, mixture placed in the vacuum for 15 minutes to remove air bubbles present in the blend. [Figure 32]



Figure 32: Vacuum System

After one day of curing, sample is placed inside an oven for 1 day at 60°C as post-curing process.

In the table, all of the information about self-healing preparation are summarized,

Table 5: Self-healing preparation

Steps	Ratio	Centrifuging speed(rpm)	Time	Temp	P(Torr)
Dissolving the Grubbs catalyst into acetone	GC:Acetone = 15-25 mg/ml	-	-	RT	Atm.
Mixing with epoxy(Epon828) in vacuum mixer	EP:GC = 100:2.4 (by weight)	1200	120 sec	RT	40(V)
Blending with microcapsule	EP:MC:GC = 100:21:1.4 (by weight)	1200	120 sec	RT	40(V)
Mixing with curing agent (Epicure-3046) in vacuum mixer	Ep:CA:MC:GC = 100:40:7:2.4 (by weight)	1200	120 sec	RT	40 (V)
Curing in autoclave	-	-	13 hours	40°C	40 psi
Post curing	-	-	24 hours	50°C	atm.

As seen in the Table 5, to make the self-healing composite, following ratio were considered:

Ep: CA:MC: GC=100:40:7:2.4 (by weight)

Where Ep is the epoxy, CA is curing agent, MC is microcapsule and GC is Grubbs catalyst. All the necessary components to make self-healing resin are summarized in Table 6;

Table 6: Self-healing elements

	Material	Commercial Name	Supplier
1	Epoxy	EPON 828	Miller-Stephenson
2	Catalyst	Grubbs	Aldrich
3	Hardening agent	EPICURE 3046	Miller-Stephenson
4	Microcapsule	DCPD	Concordia Uni.

3.1.1. Chemical Elements

3.1.1.1.Epon

Epon 828 is bought from Miller-Stephenson [Figure 33]. This is a basic element as host matrix to make self-healing material. Also mixtures of Epon as a resin with hardener (e.g. Epicure) have many advantages such as low room temperature viscosity, long working life, low moisture absorption, Superior epoxy performance, flexibility, reactivity, high elongation, adjustable cure times, corrosion resistance, heat resistance and fire retardation. Epon is a viscous material in the room temperature and needs sometimes to be heated before using. Table 7 shows the Epon specifications.

Table 7: Epon specifications

Product	Chemical Type	Viscosity at 25° C (P)	Weight per Epoxide	Density (lb/gal)	Comments
EPON 828	DGEBA	110 –150	185 –192	9.7	Predominant liquid epoxy product, widely used in multiple applications.

**Figure 33: Epon 828**

3.1.1.2. Hardening Agent

Adding the hardener agent to the resin is crucial for polymerization. Because of chemical reaction, resin starts to be harder. In present study, Epicure 3046 was used as a hardener agent, and specifications are available in the Table 8. [Figure 34]

Table 8: Hardening agent specifications

Product	Chemical Type	Gel Time at 25°C (min)	Density (lb/gal)	Viscosity at 25°C (cP)	Comments
Epikure 30	Poly amido amine	270	7.8	120-280	Long pot life, general purpose curing agent.

**Figure 34: Hardening agent (Epikure 3046)**

3.1.1.3. Microcapsule

Microcapsules of different diameters are used as a container for healing agent. In the present work, 5-ethylidene-2-norbornene (5E2N) and dicyclopentadiene

(DCPD) monomers and combination of the two are used as healing agents. Our microcapsules were manufactured by INRS-EMT PhD student (Mrs Hasna Hena Zama). [Figure 35]



Figure 35: Microcapsule less than 200 microm eter diameter

3.1.1.4.Catalyst

Catalyst helps to chemical reaction of self-healing materials for filling and bonding the cracks. Grubbs catalyst 1st generation bought form Aldrich. [Figure 36]

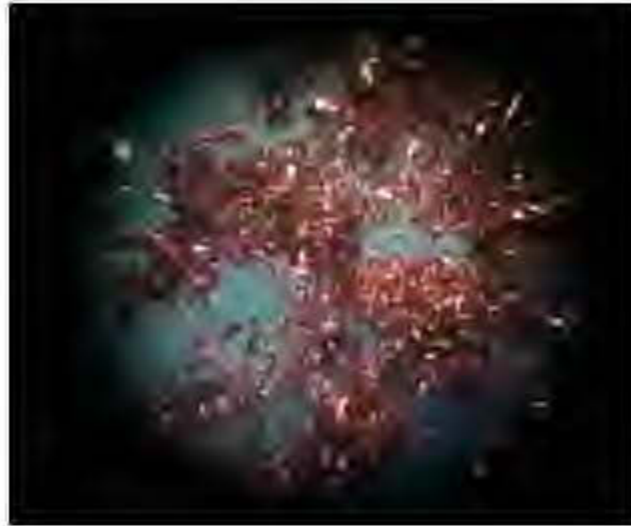


Figure 36: Grubbs catalyst under the microscope

3.1.1.5.CNT

For this study, CNT from MPB Inc. were utilized.

3.1.2. Oven

Last step of self-healing process is the post curing process. After mixing the self-healing materials, remain under the room temperature for 24 hours and then transfer in the oven at 60 °C for 24 hours as post curing.



Figure 37: Oven for post curing process.

Figure 37 shows the used oven and model is Fisher Scientific 737G.

3.1.3 Microscope

Two optical microscopes were used. A Leica Zoom 2000 for regular analyse. This microscope can zoom up to 45X. [Figure 38]



Figure 38: Leica zoom 2000 microscope

The second one is OMAX A35140U, which can work up to 100 X. OMAX has software and digital photography option. [Figure39]



Figure 39: OMAX A35140U microscope

3.1.4. Thermal shock

For making cracks in the samples and evaluating the self-healing efficiency, thermal shock test using liquid nitrogen and heating inside an oven was applied. For our RF antenna, first they were placed in liquid nitrogen at -196°C for 1 minute, and then transferred to an oven at 55°C . This cycle repeated 2 times [Figures 40 and 41]. Thermal shock experiments were performed at INRS-EMT (Varenes, Quebec).

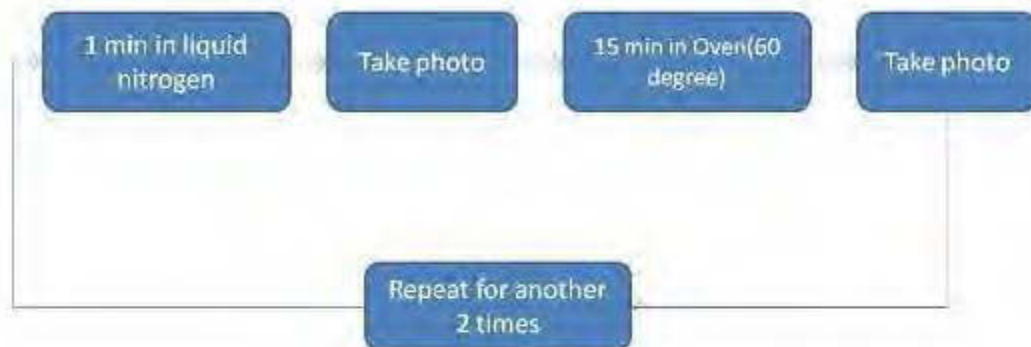


Figure 40: Schematic picture of Thermal shock test



Figure 41: Thermal shock for RF antenna

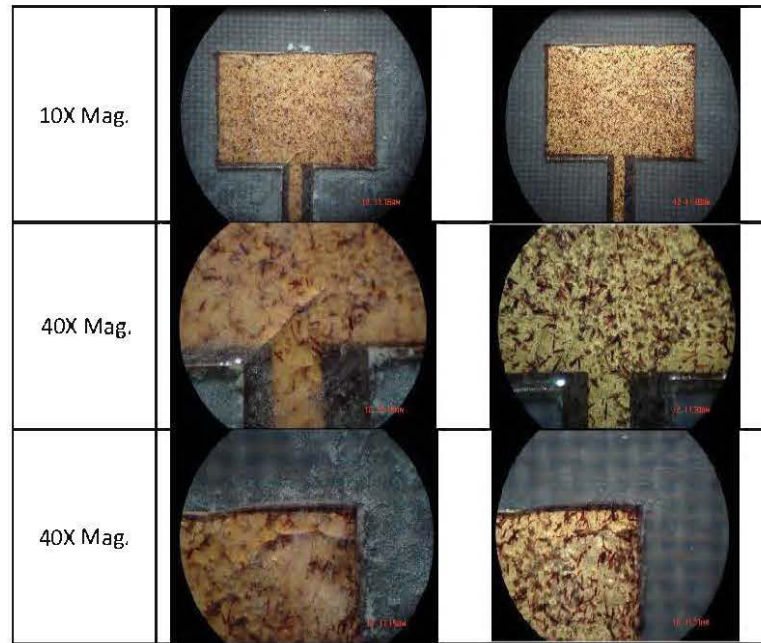


Figure 42: Thermal shock for antenna with self-healing material after first liquid nitrogen, (right) after first oven

In the Figure 42, we can see microscope images of samples before and after the thermal shock tests.

Figures 43 showing a crack which propagates in the lower part of antenna. It is shown within the different magnified scales. After the second oven and liquid nitrogen, a crack is made which is much longer than the first one and it starts from corner into the center. [Figure 43]

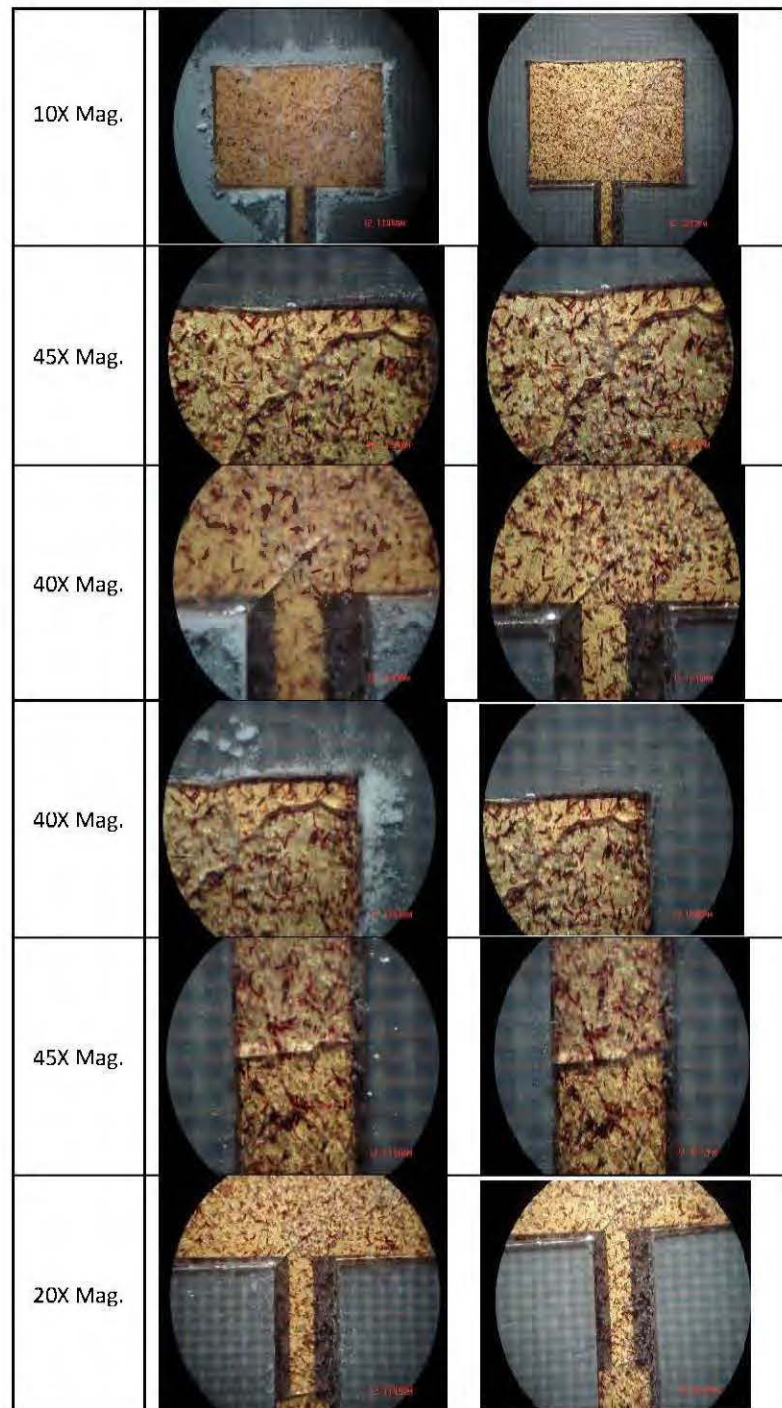


Figure 43: Thermal shock for antenna with self-healing material, (left) After Second Liquid Nitrogen, (right) After Second Oven

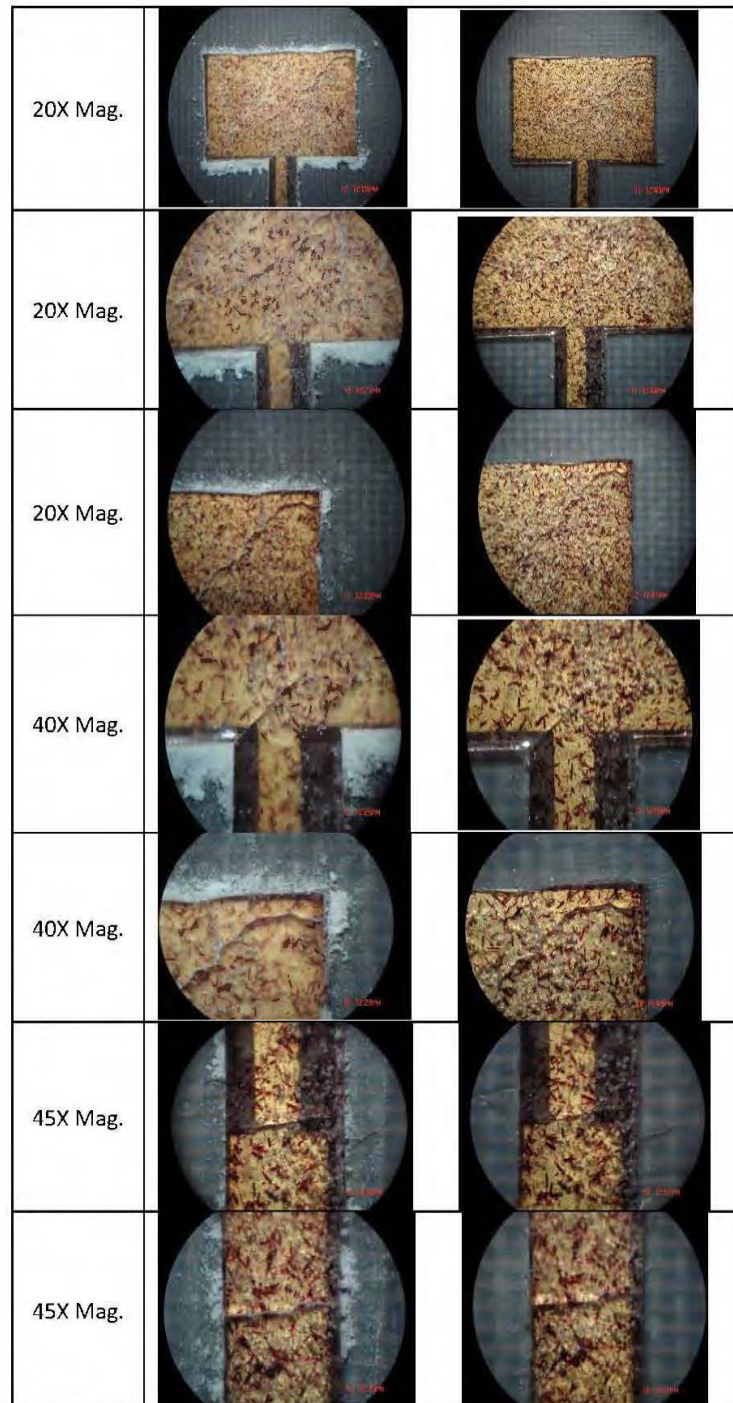


Figure 44: Thermal shock for antenna with self-healing material, (left) after third liquid nitrogen, (right) after third oven

After the specimen was placed in the liquid nitrogen for second one, except of previous crack, some other group of cracks are propagated. In the Figure 44, you can see the one in the head of antenna, also another crack in the lower part. It is obvious that a crack on the right top corner of Antenna [Figures 44].

2

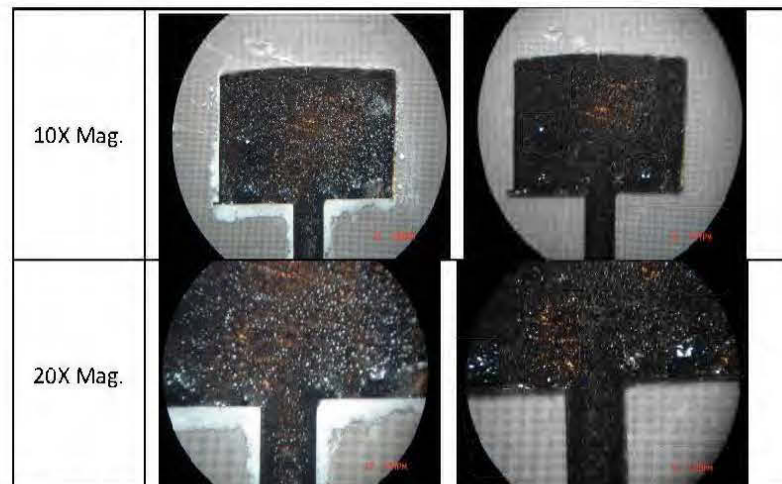


Figure 45: Thermal shock for antenna with self-healing material plus CNTs, (left) After First Liquid Nitrogen, (right) After First Oven

Antenna with self-healing material plus CNTs shows few and narrow cracks after the first liquid nitrogen and oven [Figure 45].

In the Figure 46, some longer cracks are found after the second liquid nitrogen and oven, which is almost similar to antenna with self-healing material after the same cycle.

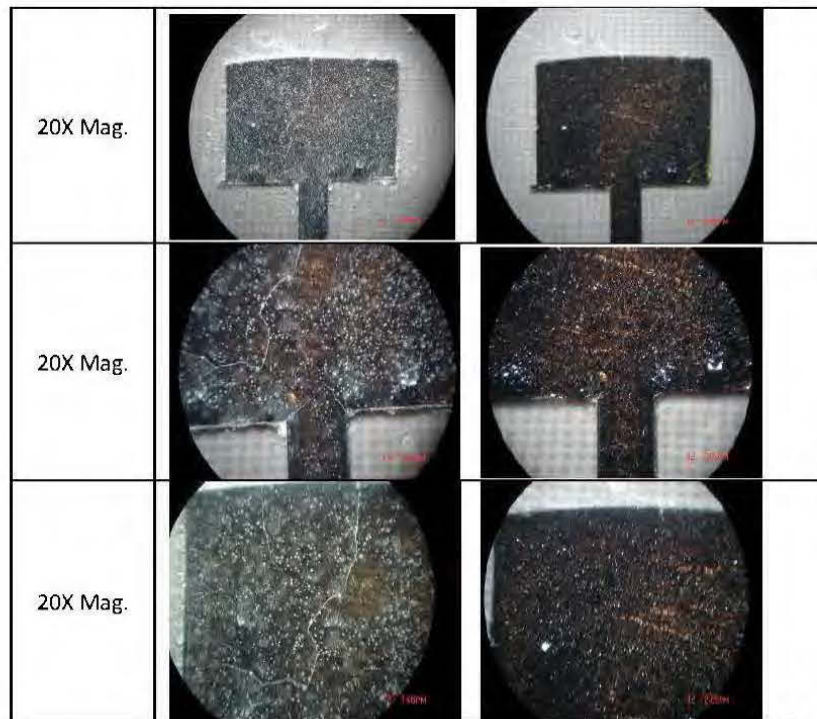


Figure 46: Thermal shock for antenna with self-healing material plus CNTs, (left) After Second Liquid Nitrogen, (right) After Second Oven

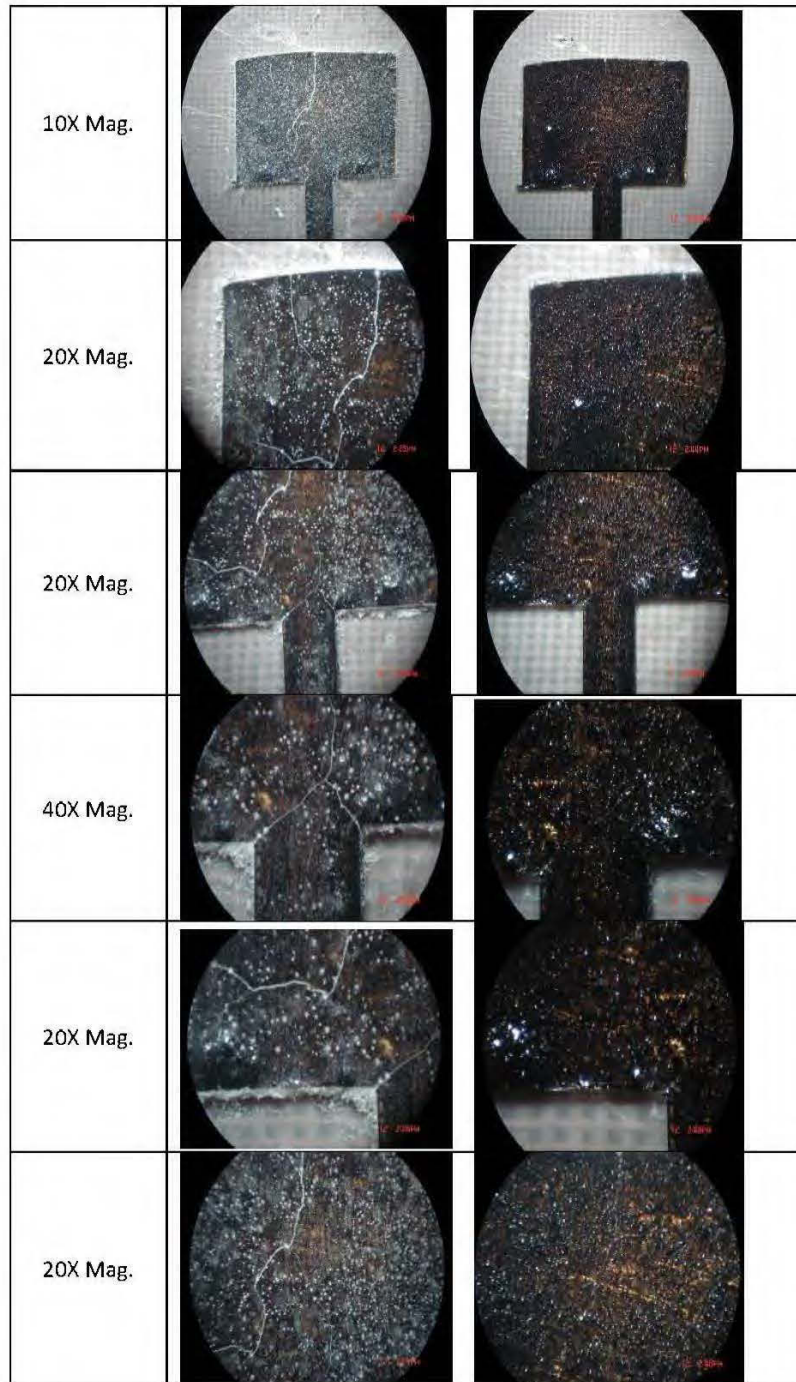


Figure 47: Thermal shock for antenna with self-healing material plus CNTs, (left) After Third Liquid Nitrogen, (right) After Third Oven

Figure 47 shows that more cracks are generated after the third liquid nitrogen and oven. They are distributed in the different places of antenna and apparently are similar to antenna with self-healing material after the third cycle.

3.2. RF Part

3.2.1. Antenna

Two RF patch antennas operating at 2.5 GHz frequency were provided by Prof. Nedil (UQAT).



Figure 48: RF Patch antenna

3.2.2. Vector Network Analyzer (VNA):

Vector Network analyser (VNA) is used for measuring the response of devices at RF. It is then possible to characterise RF response of the antenna device. Current study used VNA in department of electrical engineering at Ecole Polytechnique de Montreal.

3.2.3. Anechoic Chamber:

Anechoic chamber is an indoor antenna range. Inside the chamber, walls and other components lined with special electromagnetic wave absorb ring material. With anechoic chamber, measuring the radiation pattern (variation of the radiated power by antenna) is possible.

For our study, anechoic chamber department of Electrical Engineering Faculty of Ecole Polytechnique de Montreal was utilized.



Figure 49: Anechoic chamber in the Ecole Polytechnique de Montreal

The walls, ceilings and floor are lined with specific electromagnetic wave absorbing material. Indoor ranges are desirable because the test conditions can be much more tightly controlled than that of outdoor ranges. The material is often jagged in shape as well, making these chambers quite interesting to see. The jagged triangle shapes are designed so that what is reflected from them tends to spread in random directions, and what is added together from all the random reflections tends to add incoherently and is thus suppressed further.

3.3. Experimental Results

3.3.1. VNA

By VNA, we could measure S-parameters for the both antennas in each step. Figure 50 shows s-parameters for antenna 1 with different conditions (antenna without any material, with self-healing and with self-healing after the thermal shock). As you see, s-parameters for antenna with self-healing material is more narrow and longer comparing to other two different materials.

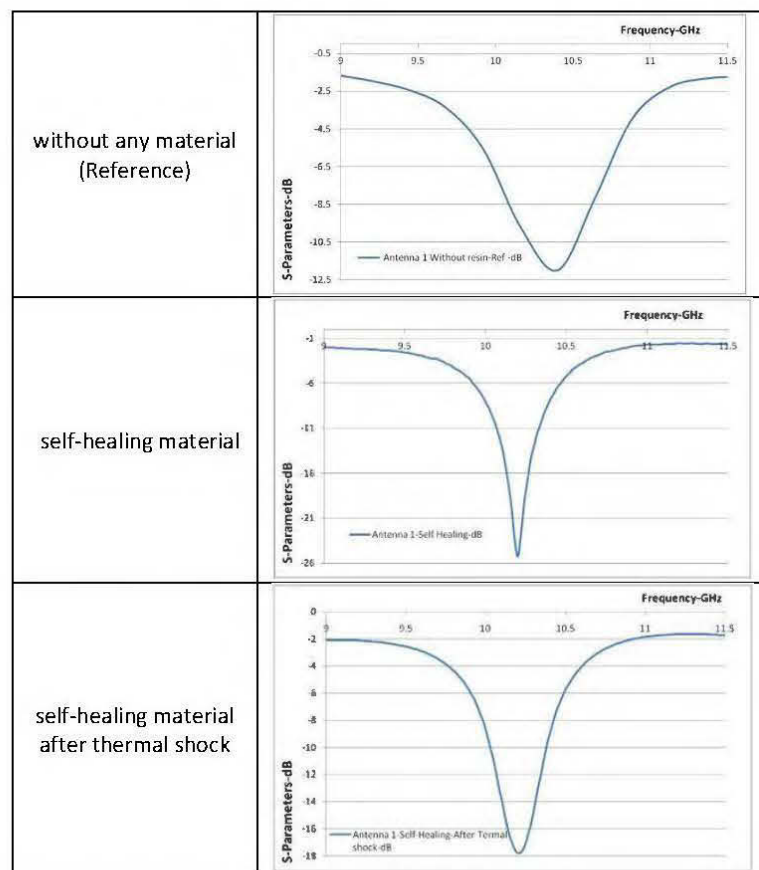


Figure 50: Measured s-parameters for antenna 1 by VN

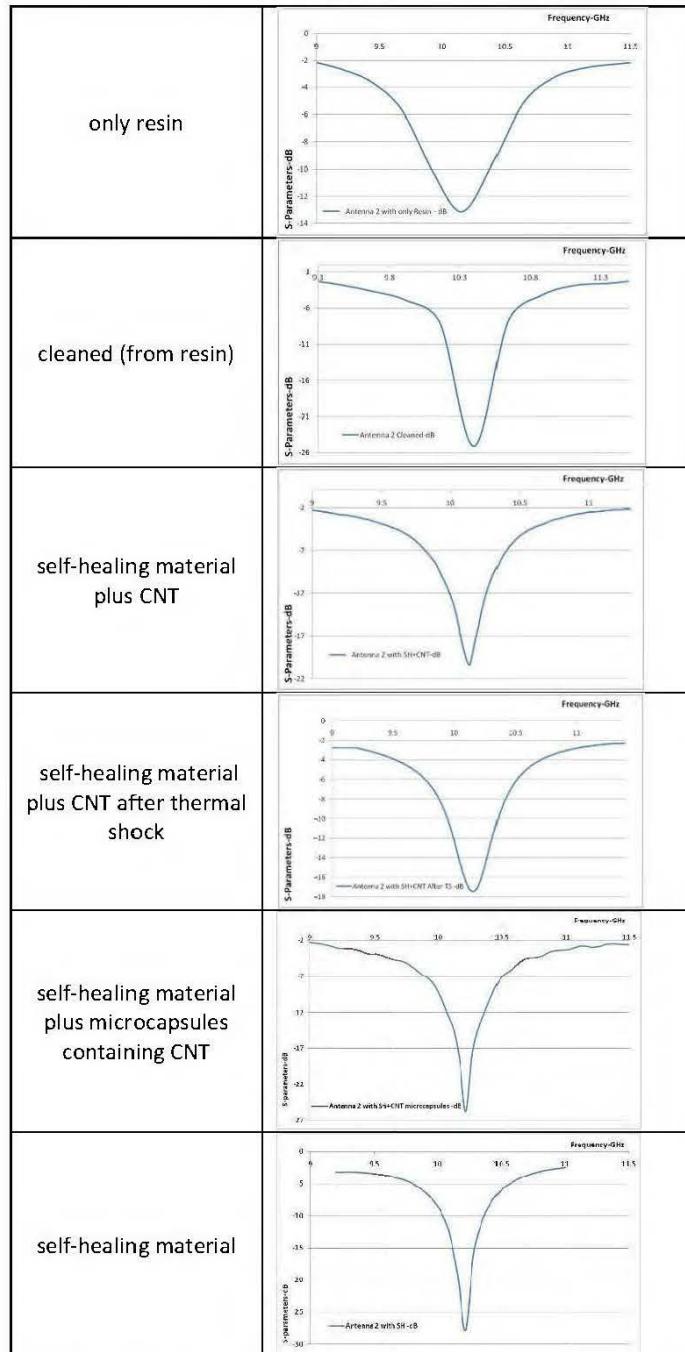


Figure 51: Measured s-parameters for antenna 2 by VNA

Figure 51 shows s-parameters for antenna 2. Antenna tested in the different conditions; cleaned(Reference), only resin, self-healing material plus CNT, self-healing material plus CNT after the thermal shock, self-healing material plus microcapsules containing CNT and only self-healing material. Similar to antenna 1, Here antenna with only self-healing demonstrates narrower and longer peak.

3.3.2. Anechoic chamber

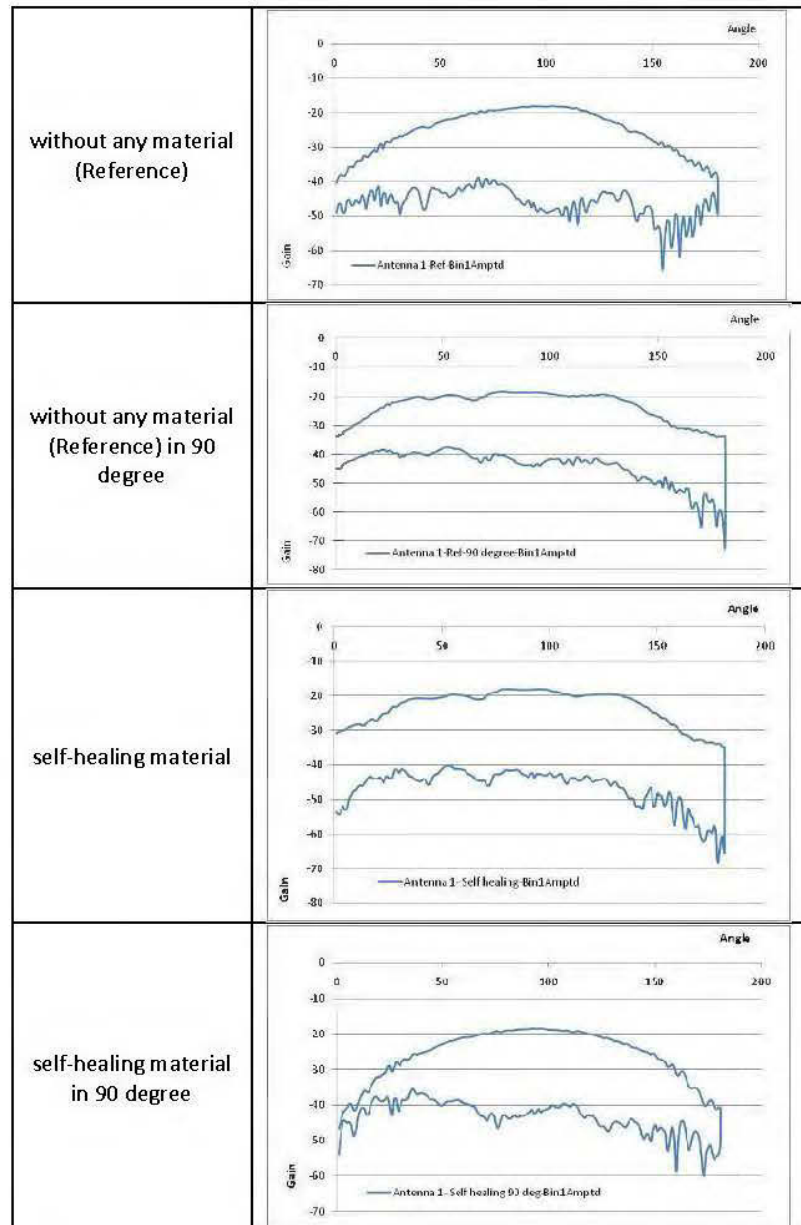


Figure 52: Radiation pattern by anechoic chamber for antenna 1

Figure 52 and 53 show radiation pattern which is measured by anechoic chamber for antenna1 in the different conditions. As you see in the Figure 52, radiation pattern of antenna without any material and antenna with self-healing material in the 0 degree are different.

Figure 53 exhibits Co-polar and Cross-polar of radiation pattern for antenna 1 with self-healing material.

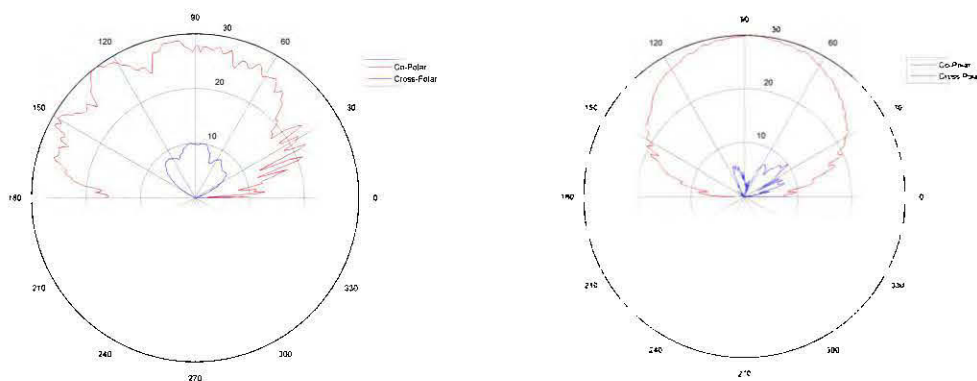


Figure 53: Radiation pattern for antenna 1 with self-healing material in 0 degree(left) and 90° degree(right)

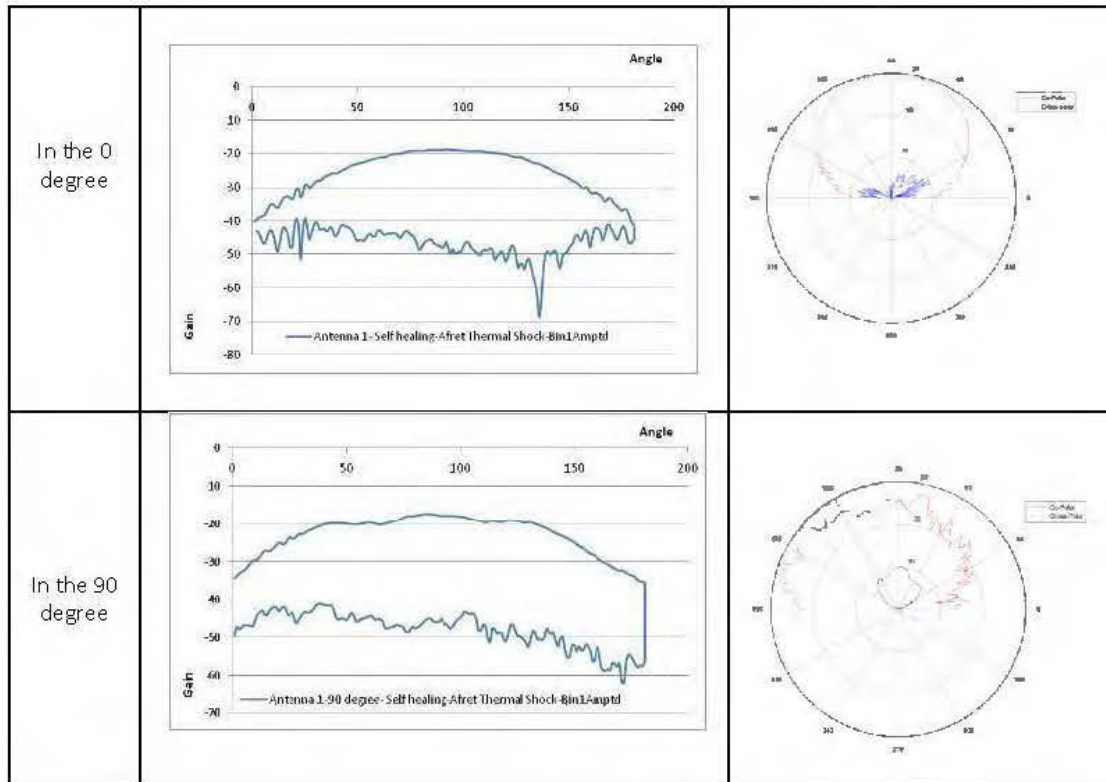


Figure 54: Radiation pattern for antenna 1 with self-healing material after thermal shock

Also, radiation pattern of antenna 1 with self-healing material after thermal shock is measured. [Figure 54]

Radiation pattern for antenna 2 is shown on the Figure 55. Here, antenna covered with only resin.

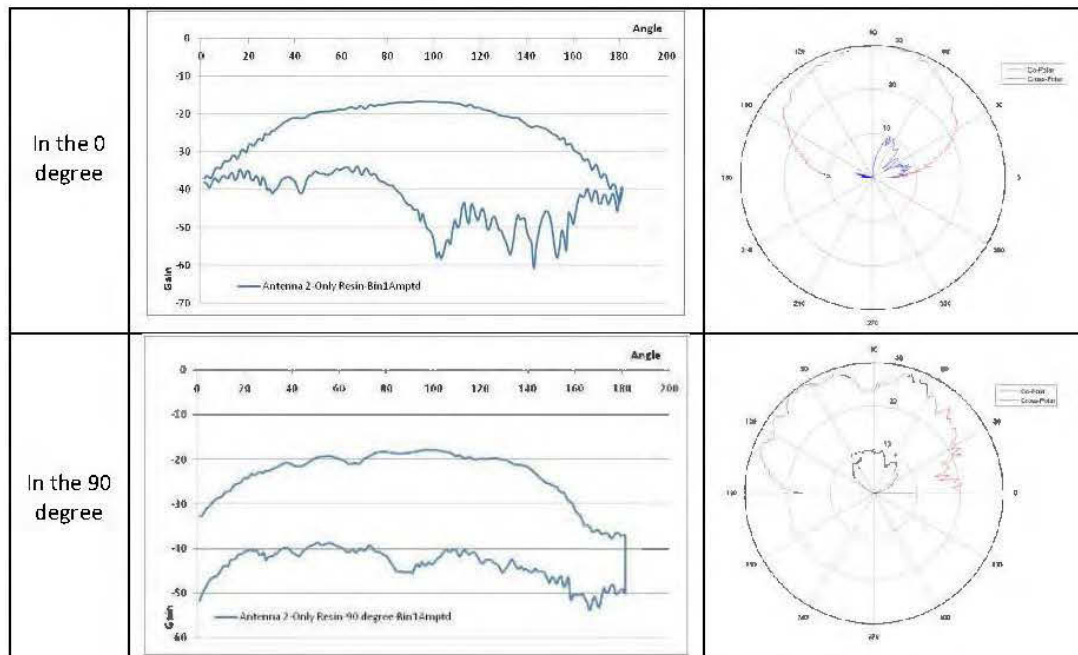


Figure 55: Radiation pattern for antenna 2 with only resin

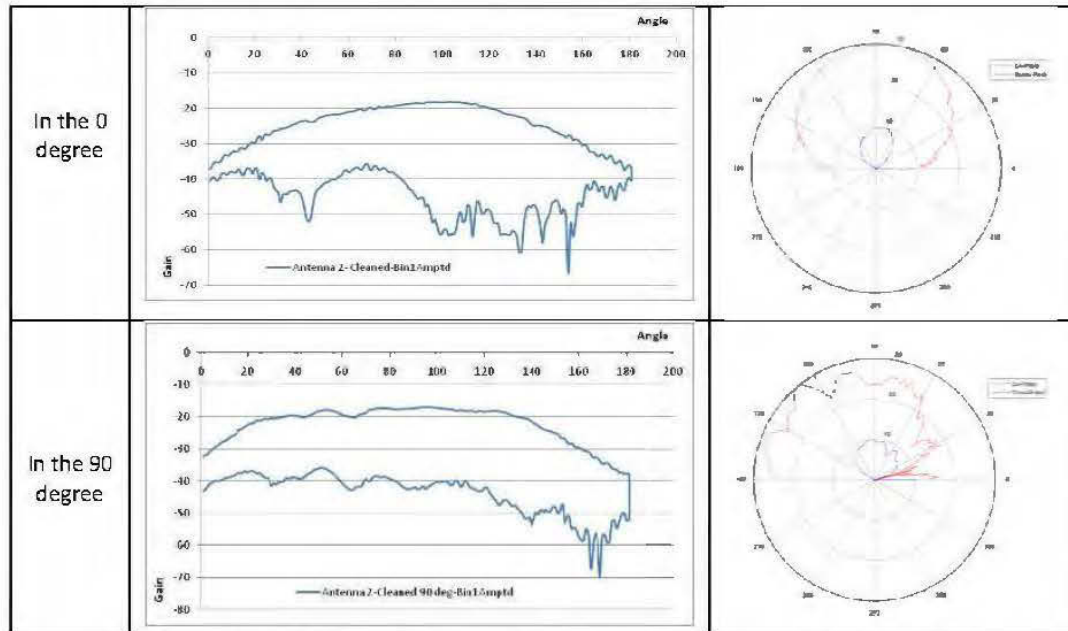


Figure 56: Radiation pattern for cleaned (from resin) antenna 2

Then, antenna cleaned from resin and measured for radiation pattern again [Figure 56].

Therefore, antenna 2 covered with self-healing material plus CNTs. Figure 57 shows corresponding radiation pattern in 0 and 90 degrees. Compare to antenna 2 with only resin, the pattern is different. Antenna 2 with resin shows more curvy pattern.

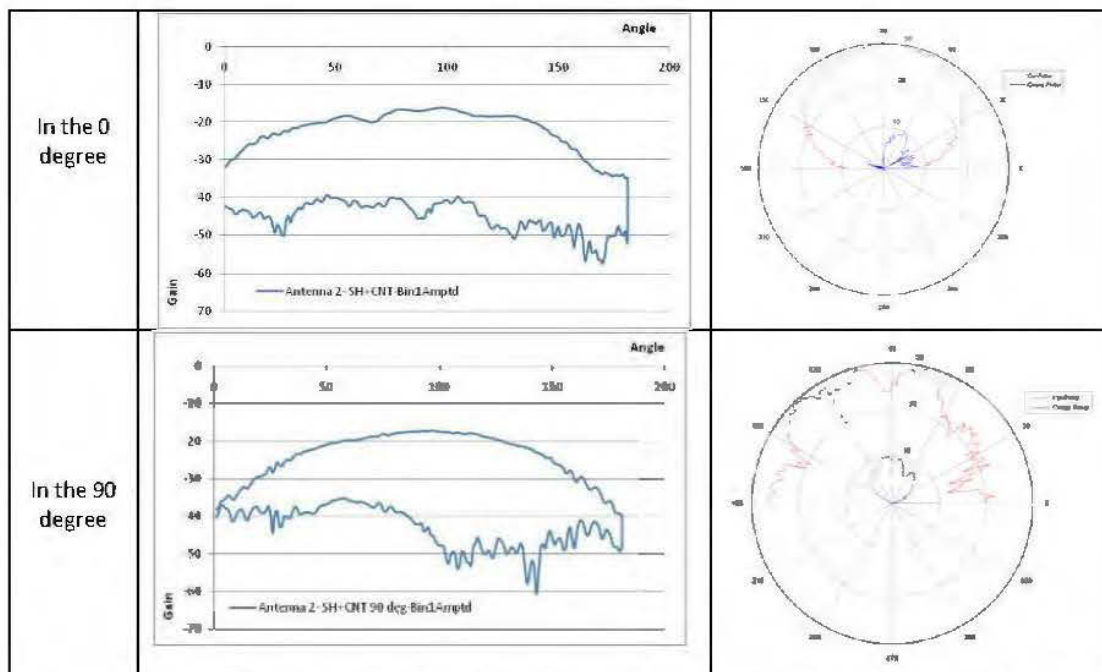


Figure 57: Radiation pattern for antenna 2 with self-healing material plus CNT

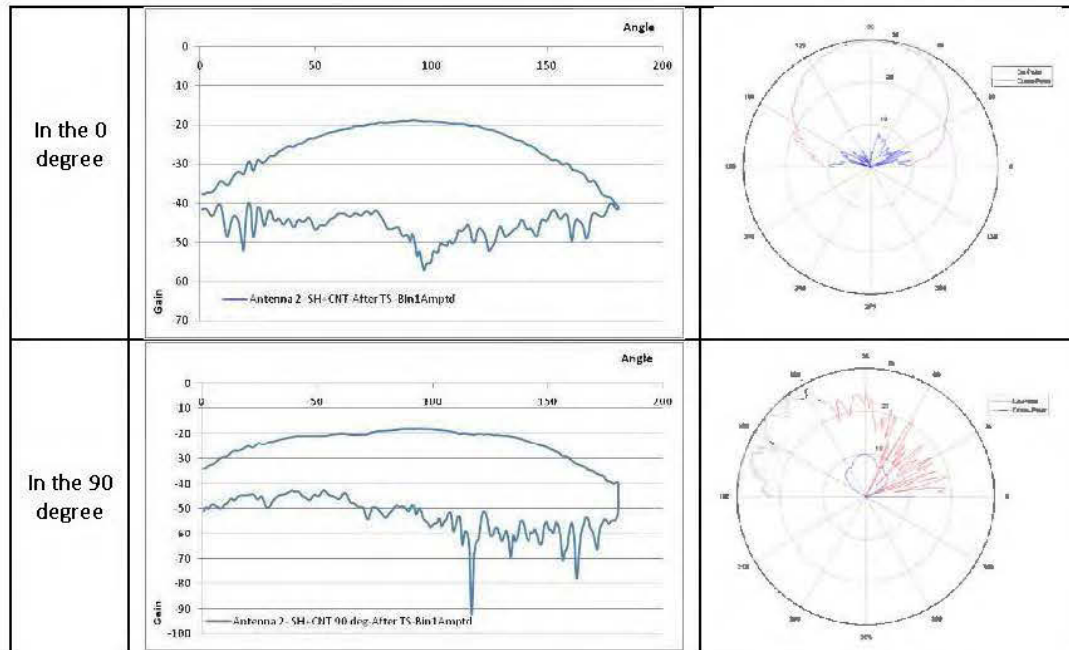


Figure 58: Radiation pattern for antenna 2 with self-healing material plus CNT after thermal shock

Afterward, to making thermal shock, antenna 2 with self-healing material plus CNTs placed in the liquid nitrogen and oven respectively. Radiation patterns in the 0 and 90 degrees for antenna 2 with self-healing material plus CNTs after thermal shock are shown in the Figure 58. The pattern in the 0 degree is similar to antenna 2 with only resin and much different with the same material before the thermal shock.

Then, microcapsules containing the CNT added to self-healing material and deposited on the antenna 2. Radiation pattern is available in the Figure 59.

Pattern in 0 degree is completely deferent from the others and 90 degrees is similar to antenna 2 with only resin.

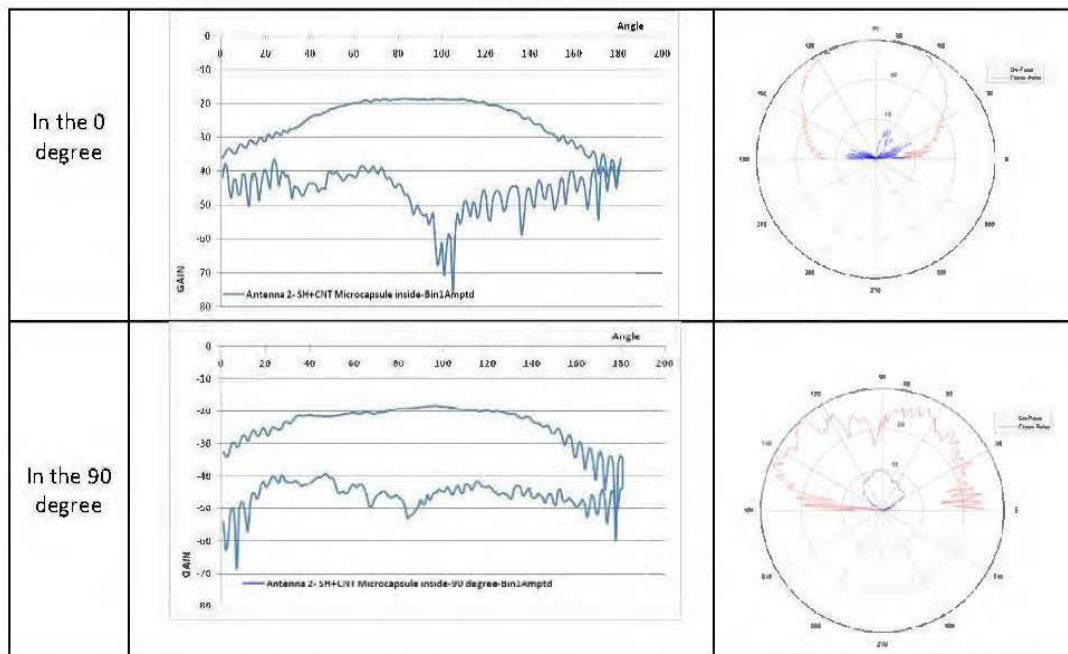


Figure 59: Radiation pattern for antenna 2 with self-healing material with microcapsules containing CNT

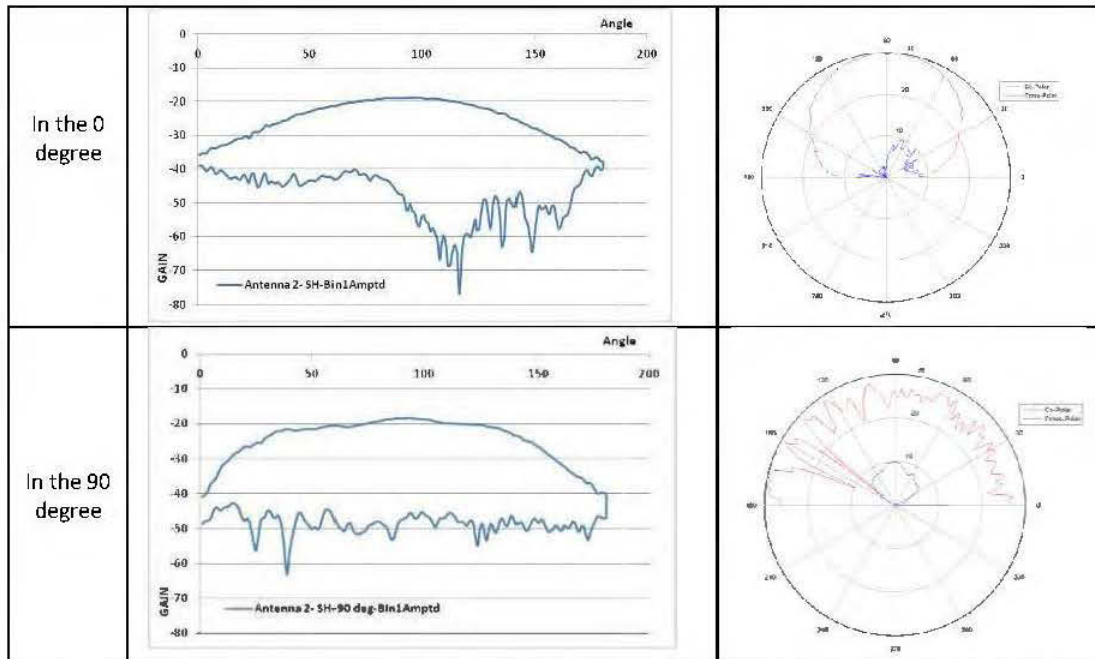


Figure 60: Radiation pattern for antenna 2 with self-healing material

Finally, radiation pattern for antenna 2 with only self-healing material is shown in the Figure 60. Pattern in the 0 degree is similar to antenna with self-healing material plus microcapsule containing CNT. 90 degree pattern is different from the others.

In the Table 9 and 10, all of the information about radiation pattern for antenna 1, 2 showed respectively;

Table 9: Summary of radiation pattern information for antenna 1

	0 degree position		90 degree position	
	Maximum	Max peak of GAIN	Maximum	Max peak of GAIN
Cleaned(Ref.)	-18.08		-18.17	
SH	-17.92	Maximum	-18.38	
SH+CNT-After Thermal Shock	-18.60		-17.38	Maximum

As you see, in the 0 degree, antenna with self-healing and also in the 90 degree, antenna with self-healing plus CNTs after thermal shock showing higher gains.

Table 10: Summary of radiation pattern information for antenna 2

	0 degree position		90 degree position	
	Maximum	Max peak of GAIN	Maximum	Max peak of GAIN
Cleaned	-18.047		-16.9204	
Only Resin	-16.6249	Maximum	-17.8447	
SH+CNT	-17.0806		-16.1792	Maximum
SH+CNT Microcapsule Inside	-18.4753		-18.1325	
SH+CNT-After Thermal Shock	-18.7772		-18.0079	

In the antenna 2, covered antenna with only resin in the 0 degree has maximum gain, and antenna with self-healing plus CNTs is maximum for 90 degrees.

CHAPTER 4

DISCUSSION

The focus of our present work is on two main goals:

- How self-healing material affects the electromagnetic properties of the RF patch antenna? And
- Efficiency of the self-healing process for the case of cracks and fracture in these RF devices.

4.1. Irradiation Properties

First, S-parameters for antennas with and without self-healing coatings are analyzed. From Figure 90, in the reference antenna 1 (i.e. without Self-healing coating), a shift in the resonance frequency can be clearly when self-healing is applied and also after thermal shock test. Regarding the S-parameters (Figure 61), the maximum shift value is attributed to sample with self-healing material. (Table 11)

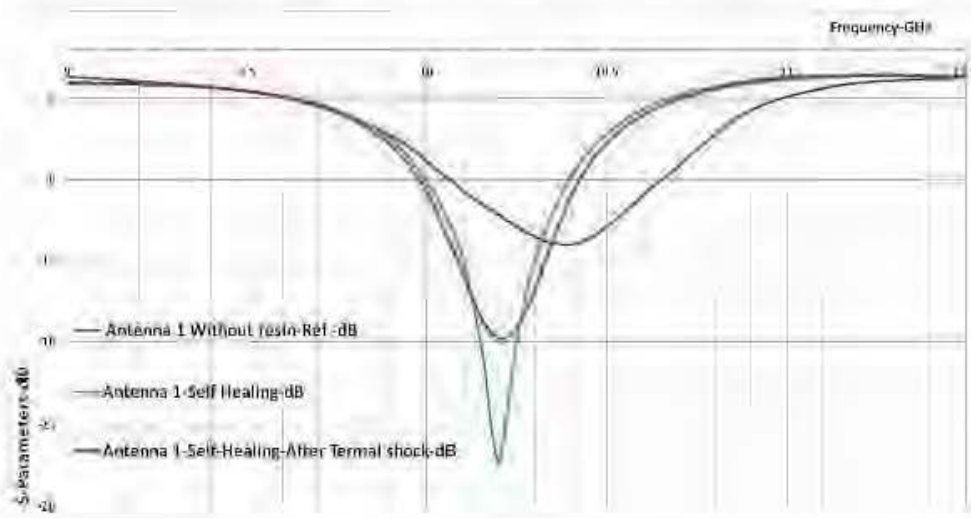


Figure 61: Measured s-parameters for antenna 1

Table 11: Measured s-parameters by VNA and calculated information for antenna 1

	Frequency GHz	Δ Frequency	S-parameters dB	X	Percent of X in $\text{dB}=10\text{Log}(1+X)$	Status	Difference value (dB)
Antenna 1-without resin(Ref)	10.40	-	-12.00	-0.94	93.69	Ref.	-
Antenna 1 with SH	10.13	0.22	-23.50	-1.00	99.55	Increased	11.50
Antenna 1 with SH-After Thermal shock	10.20	-0.20	-17.78	-0.98	98.33	Decreased	5.78

For Antenna 2, when the self-healing is applied, S-parameters with different materials are showed in the Figure 62. As we can see, compared to cleaned and original antenna, there is shift for frequency in all of the samples.

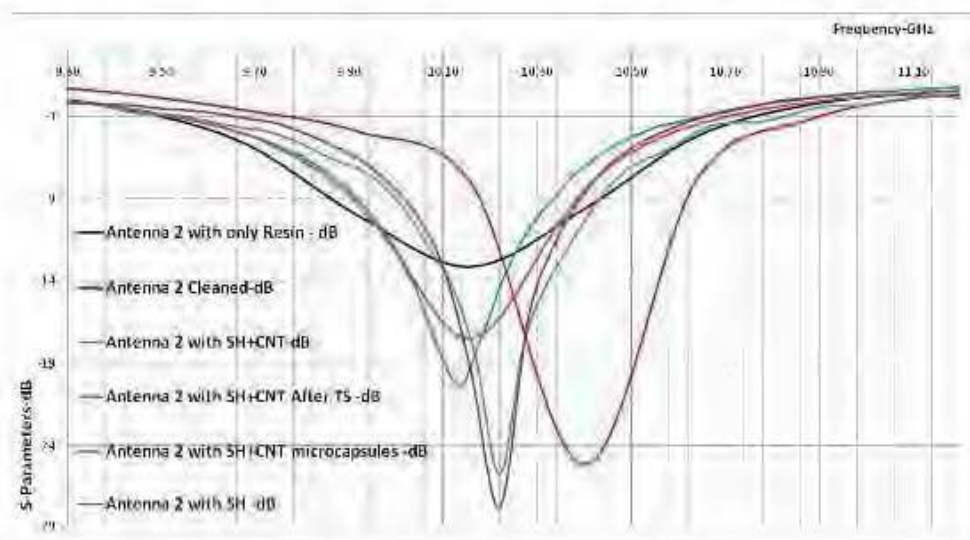


Figure 62: Measured s-parameters with different materials for antenna 2

Table 12: Measured s-parameters by VNA and calculated information for antenna 2

	S-parameters	Frequency	Δ Frequency	X	Percent of X in $\text{dB}=10\log(1+X)$	Status	Difference value(dB)
Antenna 2-Cleaned	-25.13	10.40	-	-1.00	99.69	Ref.	
Antenna 2-SH+CNT	-20.33	10.14	-0.26	-0.99	99.07	Decreased	-4.80
Antenna 2-SH+CNT Microcapsules	-17.9	10.36	-0.11	-0.98	98.38	Decreased	-7.23
Antenna 2-SH+CNT After Thermal shock	-17.46	10.16	-0.24	-0.98	98.20	Decreased	-7.67
Antenna 2-Resin	-13.13	10.16	-0.24	-0.95	95.14	Decreased	-12.00
Antenna 2-SH	-27.847	10.22	-0.18	-1.00	99.84	Increased	2.72

Regarding to values of Table 12, highest S-parameters belong to self-healing material plus CNTs (after reference antenna). With adding the microcapsules contain CNTs, resonance frequency of the antenna is decreased less than the other materials (closer to original).

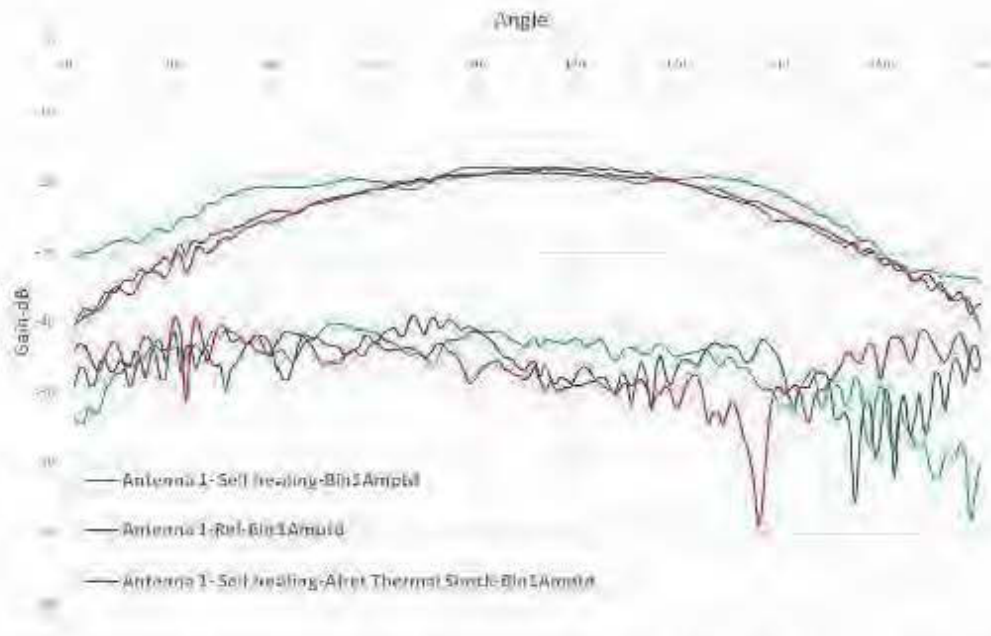


Figure 63: Radiation pattern by anechoic chamber for antenna 1 in the 0 degree

Antenna with only resin epoxy has the largest difference rather to original antenna. For analyzing the radiation pattern and the Gain of antenna, information for antenna 1 with different materials and directions demonstrates in Figures 63 and 64.

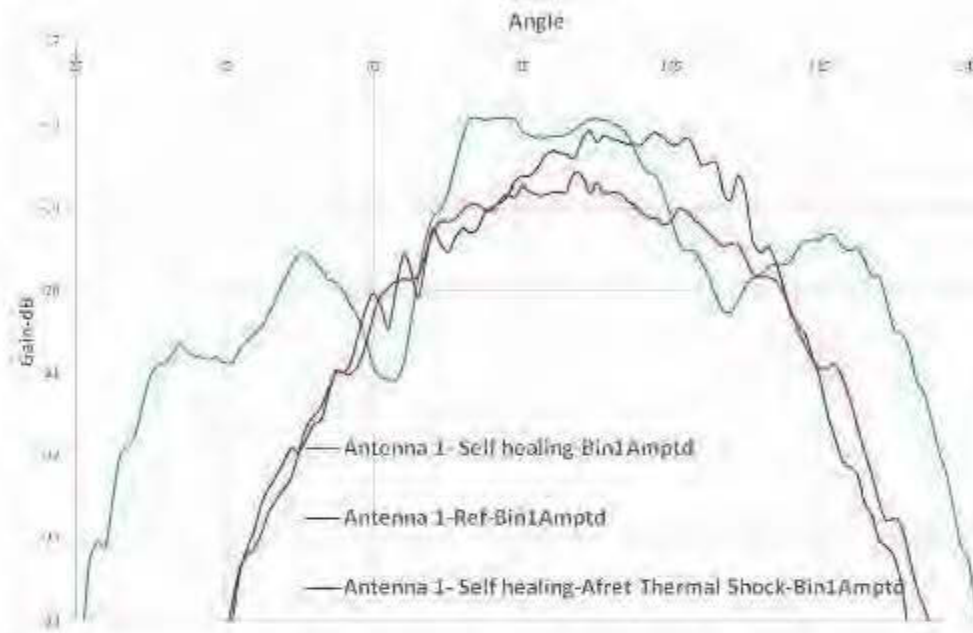


Figure 64: Zoomed of peak area of Radiation pattern by anechoic chamber for antenna 1 in the 0 degree

Table 13: Radiation pattern description for antenna 1

	Min		
Position	0 degree position	Max peak of GAIN	Diffrencece
Antenna 1-Ref	-18.08	-	-
Antenna 1- Self healing	-17.92	Max	-0.16
Antenna 1- Self healing-Afret Thermal Shock	-18.60	-	0.52

For antenna 1, sample with self-healing material has higher gain and shows maximum gain. (Table 13)

Figure 65 shows the radiation patterns for antenna 1 without any material, with self-healing material and the one with self-healing material after thermal shock.

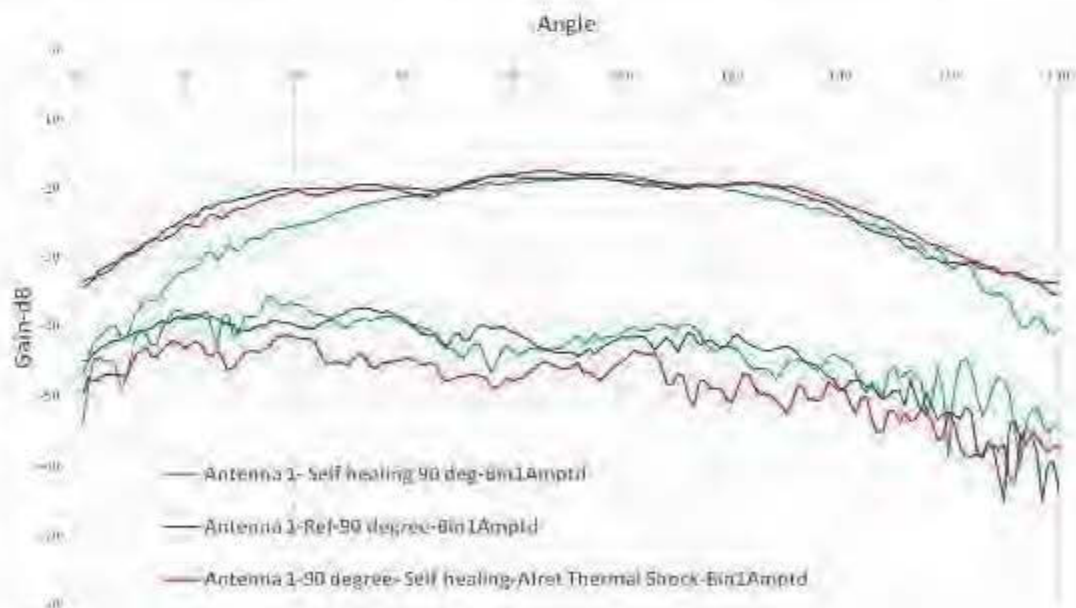


Figure 65: Radiation pattern by anechoic chamber for antenna 1 in the 90 degree



Figure 66: Zoomed of peak area of Radiation pattern by anechoic chamber for antenna 1 in the 90 degree

For better view, a zoomed scale of peak region of radiation pattern for antenna 1 without any material, with self-healing material and the one with self-healing material after thermal shock is shown in the Figure 66. As you see, one with self-healing material after thermal shock represent the higher gain compare to the others.

Table 14: Radiation pattern description in different direction for antenna 1

Position	Min 90 degree position	Max peak of GAIN	Diffrenece
Antenna 1-Ref	-18.17	-	-
Antenna 1- Self healing	-18.38	-	0.21
Antenna 1- Self healing-Afret Thermal Shock	-17.38	Max	-0.79

Table 14 summarize the gain information for antenna 1 in the different conditions and confirms that one with self-healing material after thermal shock has higher gain. For the antenna 2, there is more different materials which are deposited on the surface. Figures 67 and 68 showing the related radiation patterns in the 0 degree.

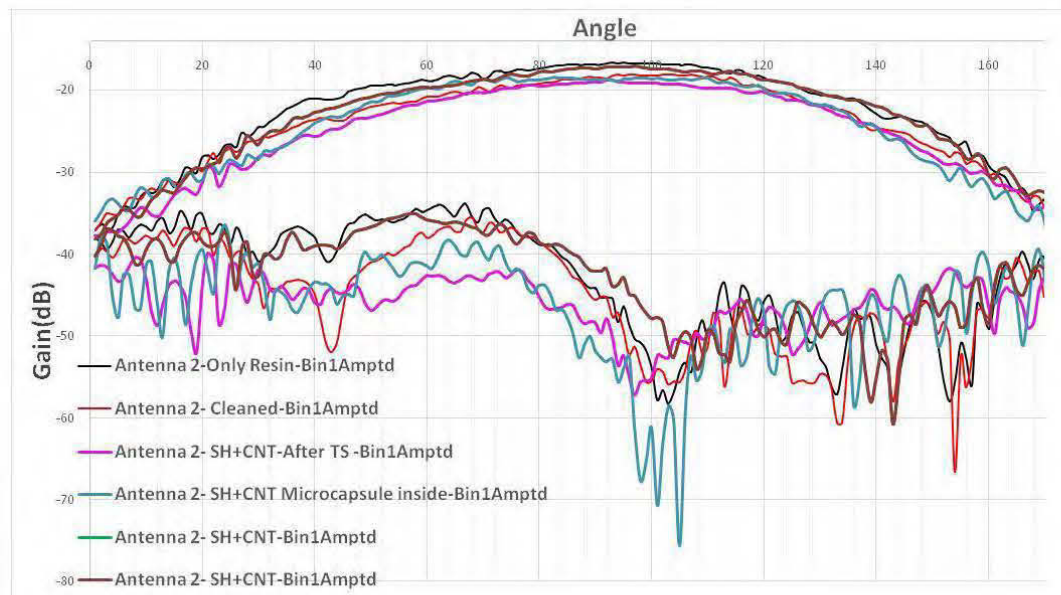


Figure 67: Radiation pattern by anechoic chamber with different materials for antenna 2 in the 0 degree

Antenna 2 was tested with different conditions,

- only resin
- Cleaned from resin
- Self-healing
- Self-healing + CNT
- Self-healing + microcapsules containing CNT
- Self-healing + CNT after the thermal shock

Figure 68 showing a zoomed scale of peak area of previous picture (Figure 67), and this is clear that antenna with only resin has higher gain.

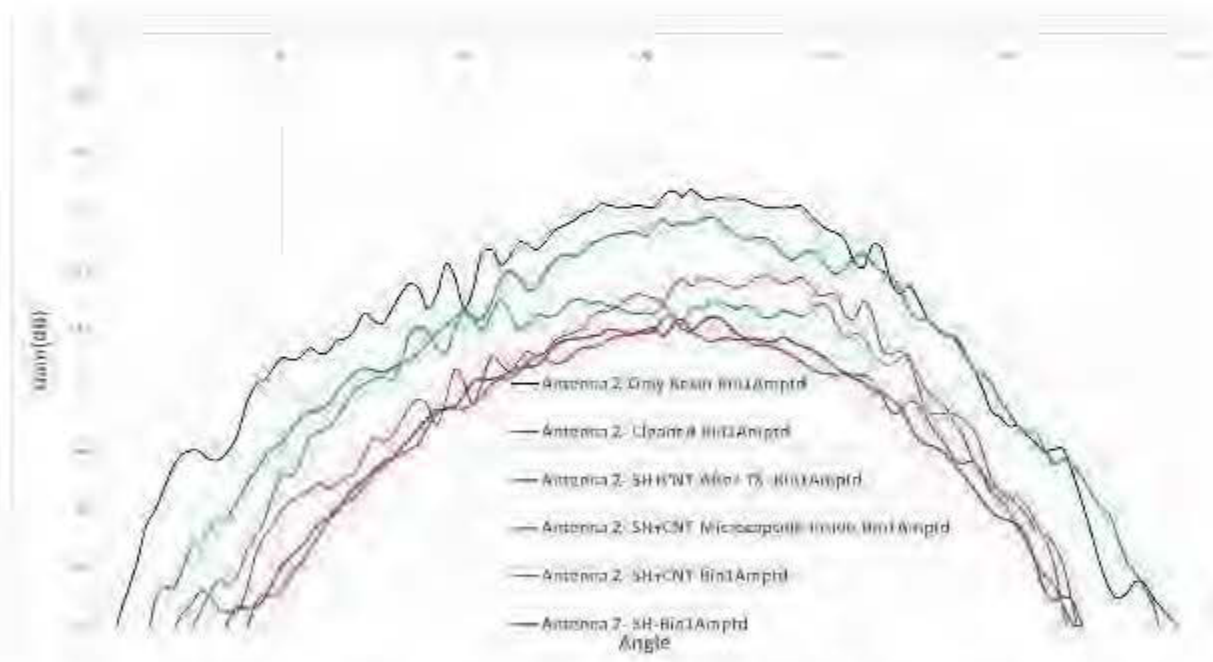


Figure 68: Zoomed of peak area of Radiation pattern by anechoic chamber with different materials for antenna 2 in the 0 degree

Table 15: Radiation pattern description for antenna 2

First position(0 degree)				
Position	Maximum	Max peak of GAIN	Diffrence	Average in 90-110degree
Antenna 2- Cleaned	-18.05	-	-1.42	-18.24
Antenna 2-Only Resin	-16.62	Max	-	-16.87
Antenna 2- SH+CNT	-17.08	-	-0.46	-17.42
Antenna 2- SH+CNT Microcapsule inside	-18.48	-	-1.95	-18.66
Antenna 2- SH+CNT-After Thermal Shock	-18.78	-	-2.15	-19.22
Antenna 2- SH	-18.78	-	-2.15	-0.68

The maximum value of gain is attributed to antenna with only resin epoxy as coating. So, in the 0-degree position, resin epoxy coating has the highest effect on the gain of the antenna. [Table 15]

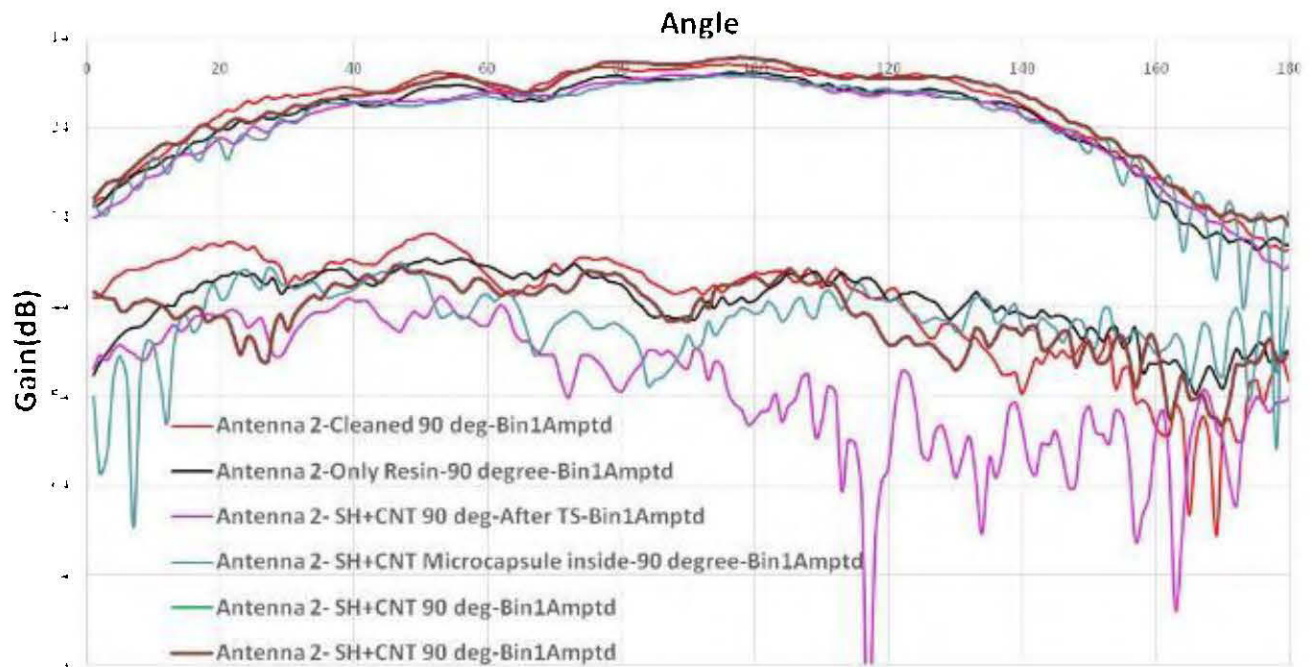


Figure 69: Radiation pattern by anechoic chamber with different materials for antenna 2 in the 90 degree

Figure 69 and 70 showing the radiation pattern in 90-degree position.

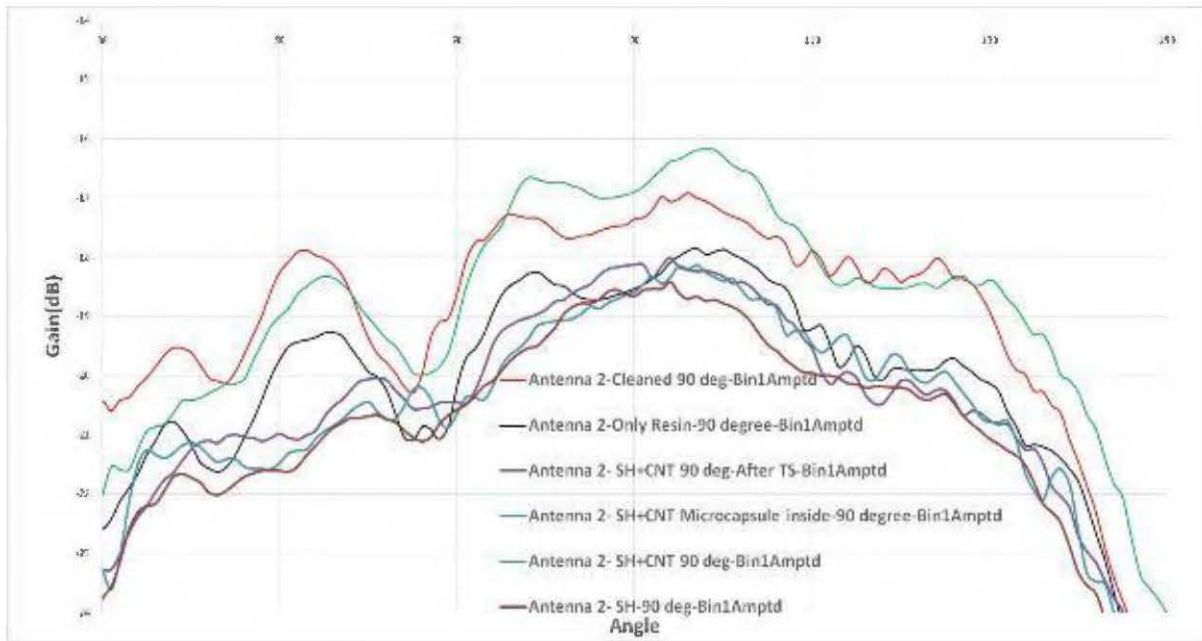


Figure 70: Zoomed of peak area of radiation pattern by anechoic chamber with different materials for antenna 2 in the 90 degree

For better understanding, in the Figure 70, peak area of radiation pattern is magnified. Picture exhibit a same trend for all of the different materials on the antenna, but as we can see, antenna with self-healing material plus CNTs has maximum gain.

Table 16: Radiation pattern description in different direction for antenna 2

Position in 90 degree				
Position	Maximum	Max peak of GAIN	Differece	Average in 90-110degree
Antenna 2-Cleaned 90 deg	-16.92	-	0.74	-17.39
Antenna 2- SH+CNT 90 deg	-16.18	Max	-	-16.75
Antenna 2-Only Resin-90 degree	-17.84	-	1.67	-18.29
Antenna 2- SH+CNT 90 deg-After Thermal shock	-18.01	-	1.83	-18.52
Antenna 2- SH+CNT Microcapsule Inside-90 degree	-18.13	-	1.93	-18.61
Antenna 2- SH-90 deg	-18.42	-	2.24	-19.03

Information of radiation pattern in the 90-degree position for antenna 2 is summarized in the table 16. Regarding to the values in the table 16, antenna with self-healing material plus CNTs has the maximum gain comparing to the others and especially to the cleaned antenna.

4.2. Self-Healing

For evaluate the self-healing quality and quantity, two methods used:

- Thermal shock
- Visual inspection by microscope

In the thermal shock, samples placed in too low temperature and then in hot temperature rapidly to making the artificial cracks. Here, two antennas with different materials are investigated. First antenna, covered by self-healing material

and one week after the thermal shock test, one crack zone in the different magnifications showed in following figures.



Figure 71: Zoomed selected damaged area of antenna in 4X

In Figure 71, one damaged area is selected and then by microscope is magnified in 4X. In 4X magnification, one crack with two derivations can be seen clearly. Also, microcapsules and catalyst in the surface can be seen.

In the Figure 72 to 74, there are different focus modes for 10X magnification.

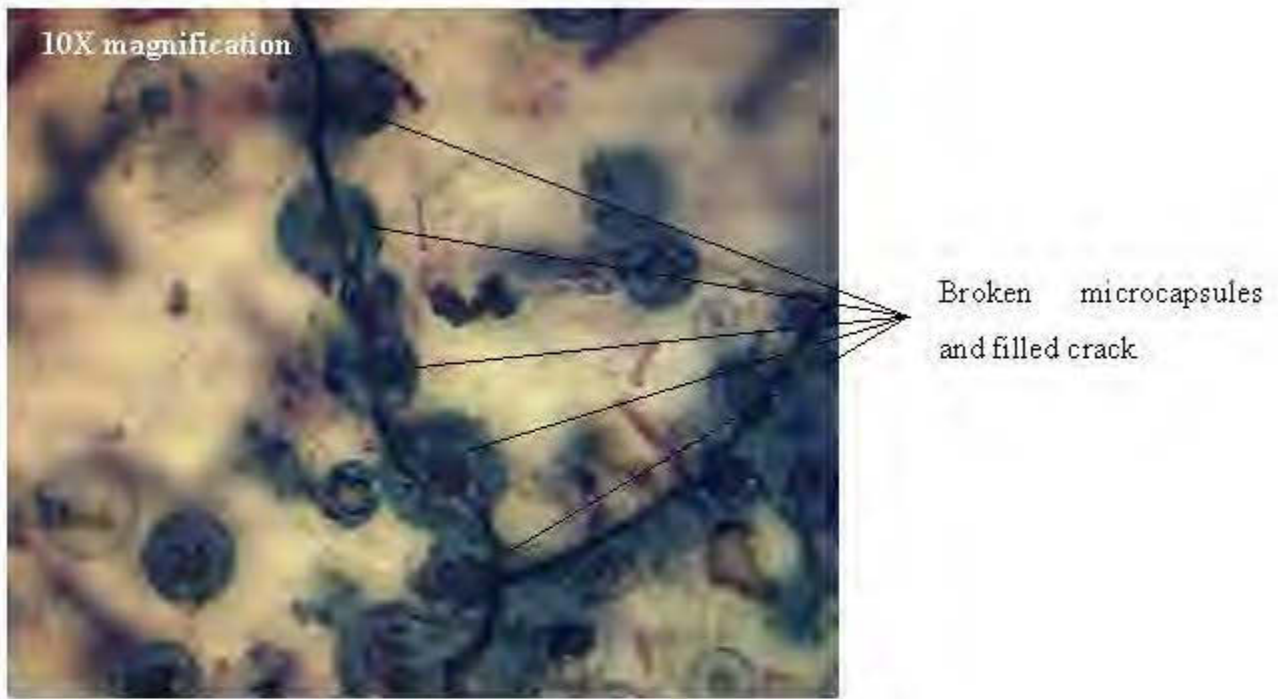


Figure 72: Many broken microcapsules in 10X

AS you see in the figure 72, there is a path of crack and some of the self-healing microcapsules are broken in this line. Now, space of the crack is filled by released material of microcapsules.



Figure 73: Well distributed catalyst in the resin bas(10X)

In the figure 73, Grubbs catalyst demonstrated. Regard to figure, a well distribution of catalyst seen in the resin.

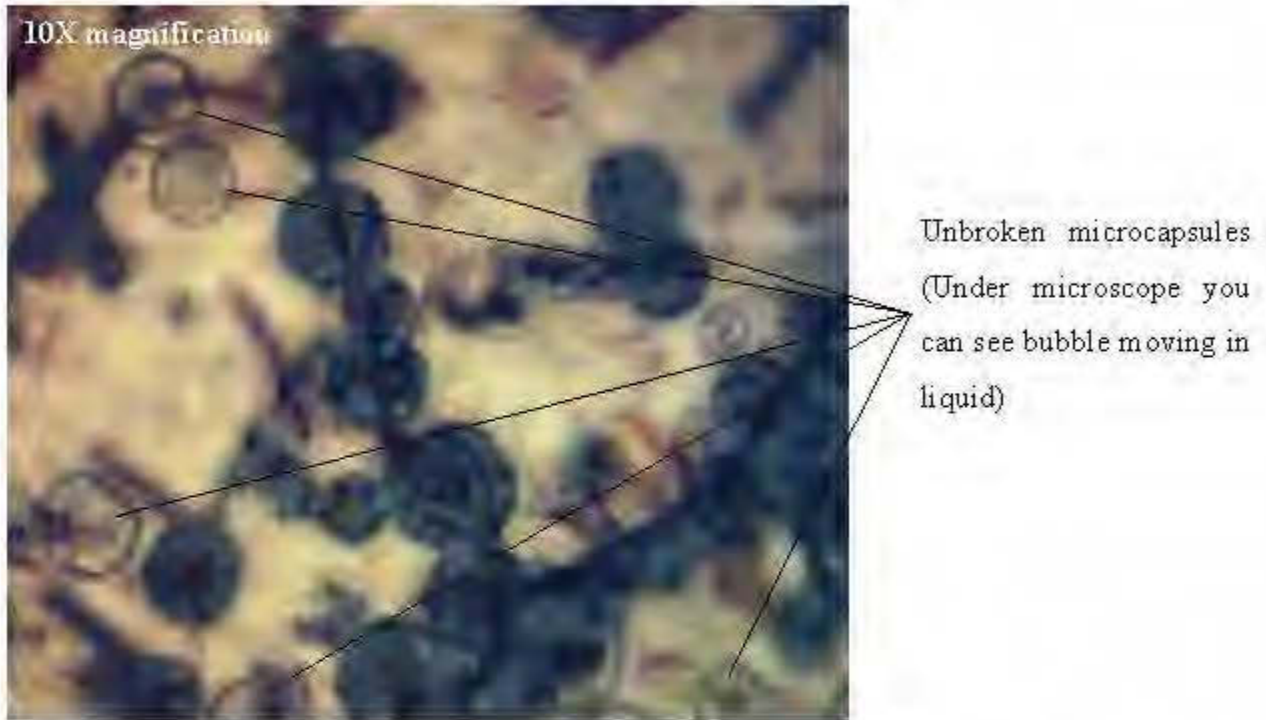


Figure 74: Many Unbroken microcapsules in 10X

In the case of cracks and/or fracture, those microcapsules which are located in the path of crack, start to break. When, a microcapsule is broken, healing agent can escape from inside of microcapsule, and meet catalysts and start chemical bonding (i.e. polymerization). In the Figure 74, there are some unbroken microcapsules which are not in the path of any crack, so they remain without any fracture.

With magnification, more details can be considered. In the Figure 75, broken microcapsules and filled crack are shown.

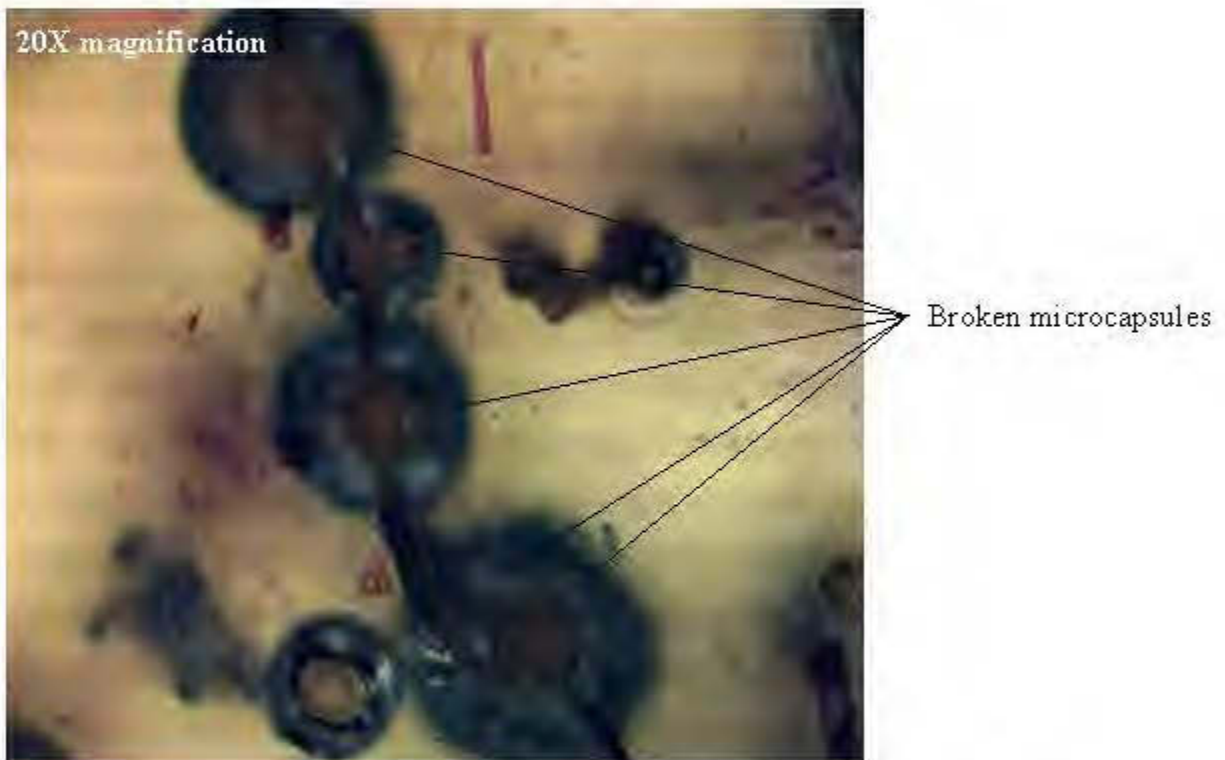


Figure 75: Broken microcapsules in the path of crack (20X)

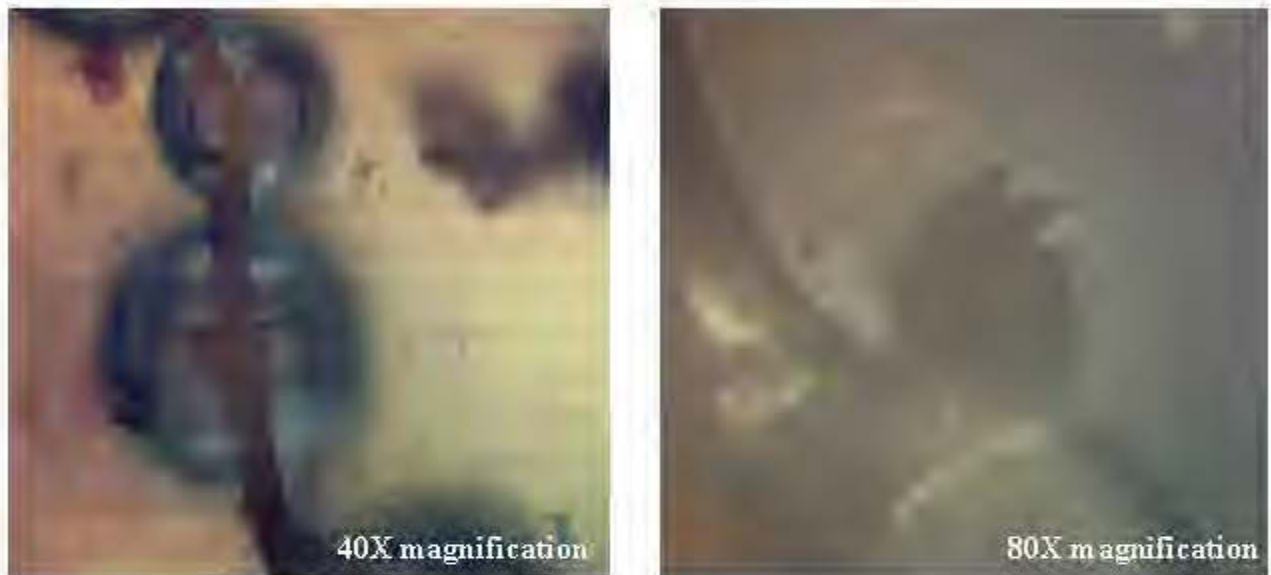


Figure 76: More magnified broken microcapsules in the path of crack (40X, 80X)

Maximum magnifications of a damaged zone with broken microcapsule, demonstrated in Figure 76. These pictures confirm that microcapsules are broken completely and crack is filled with self-healing material.

Also, for the antenna with self-healing plus CNTs, a damaged zone is selected to more investigation.

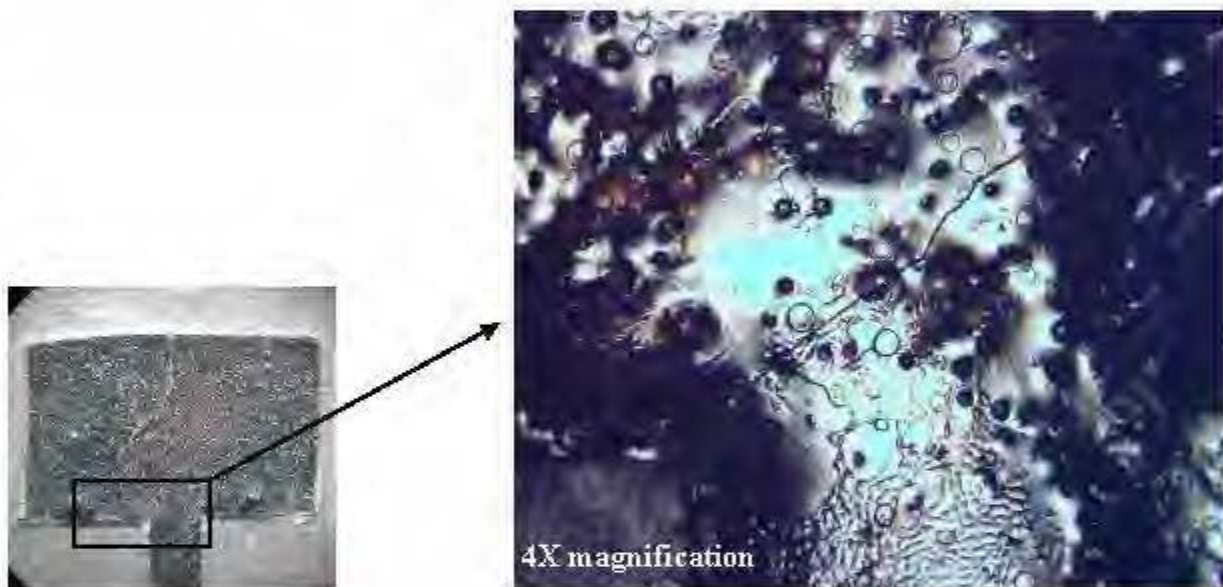


Figure 77: Zoomed selected damaged area of antenna with self-healing plus CNTs in 4X

After the thermal shock, because of the temperature gradient, sample start to crack in the different zones. (Figure 77)

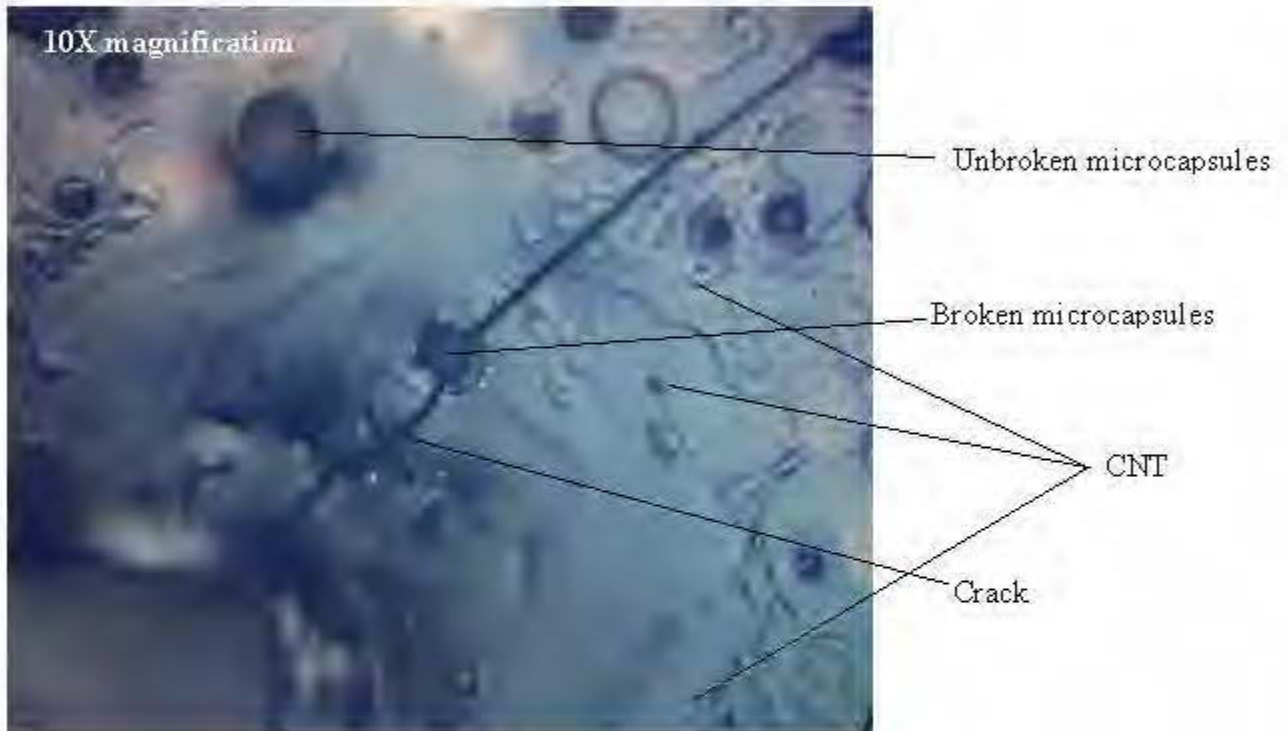


Figure 78: Surface of damaged zone in 10X

Figure 78 confirms that a crack is happening in the sample. In this figure, one microcapsule is placed in path of crack, so it is broken. Also, CNT can be clearly seen in the background.

Here, unbroken and broken microcapsules are shown in the figure 79. You can see that crack lead to breaking a microcapsule which is on the line of crack, but at the same time, there is another microcapsule which is unbroken because it is not on the crack way then there is no collision.

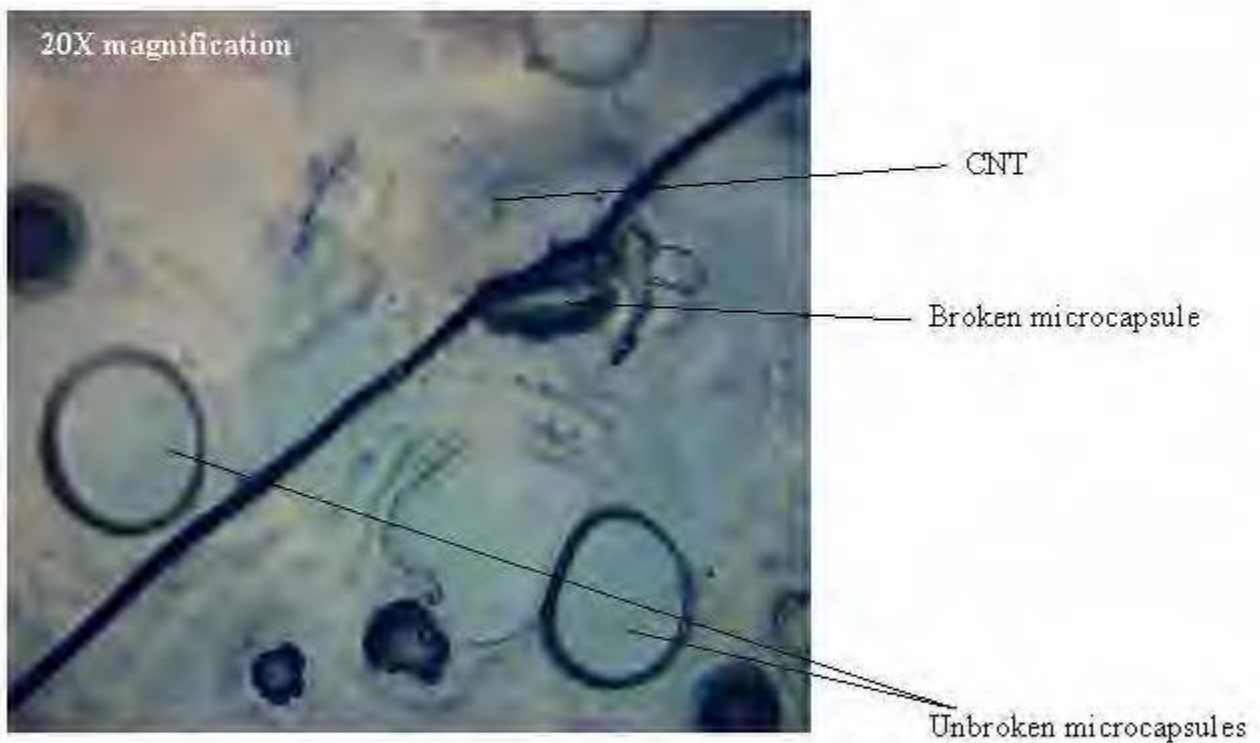


Figure 79: Surface of damaged zone in 20X

Different focus points, shows a good distribution of CNTs inside of resin. [Figure 80]

Clearly, self-healing material is well-distributed within the specimen and reliability of self-healing is increased.



Figure 80: Different focus points in 20X

Corresponding to microscopic pictures, for both samples, self-healing is happening and cracks are filled. CNTs can increase the electrical properties in the case of any cracks.

To further investigate the role of CNTs in terms of electrical contribution, here is a need to additional experiments.

In the tables 17 to 20, all of the irradiation properties for both antennas and with different conditions are compared. S-parameters are independent of different positions of anechoic chamber, and for both positions are the same, but they are placed on the table for better comparison. Table 17, shows the comparison in the first position (0° degree) of anechoic chamber.

Table 17: Comparison of irradiation properties in the first position of anechoic chamber test (0° position)

Parameter	Frequency	Δ Frequency	S-parameters	Total Area of Signal	Min angle	Middle angle	Max angle	Comment
Instrument	VNA	VNA	VNA	VNA	Anechoic chamber	Anechoic chamber	Anechoic chamber	
Dimension	GHz	GHz	dB	-	dB	dB	dB	
Ref 1	10.4	--	-25.13	-11754.06	-37.1	-18.04	-35.91	-
Resin alone	10.16	-0.24	-13.13	-11298.97	-37	-16.62	-42.02	·S-parameters is decreased ·Gain in 0 degree is increased
Resin+Hardener+Catalyst+Microcapsules+CNT	10.14	-0.26	-20.33	-8351.87	-31.83	-16.17	-34.96	·S-parameters is decreased ·Gain in 0 degree is increased
Resin+Hardener+Catalyst+MicrocapsulesCNT	10.26	-0.14	-17.9	-28845.61	-35.97	-18.47	-39.19	·S-parameters is decreased ·Gain in 0 degree is decreased
Resin+Hardener+Catalyst+Microcapsules	10.22	-0.18	-27.84	-2191.58	-35.77	-18.98	-36.85	·S-parameters is increased ·Gain in 0 degree is decreased
Ref 2	10.4	--	-12	-10096.72	-40.38	-18.08	-37.37	-
Resin+Hardener+Catalyst+Microcapsules	10.18	-0.22	-23.5	-7101.80	-30.83	-17.92	-34.54	·S-parameters is increased. ·Gain in 0 degree is increased

Among of different materials, when only (Resin+Hardener) + Catalyst + Microcapsules (self-healing material) is used, S-parameters are less than the reference antenna. But for other materials, S-parameters are increased. Antenna with only Resin, demonstrate a higher difference compared to reference for S-parameters. Also, when a material is deposited on the surface of antenna, frequency is shifted. In the case of (Resin+Hardener) + Catalyst + Microcapsules plus CNTs, shifting of frequency is higher than the others. Total area of signal shows the total area of S-parameters peak.

For better comparison, three points in beginning (0° degree), middle (90° degree) and the end (180° degree) of the Gain graph for each antenna with different conditions were selected.

When only Resin, (Resin+Hardener) + Catalyst + Microcapsules and also (Resin+Hardener) + Catalyst + Microcapsules + CNTs used for antennas, Gain is less negative in the middle point of the graph (90° degree). Totally, in this position, antenna with Only Resin shows higher gain of antenna.

In anechoic chamber, antenna rotates in 90° degree for another direction. Figure 81 demonstrates the different views of test.

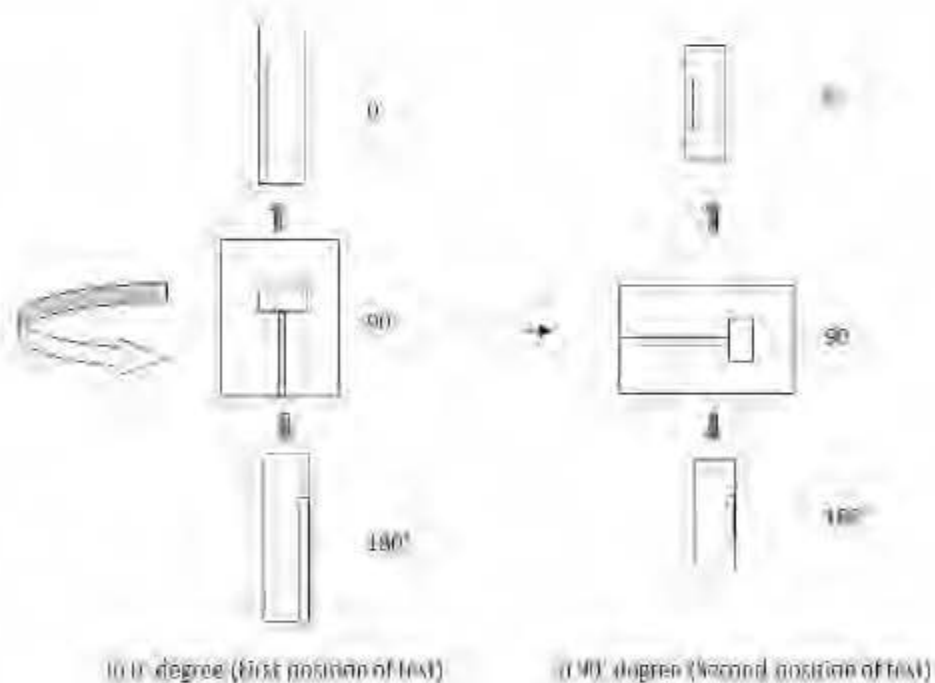


Figure 81: Two positions in anechoic chamber test

In the second position of test (90° degree), comparison is showed in table 18. In this case, gain of antenna is more negative for all of the conditions. But for self-healing material (Resin+Hardener+Catalyst+Microcapsules), Gain is more negative.

Table 18: Comparison of irradiation properties in the second position of anechoic chamber test (90° position)

Parameter	Frequency	Δ Frequency	S-parameters	Total Area of Signal	Min angle	Middle angle	Max angle	Comment
Instrument	VNA	VNA	VNA	VNA	Anechoic chamber	Anechoic chamber	Anechoic chamber	
Dimension	GHz	GHz	dB	-	dB	dB	dB	
Ref 1	10.4	-	-25.13	-11754.06	-32.43	-16.92	-37.67	-
Resin alone	10.16	-0.24	-13.13	-11298.97	-32.80	-17.84	-37.11	-S-parameters is decreased -Gain in 0 degree is decreased
Resin+Hardener+Catalyst+Microcapsules+CNT	10.14	-0.26	-20.33	-8351.87	-38.16	-17.08	-39.29	-S-parameters is decreased -Gain in 0 degree is increased
Resin+Hardener+Catalyst+Microcapsules:CNT	10.26	-0.14	-17.9	-28845.61	-32.53	-18.13	-33.42	-S-parameters is decreased -Gain in 0 degree is decreased
Resin+Hardener+Catalyst+Microcapsules	10.22	-0.18	-27.84	-2191.58	-40.89	-18.55	-39.84	-S-parameters is Increased -Gain in 0 degree is decreased
Ref 2	10.4	-	-12	-10096.72	-33.56	-18.16	-33.56	-
Resin+Hardener+Catalyst+Microcapsules	10.18	-0.22	-23.5	-7101.80	-46.63	-18.37	-40.79	-S-parameters is increased. -Gain in 90 degree is decreased.

Irradiation properties of the two antennas with different materials after the thermal shock test are compared to know the effect of thermal shock on the samples. (Tables 19, 20)

With Resin+Hardener+Catalyst+Microcapsules+CNTs, S-parameter is less negative but for only self-healing material (Resin+Hardener+Catalyst+Microcapsules) is more negative. In the Table 19, for 0° position, gain of antenna is more negative for both antennas. (Middle angle)

Table 19: Comparison of irradiation properties in the first position of anechoic chamber test (0° position) after the thermal shock

Parameter	Frequency	Δ Frequency	S-parameters	Total Area of Signal	Min angle	Middle angle	Max angle	Comment
Instrument	VNA	VNA	VNA	VNA	Anechoic chamber	Anechoic chamber	Anechoic chamber	
Dimension	GHz	GHz	dB	-	dB	dB	dB	
Ref 1	10.4	-	-25.13	-11754.06	-37.1	-18.04	-35.91	-
Resin+Hardener+Catalyst+Microcapsules+CNT After Thermal Shock	10.16	-0.24	-17.46	-20703.31	-37.75	-18.77	-40.39	-S-parameters is less negative -Gain in 0 degree is more negative
Ref 2	10.4	-	-12	-10096.72	-40.38	-18.08	-37.37	-
Resin+Hardener+Catalyst+Microcapsules After Thermal Shock	10.2	-0.2	-17.78	-16572.48	-40.04	-18.59	-40.63	-S-parameters is more negative -Gain in 0 degree is more negative

Also, same conditions in different angle (90° degree) are studied on Table 20. Here, S-parameter for Resin+Hardener+Catalyst+Microcapsules+CNTs is less negative and in contrast, for only self-healing material is more negative.

Table 20: Comparison of irradiation properties in the first position of anechoic chamber test (90° position) after the thermal shock

Parameter	Frequency	Δ Frequency	S-parameters	Total Area of Signal	Min angle	Middle angle	Max angle	Comment
Instrument	VNA	VNA	VNA	VNA	Anechoic chamber	Anechoic chamber	Anechoic chamber	
Dimension	GHz	GHz	dB	-	dB	dB	dB	
Ref 1	10.4	-	-25.13	-11754.06	-37.1	-18.04	-35.91	-
Resin+Hardener+Catalyst+Microcapsules+CNT After Thermal Shock	10.16	-0.24	-17.46	-20703.31	-34.02	-18	-39.48	-S-parameters is less negative -Gain in 0 degree is less negative
Ref 2	10.4	-	-12	-10096.72	-40.38	-18.08	-37.37	-
Resin+Hardener+Catalyst+Microcapsules After Thermal Shock	10.2	-0.2	-17.78	-16572.48	-34.29	-17.38	-35.25	-S-parameters is more negative -Gain in 0 degree is less negative

Also, compared with reference antenna, the Gain of antenna for both materials is less negative.

CHAPTER 5

CONCLUSIONS AND OUTLOOK INTO THE FUTURE

- Our object was the protection by the self-healing material an RF antenna that aim at operating in the underground mine workplace. A self-healing coating was successfully deposited onto the patch antenna. With adding new material on the antenna, no perturbations in the irradiation properties of RF antenna were observed, but also we received an improving in S-parameters and gain of antenna. (Based on being less or more negative value)
- With adding the microcapsules containing CNTs, resonance Frequency of antenna is decreased less than the other materials (closer to original).
- Resin only, Resin+Hardener+Catalyst+Microcapsules+CNTs and Resin+Hardener+Catalyst+Microcapsules containing CNTs, lead to less negative value of S-parameters.
- In the 0° degree, Resin only, Resin+Hardener+Catalyst+Microcapsules+CNTs and Resin+Hardener+Catalyst+Microcapsules (self-healing material) make less negative gain of antenna.
- In the 90° degree, all the samples were showing more negative values of the gain of the antenna.
- For anechoic chamber, after Thermal shock test, the antenna with self-healing + CNT is more negative but when it is rotated to 90 degrees as H plane, showed less negative GAIN.
- Size of microcapsules containing the CNTs was different. Microcapsules containing CNTs tended to be agglomerated. One probable reason is, this kind of microcapsules are more brittle and during the preparation are broken.

FUTURE WORKS

One of the future works could be using self-healing material as painting to self-healing corrosion for antenna and RF instruments in the humid workplaces.

Other explorative ways for RF self-healing is using the Graphene as a conductive element in the resin. Instead of utilizing CNT, we can add Graphene and because their specific shapes and properties, electrical conductivity can be increased. (Table 21)

Another work could be the thermal cycling of temperature simulation of underground mines ambient.

Table 21: Review table of papers about Graphene self-healing

Title	Method
Self-healing of defected graphene	<ul style="list-style-type: none"> * For electronics applications, defects in graphene are usually undesirable because of their ability to scatter charge carriers, thereby reduce the carrier mobility. * The self-healing is attributed to recombination of mobile carbon atoms with vacancies. With increasing level of plasma induced damage, the self-healing becomes less effective. * They employ argon plasma bombardment to produce structural defects in graphene and study healing of defects by thermal annealing.[Chen 2013]
Graphene Field-Effect Transistors with Gigahertz-Frequency Power Gain on Flexible Substrates	<ul style="list-style-type: none"> * Development of flexible electronics operating at radiofrequencies (RF) requires materials that combine excellent electronic performance and the ability to withstand high levels of strain. * Fabrication graphene field-effect transistors (GFETs) on flexible substrates from graphene grown by chemical vapour deposition (CVD).[Petrone 2012]
SOLVENT-BASED SELF-HEALING POLYMERIC MATERIALS	<ul style="list-style-type: none"> * Mechanical damage to bulk polymers typically begins as a micro crack, which can lead to eventual failure of the material if there is no method to inhibit crack growth. * In order to maximize the amount of current measured from these types of experiments, future experiments could include encapsulating graphene particles and other carbon-containing materials, then monitoring their electronic behaviour upon microcapsule rupture.[Caruso 2010]
A Rapid and Efficient Self-Healing Thermo-Reversible Elastomer Cross linked with Graphene Oxide	<ul style="list-style-type: none"> * A self-healing thermoreversible elastomer based on Graphene oxide nanocomposites. * These self-healing elastomers should be useful toward applications such as protecting barrier for electronic wires and devices, sealing layer for gas systems, etc. * when combined with electrical fillers, these elastomers should also display electrical conductivities that are useful towards stretchable self-healing conductive wires.[Wang 2013]
A strong and stretchable self-healing film with self-activated pressure sensitivity for potential artificial skin applications	<ul style="list-style-type: none"> * They show that graphene and polymers can be integrated into a thin film which mimics both the mechanical self-healing and pressure sensitivity behaviour of natural skin without any external power supply. * Integration graphene and polymers into a thin film which mimicked both the mechanical self-healing and pressure sensitivity behaviour of natural skin without any external power supply.[Hou 2013]

REFERENCES

1 - [Abhilash 2011], 2013, Abhilash Goyal, "Methodologies for Low-Cost Testing and Self-Healing of RF Systems", Georgia Institute of Technology, Thesis.

2 - [Aissa 2013], 2013, "B. Aissa, M. Nedil, M. A. Habib, E. Haddad, W. Jamroz, D. Therriault, Y. Coulibaly, and F. Rosei", "Fluidic patch antenna based on liquid metal alloy/single-wall carbon-nanotubes operating at the S-band frequency", MPB Co., APPLIED PHYSICS LETTERS 103, 063101 (2013).

3 - [Aissa 2014], 2014, Dr. B. Aissa, Dr. E. Haddad, "Mitigation of small Debris (0.1-10 mm). Effect in Space- Monitored with Fiber sensors and self-repairing materials- Application to COPVs.", MPB Communications Inc., 151 Hymus Boulevard, Montréal, QC, H9R 1E9, MPB Document Self-Healing-Debris-NPI-TN1.

4 - [Bailey 2015], 2010, Brennan M. Bailey, Yves Leterrier, S.J. Garcia, S. van der Zwaag, Véronique Michaud, "Electrically conductive self-healing polymer composite coatings", Ecole Polytechnique Fédérale de Lausanne (EPFL), Progress in Organic Coatings 85 (2015) 189–198.

5 - [Blaiszik 2010], 2010, B.J. Blaiszik, S.L.B. Kramer, S.C. Olugebefola, J.S. Moore, N.R. Sottos, and S.R. White, "Self-Healing Polymers and Composites", Annu. Rev. Mater. Res. 2010. 40:179–211.

6 - [Blaiszik 2011], 2011, Benjamin J. Blaiszik, Sharlotte L. B. Kramer, Martha E. Grady, David A. McIlroy, Jeffrey S. Moore, Nancy R. Sottos, and Scott R. White, "Autonomic Restoration of Electrical Conductivity ", Department of Materials Science and Engineering, Beckman Institute for Advanced Science and Technology, University of Illinois at Urbana-Champaign, Adv. Mater. 2011, XX, 1–4.

7 - [Boesen 2011], 2011, Michael Reibel Boesen, Didier Keymeulen, Jan Madsen, Thomas Lu, Tien-Hsin Chao, "Integration of the Reconfigurable Self-Healing eDNA Architecture in an Embedded System", Technical University of Denmark, 978-1-4244-7351- ©2011 IEEE.

IEEEAC paper#1453, Version 4, Updated 2010:10:26.

8 - [Caruso 2010], 2010, MARY M. CARUSO, "SOLVENT-BASED SELF-HEALING POLYMERIC MATERIALS", PhD thesis, University of Illinois at Urbana-Champaign, 2010.

9 - [Chahat 2014], 2013, Nacer Chahat, Maxim Zhadobov and Ronan Sauleau, "Antennas for Body Centric Wireless Communications at Millimeter Wave Frequencies", Progress in Compact Antennas, <http://dx.doi.org/10.5772/58816>.

10 - [Chen 2013], 2013, Jianhui Chen, Tuwan Shi, Tuocheng Cai, Tao Xu, Litao Sun, "Self-healing of defected graphene", School of Physics, Peking University, Beijing 100871, People's Republic of China, APPLIED PHYSICS LETTERS 102, 103107 (2013).

11 - [Dadi 2012], 2012, Gabriel Dadi, "SmartCoats: Intelligent and Innovative Material Coatings", White Paper (Draft: 06/18/2012), Breakthrough Strategy Committee.

12 - [Dickey 2014], 2014, Michael D. Dickey, "Emerging Applications of Liquid Metals Featuring Surface Oxides", North Carolina State University, dx.doi.org/10.1021/am5043017 | ACS Appl. Mater. Interfaces 2014, 6, 18369–18379.

13 - [El Azhari 2015], 2015, Moulay El Azhari, Mourad Nedil, Ismail Ben Mabrouk, Khalida Ghanem, and Larbi Talbi, "Characterization of an Off-Body

Channel at 2.45GHz in an Underground Mine Environment", Progress In Electromagnetics Research M, Vol. 43, 91–100, 2015.

14- [Francesconi 2013], 2013, A. Francesconi, C. Giacomuzzo, A.M. Grande, T. Mudric, M. Zaccariotto, "Comparison of self-healing ionomer to aluminium-alloy bumpers for protecting spacecraft equipment from space debris impacts", Advances in Space Research 51 (2013) 930–940.

15 - [Frei 2013], 2013, Regina Frei, Richard McWilliam, Benjamin Derrick, Alan Purvis, Asutosh Tiwari, Giovanna Di Marzo Serugendo, "Self-healing and self-repairing technologies", Int J Adv Manuf Technol (2013) 69:1033–1061.

16 - [Gao 2012], 2012, A.-M. Gao, Q.-H. Xu, H.-L. Peng, W. Jiang, and Y. Jiang, "Performance Evaluation of Uwb On-Body Communication Under Wimax Off-Body Emi Existence", Key Lab of Ministry of Education for Design and EMC of High-Speed Electronic Systems, Shanghai Jiao Tong University, Shanghai 200240, Progress In Electromagnetics Research, Vol. 132, 479–498, 2012, China.

17 - [Hou 2013], 2014, Chengyi Hou, Tao Huang, Hongzhi Wang, Hao Yu, Qinghong Zhang & Yaogang Li, "A strong and stretchable self-healing film with self-activated pressure sensitivity for potential artificial skin applications", State Key Laboratory for Modification of Chemical Fibers and Polymer Materials, College of Materials Science and Engineering, Donghua University, 201620 (People's Republic of China), SCIENTIFIC REPORTS | 3: 3138 | DOI: 10.1038/srep03138.

18 - [Huiskamp 2015], 2015, M. Huiskamp, "Signal Characterization for Self-Healing RF-Power Amplifiers", University of Twente, Thesis.

19 - [Kang 2014], 2014, Hong Suk Kang, Hee-Tak Kim, Jung-Ki Park, and Seungwoo Lee, "Light-Powered Healing of a Wearable Electrical Conductor", Korea

Advanced Institute of Science and Technology (KAIST), DOI: 10.1002/adfm.201401666, Adv. Funct. Mater. 2014, 24, 7273–7283.

20 - [Kishore 2014], 2014, C. Maruthi Ratna Kishore, "Concept and Working Of Different Types Of Fuses – Protection From Short Circuit Damages – A Bird’s Eye View", Electrical and Electronics Engineering. Dept, Rise group of Institutions Ongole-523001, Andhra Pradesh, India, IOSR Journal of Electrical and Electronics Engineering (IOSR-JEEE), e-ISSN: 2278-1676, p-ISSN: 2320-3331, Volume 9, Issue 5 Ver I (Sep–Oct. 2014), PP 44-49, www.iosrjournals.org.

21 - [Odom 2012], 2012 , Susan A. Odom, Timothy P. Tyler, Mary M. Caruso, Joshua A. Ritchey, Matthew V. Schulmerich, Scott J. Robinson, Rohit Bhargava, Nancy R. Sottos, Scott R. White, Mark C. Hersam, and Jeffrey S. Moore, "Autonomic restoration of electrical conductivity using polymer-stabilized carbon nanotube and graphene microcapsules", University of Illinois at Urbana-Champaign, APPLIED PHYSICS LETTERS 101, 043106 (2012).

22 - [Pallaeu 2013], 2013, Etienne Palleau, Stephen Reece, Sharvil C. Desai, Michael E. Smith, and Michael D. Dickey, "Self-Healing Stretchable Wires for Reconfigurable Circuit Wiring and 3D Microfluidics ", North Carolina State University, DOI: 10.1002/adma.201203921, Adv. Mater. 2013, 25, 1589–1592.

23 - [Petroni 2012], 2012, Nicholas Petrone, Inanc Meric, James Hone, and Kenneth L. Shepard, "Graphene Field-Effect Transistors with Gigahertz-Frequency Power Gain on Flexible Substrates", Department of Mechanical Engineering and Department of Electrical Engineering, Columbia University, New York, Nano Lett. 2013, 13, 121–125.

24 - [Raheem 2011], 2011, Soliu Adegboyega Raheem, "Remote Monitoring of Safe and Risky Regions of Toxic Gases in Underground Mines: A Preventive Safety Measures", African Institute for Mathematical Sciences (AIMS).

25 - [Wang 2013], 2013, Chao Wang, Nan Liu, Ranulfo Allen, Jeffrey B.-H. Tok, Yinpeng Wu, Fan Zhang, Yongsheng Chen, and Zhenan Bao, "A Rapid and Efficient Self-Healing Thermo-Reversible Elastomer Crosslinked with Graphene Oxide", Department of Chemical Engineering Stanford University, *Adv. Mater.* 2013, 25, 5785–5790.

Annex

In this master's report, in the first part of it, with huge quantity of manmade Micro-Meteorites Orbital Debris (MMOD) in the space, there is concern about damage potential of them for spacecraft, satellite and space instruments. This debris with a few microns to centimetre size and high kinetic energy can have velocity up to 20 km/s. For decreasing of the possible damage and also health monitoring of system, new generation of smart material can be suitable option. Self-healing material can repair them with or without external influence. And also self-healing composite can decrease the velocity and intensity of impact. Also, for self-healing like microcapsules, ionomers, ceramics and etc, used and researcher group analysed the results. Additionally, for the health monitoring, Fiber sensor, in particular Fiber Bragg Grating (FBG) because of their proper characteristics can be used. There are too many debris coming from manmade instruments in the space. Their number is exponentially increasing with higher probability of hitting functional satellites.

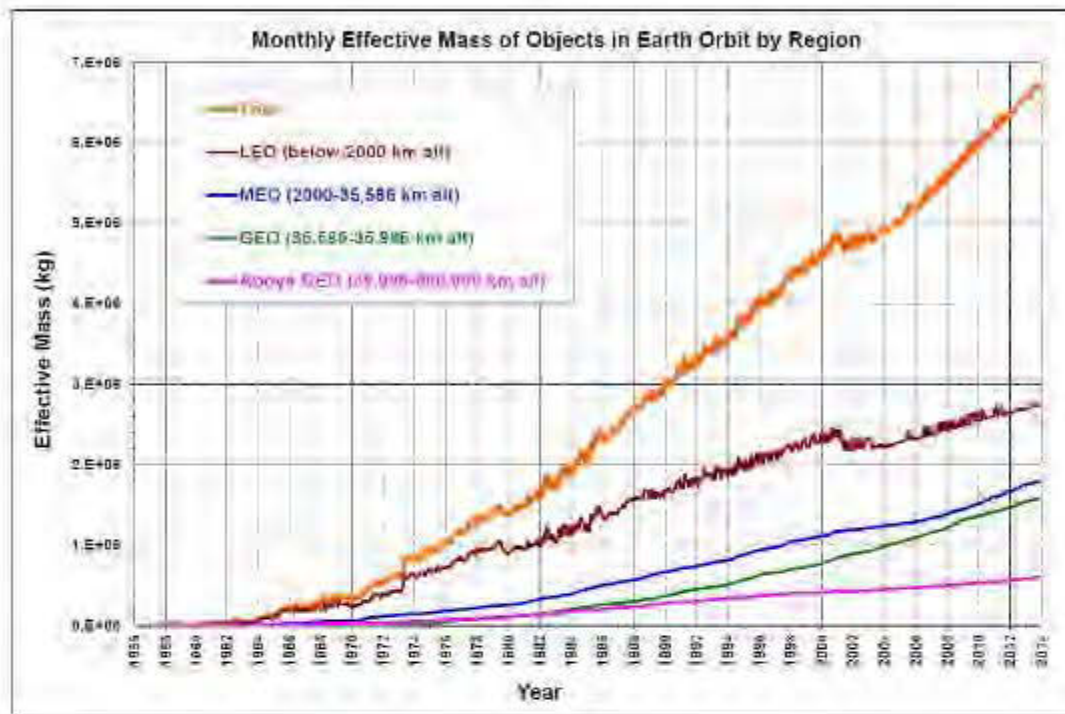


Figure 82: Monthly Effective Mass of Objects in Earth Orbit by Region (officially catalogued by the U.S. Space Surveillance Network. Divided into orbital altitude regions, “effective mass” accounts for the fraction of its orbit that an object may spend in the different regions).

On 27 October 2014, the International Space Station (ISS) performed a manoeuvre to avoid the close approach of 8 cm diameter debris from the 2009 collision of the satellites Iridium 33 (US functional) and Cosmos 2251 (Russia obsolete).

We take profit from two innovative technologies that were developed recently, to reduce the effects of the debris:

- The self-healing material that makes possible an autonomous repair of cracks and holes in a composite.

- The fiber sensors that can be embedded in various materials to detect the impact by the debris. The fiber sensors permit to monitor the health of these structures (measure their strain and temperature).

We focus on the space applications, in particular to the protection of Composite Over-Wrapped Pressure Vessels (COPVs) tanks. These tanks are being used as fuel reservoir; they are sensitive to debris since any small puncture will lead to the leak of all the fuel.

Fiber Sensors

Fiber sensors can convert the mechanical and temperature changes to an optical signal variation, which can have monitored with special instruments. Normally, the fiber sensors include three parts: core of fused silica of about 10 μm diameter, that transmits the light, covered by ad a cladding of about 125 μm , a first protective flexible layer of polyimide or acrylic is added. A second-thick plastic layer can be added to protect against the mechanical forces and avoids the breaking [Figure 83].

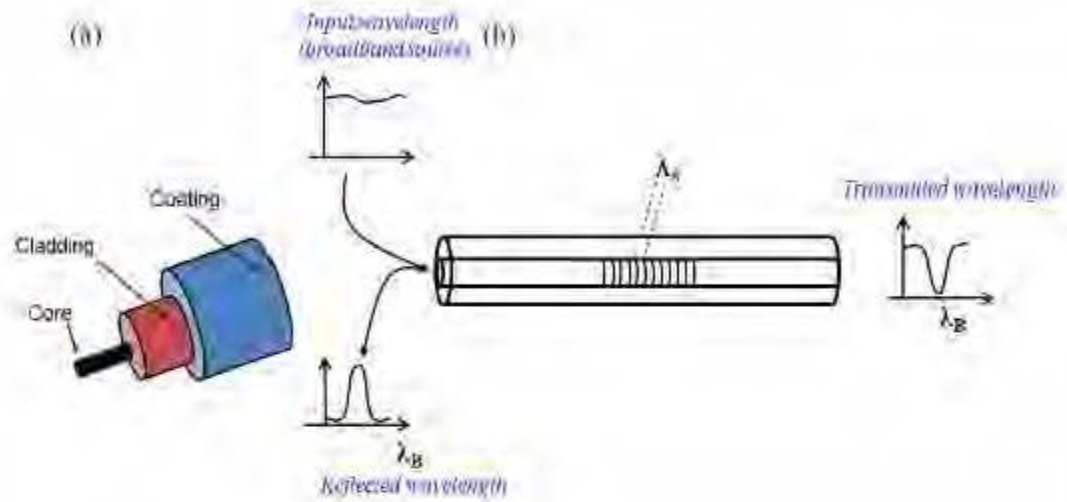


Figure 83: (a) Schematic of the optical fiber (b) Light phenomena in the FBG sensor. [Aissa 2014]

